University of Alberta

Adaptive Responses of Paralyzed Skeletal Muscle to Altered Activity After Spinal Cord Injury

by

Robinson Luke Whitney Harris

©

A thesis submitted to the Faculty of Graduate Studies and Research
in partial fulfillment of the requirements for the degree of

Doctor of Philosophy

Centre for Neuroscience

Edmonton, Alberta
Fall, 2007

Library and Archives Canada

Published Heritage Branch

395 Wellington Street
Ottawa ON K1A 0N4
Canada

Bibliothèque et Archives Canada

Direction du Patrimoine de l'édition

395, rue Wellington
Ottawa ON K1A 0N4
Canada

Your file Votre référence
ISBN: 978-0-494-32974-0
Our file Notre référence
ISBN: 978-0-494-32974-0

NOTICE:
The author has granted a non-exclusive license allowing Library and Archives Canada to reproduce, publish, archive, preserve, conserve, communicate to the public by telecommunication or on the Internet, loan, distribute and sell theses worldwide, for commercial or non-commercial purposes, in microform, paper, electronic and/or any other formats.

The author retains copyright ownership and moral rights in this thesis. Neither the thesis nor substantial extracts from it may be printed or otherwise reproduced without the author's permission.

AVIS:
L'auteur a accordé une licence non exclusive permettant à la Bibliothèque et Archives Canada de reproduire, publier, archiver, sauvegarder, conserver, transmettre au public par télécommunication ou par l'Internet, prêter, distribuer et vendre des thèses partout dans le monde, à des fins commerciales ou autres, sur support microforme, papier, électronique et/ou autres formats.

L'auteur conserve la propriété du droit d'auteur et des droits moraux qui protège cette thèse. Ni la thèse ni des extraits substantiels de celle-ci ne doivent être imprimés ou autrement reproduits sans son autorisation.

In compliance with the Canadian Privacy Act some supporting forms may have been removed from this thesis.

While these forms may be included in the document page count, their removal does not represent any loss of content from the thesis.

Conformément à la loi canadienne sur la protection de la vie privée, quelques formulaires secondaires ont été enlevés de cette thèse.

Bien que ces formulaires aient inclus dans la pagination, il n'y aura aucun contenu manquant.

Canada

ABSTRACT

Central nervous system injury leads to the paralysis of skeletal muscles innervated below the level of the lesion. Depending on the nature of the injury, this paralysis may be associated with a variety of alterations in daily muscle activity, ranging from a near-complete elimination of muscle activity to near-normal muscle activity. Using rat models of sacral spinal isolation and sacral spinal cord transection, it was demonstrated that activity in paralyzed tail muscles is almost completely eliminated early after spinal cord transection, and also that there is almost no activity after long-term spinal isolation. The absence of muscle activity in these animals resulted in tail myofiber atrophy and a slow-to-fast transformation in myosin heavy chain (MyHC)-based myofiber types. However, after long-term sacral spinal cord transection tail muscle activity recovered to no different from normal due to the development of pronounced spasticity. This spasticity-associated tail muscle activity promoted recovery from myofiber atrophy and recovery of normal MyHC-based myofiber type proportions. Spastic tail muscles also had longer and larger twitch contractions, but they become much more fatigable. Similarly, following chronic hindlimb muscle paralysis due to hemisection and unilateral deafferentation (HSDA) in adult cats there was some residual activity in the paralyzed muscles. This residual muscle activity was associated with preserved contractile force and speed in paralyzed motor units and whole muscles, as well as with preserved proportions of MyHC proteins and the myofiber types that express them. However, as also observed in spastic tail muscles, paralysis due to HSDA resulted in a dramatic reduction in muscle endurance, and this was paralleled by a transformation toward more fatigable motor unit and metabolically-classified myofiber types, as well as a reduced oxidative to glycolytic enzyme activity

ratio. Overall, the results from these models of spinal cord transection, spinal isolation, and HSDA suggest that activity in paralyzed muscles due to spasticity, for example, promotes the maintenance or recovery of some normal muscle, motor unit, and myofiber properties. However, the contractile and metabolic phenotypes of these paralyzed skeletal muscles are regulated independently, and this leads to preserved contractile properties but a reduction in fatigue resistance.

ACKNOWLEDGEMENTS

I would like to express deep gratitude to my supervisor, Dr. David Bennett, for helping me learn brevity, generosity, and intuition in my scientific endeavours, as well as for his continuing financial support. I am also deeply grateful to my co-supervisor, Dr. Ted Putman, and my committee member and surrogate supervisor, Dr. Tessa Gordon, for their ongoing mentorship and advice.

Thank you to Leo Sanelli, Ian McLean, Neil Tyreman, and Jean Pearcy for their assistance with the frustrations of experimental work and bureaucracy. I also appreciate the guidance, suggestions, and technical support so generously offered over the last several years by Dr. Monica Gorassini, Dr. Philip Harvey, Dr. John Greer, Dr. René Murphy, Michelle Rank, Karen Martins, Maria Gallo, Yang Shu, and Dr. Janka Hegedus.

Numerous friends have repeatedly expressed their confidence in my abilities. Thank you Léa-Marie, Peter, James and Tracy, James S., and Colin.

Finally, thank you to Mom, Jonathan, Dad, and Jane for your love and unflagging encouragement.

Research funding in the Bennett, Putman, and Gordon labs was provided by NSERC, CFI, CIHR, AHFMR, and NCE.

TABLE OF CONTENTS

CHAPTER 1: Introduction 1

1.1 MUSCLE ACTIVITY INCREASES WITH EXERCISE TRAINING AND ELECTRICAL STIMULATION 1

1.1.1 Muscles respond differently to changes in activity brought about by resistance training and endurance training 1

1.1.2 The effects of various chronic electrical stimulation patterns reveal the neuromuscular bases for establishing muscle speed, force, and fatigue resistance 1

1.2 ELIMINATING AND REDUCING MUSCLE ACTIVITY WITH SPINAL ISOLATION AND SPINAL CORD TRANSECTION 2

1.2.1 Spinal isolation eliminates muscle activity almost completely 2

1.2.2 Muscle properties are better preserved following spinal cord transection than following spinal isolation 3

1.3 NORMAL MUSCLE PROPERTIES CAN BE PRESERVED OR RESTORED AFTER INJURY BY USING INTERVENTIONS THAT GENERATE MUSCLE ACTIVITY 4

1.3.1 Exercise promotes recovery of paralyzed muscles in a muscle- and training-dependent manner 4

1.3.2 Human muscles recover with exercise following long-term spinal cord injury 5

1.4 SPASTICITY MAY PROMOTE RECOVERY AFTER SPINAL CORD INJURY BY GENERATING ACTIVITY IN PARALYZED MUSCLES 6

1.4.1 Spasticity after spinal cord injury in humans is characterized by velocity-dependent hypertonus, hyperreflexia, and involuntary spasms 7

1.4.2 The neurophysiological basis of spasticity involves altered motoneuronal excitability 8

1.5 RESIDUAL MUSCLE ACTIVITY AFTER PARALYSIS HAS CLINICAL AND EXPERIMENTAL IMPLICATIONS 9

1.6 OBJECTIVE AND HYPOTHESES 10

CHAPTER 2: Tail muscles become slow but fatigable in chronic sacral spinal rats with spasticity 18

2.1 INTRODUCTION 18

2.2 MATERIALS AND METHODS 19

2.2.1 Spinal cord transection 19

2.2.2 Tail muscle and nerve preparation for recording 19

2.2.3 Contractions 21

2.2.4 Analyses 21

2.3 RESULTS 22
2.3.1 Body and muscle masses of normal and chronic spinal rats. 22
2.3.2 Tail muscles of chronic spinal rats have slower and larger twitches than tail muscles of normal rats 22
2.3.3 Motor unit twitches were enhanced in chronic spinal rats 22
2.3.4 The absolute rate of rise of twitch force is not lower in chronic spinal rats; it just takes longer to develop the larger peak force 27
2.3.5 Tetani and post-tetanic twitch properties of tail muscles 27
2.3.6 Chronic spinal tail muscles fuse more easily 30
2.4 DISCUSSION 35
2.4.1 Spastic muscle activity depends on the model and muscle examined 38
2.4.2 Myofiber type changes with injury 39
2.4.3 Factors that influence fatigue after injury 40
2.4.4 Factors that don't influence twitch duration and size after injury 40
2.4.5 Possible changes in intracellular calcium buffering and sequestering 40
2.4.6 Summary 42
2.5 REFERENCES FOR CHAPTER 2 43
CHAPTER 3: Spastic tail muscles recover from myofiber atrophy and myosin heavy chain transformations in chronic spinal rats 48
3.1 INTRODUCTION 48
3.2 MATERIALS AND METHODS 50
3.2.1 Animal procedures 50
3.2.2 Spinal cord injury 50
3.2.3 24-hour EMG recordings 50
3.2.4 Muscle preparation and sectioning 52
3.2.5 Immunohistochemical staining of myofibers with antibodies against myosin heavy chain isoforms 52
3.2.6 Electrophoresis of myosin heavy chain protein isoforms 55
3.2.7 Statistical analyses 55
3.3 RESULTS 58
3.3.1 Spinal isolation eliminates spasticity 58
3.3.2 Myofiber composition is not affected by differences in the ages of the rats studied 61
3.3.3 Transformation toward a faster myofiber composition early after spinal cord transection is reversed by prolonged spasticity 61
3.3.4 Tail myofiber size is not affected by differences in the ages of the rats studied 65
3.3.5 Myofibers atrophy early after spinal cord transection but recover with prolonged spasticity 65
3.3.6 Electrophoretically-determined MyHC isoform content and computed area density are stable with long-term spinal cord transection and spasticity 71

3.4 DISCUSSION 74
3.4.1 Spasticity promotes recovery from myofiber atrophy after chronic spinal cord transection 74
3.4.2 Spasticity opposes transformation of myofiber types after chronic spinal cord transection 74
3.4.3 Recovery of myofiber types and myofiber morphology resembles the effects of exercise 75
3.4.4 Rat segmental tail muscles can be reliably assessed with routine immunohistochemical staining and gel electrophoresis 76
3.4.5 Altered muscle loading may influence tail myofiber type proportions after spinal isolation 77
3.4.6 Summary 77
3.5 REFERENCES FOR CHAPTER 3 79

CHAPTER 4: Contractile and metabolic phenotypes are independently regulated in cat medial gastrocnemius muscles and motor units following long-term hemisection and unilateral deafferentation 84

4.1 INTRODUCTION 84
4.2 MATERIALS AND METHODS 85
4.2.1 Animals and experimental models 85
4.2.2 Surgery, electrodes, and unilateral hindlimb paralysis 87
4.2.3 Chronic muscle recording 88
4.2.4 Final acute motor unit and muscle recording 89
4.2.5 Enzyme histochemistry, and immunohistochemistry for myosin heavy chain isoforms 90
4.2.6 Electrophoretic determination of relative MyHC isoform contents 94
4.2.7 Biochemical measurements of oxidative and glycolytic enzyme activities 94
4.2.8 Statistical analyses 94
4.3 RESULTS 97
4.3.1 Behavior of the paralyzed hindlimb 97
4.3.2 Muscle force, contractile speed and endurance 98
4.3.3 Motor unit contractile properties 105
4.3.4 Relationships among motor unit contractile properties 111
4.3.5 Distributions of motor unit types and motor unit forces 114
4.3.6 Relationships among muscle unit and motor axon properties 117
4.3.7 Changes in myofiber types and myofiber sizes 120
4.3.8 Changes in contractile protein isoform contents and in metabolic enzyme activities 130
4.3.9 Muscle masses 135
4.4 DISCUSSION 135
4.4.1 Muscle weakness after paralysis: force versus fatigue 135
4.4.2 HSDA is an unique model of altered use 137

4.4.3 The contractile and metabolic phenotypes of cat skeletal muscle are regulated independently following HSDA 139
4.4.4 Summary 141
4.5 REFERENCES FOR CHAPTER 4 142

CHAPTER 5: INTERPRETATIONS AND APPLICATIONS 148

5.1 SUMMARY OF RESULTS 148
5.2 MUSCLE ACTIVITY AFTER INJURY BENEFITS PARALYZED MUSCLES 149
5.3 THE ROLE OF CALCIUM IN CONTRACTION OF PARALYZED MUSCLE 150
5.4 CALCIUM- AND RATE-DEPENDENCE OF FATIGUE-RESISTANCE 151
5.5 DISCOORDINATE ALTERATIONS IN METABOLIC AND CONTRACTILE PROFILES 153
5.6 FUTURE DIRECTIONS 154
5.7 CLINICAL RELEVANCE AND APPLICATION 155
5.8 REFERENCES FOR CHAPTER 5 157

LIST OF TABLES

CHAPTER 2: Tail muscles become slow but fatigable in chronic sacral spinal rats with spasticity **18**

Table 2-1: Experimental and control animals used in assessing segmental tail muscles in chronic spinal cord-injured rats. 20

CHAPTER 4: Contractile and metabolic phenotypes are independently regulated in cat medial gastrocnemius muscles and motor units following long-term hemisection and unilateral deafferentation **84**

Table 4-1: Wet masses, in grams, of the MG and other selected hindlimb muscles from paralyzed and normal cats; the percent differences between normal and paralyzed muscle masses are also shown. 86

LIST OF FIGURES

CHAPTER 2: Tail muscles become slow but fatigable in chronic sacral spinal rats with spasticity **18**

Figure 2-1: Twitch properties of the 14th ventrolateral segmental tail muscle of old normal rats and of rats with spasticity after chronic sacral spinal cord injury, in response to supramaximal stimulation pulses. 23

Figure 2-2: Representative traces from both old normal and chronic spinal rats demonstrate that twitch contractions of segmental tail muscles can be separated into the twitches of their constituent motor units. 25

Figure 2-3: Maximum rates of twitch rise and of twitch decay determined from the derivative of the twitch. 28

Figure 2-4: Representative tetani and their relationships to twitch contractions for old normal rats and chronic spinal rats. 31

Figure 2-5: Fusion properties of segmental tail muscles. 33

Figure 2-6: Fatigue with repeated contractions of segmental tail muscles. 36

CHAPTER 3: Spastic tail muscles recover from myofiber atrophy and myosin heavy chain transformations in chronic spinal rats **48**

Figure 3-1: Representative photomicrographs show immunohistochemical staining of rat segmental tail muscles in serial cross sections. 53

Figure 3-2: Electrophoresis was used to separate MyHC isoforms in segmental tail muscle homogenates. 56

Figure 3-3: Representative tail muscle EMG records taken from 24-hour EMG recording sessions, and the mean 24-hour EMG amplitude for normal, acute spinal, chronic spinal, and spinal isolated rats. 59

Figure 3-4: The mean proportion of each myofiber type is shown for normal, chronic spinal, and spinal isolated rats; percent changes in myofiber type proportions are also shown. 62

Figure 3-5: The mean cross-sectional area of each myofiber type for normal, chronic spinal, and spinal isolated rats is shown in units of cross-sectional area (μm^2); percent changes in myofiber cross-sectional area are also shown. 66

Figure 3-6: The mean myofiber cross-sectional areas shown in Figure 3-5 are detailed according to size distributions in bins of 500 μm^2 each. 69

Figure 3-7: The relative muscle content of each MyHC isoform is shown for normal, chronic spinal, and spinal isolated rats as determined by electrophoretic separation of these isoforms; the area densities of the corresponding MyHC isoforms are shown as computed from immunohistochemical staining. 72

CHAPTER 4: Contractile and metabolic phenotypes are independently regulated in cat medial gastrocnemius muscles and motor units following long-term hemisection and unilateral deafferentation 84

Figure 4-1: Representative serial photomicrographs show similar regions of the paralyzed MG of an adult cat with long-term HSDA and of the control MG of a normal adult cat, in which myofibers have been labeled using immunohistochemical staining with antibodies against MyHC isoforms. 92

Figure 4-2: Representative serial photomicrographs show similar regions of the paralyzed MG of an adult cat with long-term HSDA and of the control MG of a normal adult cat, in which myofibers have been labeled according using histochemical staining for three enzyme complexes. 95

Figure 4-3: Typical isometric recordings of twitch and tetanic contractions of the adult cat MG muscle in response to suprathreshold stimulation of the MG nerve. 99

Figure 4-4: Time-to-peak twitch force, muscle sag during unfused tetani, maximal isometric tetanic force, and endurance index of the whole MG muscle are plotted as a function of time after HS, after HSDA-SP, and after HSDA. 101

Figure 4-5: Changes in time-to-peak twitch, sag ratio, peak tetanic force, and endurance index of the whole MG muscle are shown as a function of time after long-term HSDA. 103

Figure 4-6: Time-to-peak twitch, sag, peak tetanic force, and endurance index are shown as measured acutely both for whole muscles and for motor units. 106

Figure 4-7: Motor unit data are plotted as frequency histograms for time-to-peak twitch, sag, peak tetanic force, and endurance index. 109

Figure 4-8: For each motor unit sampled, the endurance index is plotted as a function of time-to-peak twitch, of sag, or of peak tetanic force. 112

Figure 4-9: Slow, fast fatigue resistant, fast fatigue intermediate, and fast fatigable motor units are differentiated according to cumulative force histograms, proportions of individual motor unit types, mean peak tetanic forces, and mean force densities. 115

Figure 4-10: Motor axon conduction velocity, peak-to-peak amplitude of extracellular motor axon action potential, and motor unit time-to-peak twitch are plotted against motor unit tetanic force. 118

Figure 4-11: The numbers and sizes of myofibers in the MG muscles of paralyzed and normal adult cats. 122

Figure 4-12: The number of myofibers within each of a series of size ranges is plotted as a percentage of the total number of myofibers of all types. 125

Figure 4-13: Representative distribution frequency histograms demonstrating the range of sizes of myofibers comprising a single motor unit compared to the range of sizes of all myofibers. 128

Figure 4-14: Representative lanes from SDS-PAGE gel electrophoresis, mean relative contents of each MyHC isoform, and the area density of myofiber types. 131

Figure 4-15: Biochemical activities of metabolic marker enzymes, in units of activity per milligram of soluble protein. 133

LIST OF ABBREVIATIONS USED

%Δ	percent difference
α-GPD	alpha-glycerophosphate dehydrogenase
ANOVA	analysis of variance
ATP	adenosine triphosphate
CS	citrate synthase
CSA	cross-sectional area
CV	conduction velocity
DA	unilateral deafferentation
DAB	diaminobenzidine
EDL	extensor digitorum longus
EI	endurance index
EMG	electromyography
F_{50}	stimulation frequency required for 50% of maximal force
FF	fast fatigable
FG	fast glycolytic
FI	fast fatigue intermediate
FOG	fast oxidative-glycolytic
FR	fast fatigue resistant
GAPDH	glyceraldehyde phosphate dehydrogenase
HS	hemisection
HSDA HS	combined with unilateral DA
HSDA-SP	HS combined with unilateral spared root DA
MG	medial gastrocnemius
MyHC	myosin heavy chain
NADH-TR	NADH-tetrazolium reductase
NOR, NORM	normal
OC	old chronic spinal, relative to old normal
PARA, PARAL	paralyzed
PIC	persistent inward current
P_o	peak tetanic force
P-P	peak-to-peak
PTP	post-tetanic potenitation
S	slow
SCI	spinal cord injury
SERCA	sarco/endoplasmic reticulum calcium ATPase
SI	spinal isolated, relative to old normal
SO	slow oxidative
SOL	soleus
SR	sarcoplasmic reticulum
TA	tibialis anterior
TT_{50}	force magnitude 50 ms after twitch onset
TTP	time-to-peak twitch
TTX	tetrodotoxin
YC	young chronic spinal, relative to young normal

CHAPTER 1: Introduction

1.1 MUSCLE ACTIVITY INCREASES WITH EXERCISE TRAINING AND ELECTRICAL STIMULATION

1.1.1 Muscles respond differently to changes in activity brought about by resistance training and endurance training

Luigi Galvani was the first to state conclusively that muscular contraction was the result of the flow of electricity from nerve to muscle, in his 1791 essay, "The Effect of Electricity on Muscular Motion" (Galvani and Giovanni 1953). Experimentally, intervening in this flow of electricity from nerve to muscle has become the most important method of investigating adult muscle properties, either acutely or chronically. One chronic approach to examining muscle plasticity is through exercise training. Exercise training is responsible for substantial endogenous increases in muscle activity. A heavy training regimen increases the daily number of nerve impulses delivered to the muscles performing the exercise, at higher rates and in longer blocks of activity than would be experienced during normal, lower-intensity activity. In the case of resistance training, this results in trained motor units that are capable of firing at higher frequencies, that generate more force, that generate force more quickly, that are recruited earlier in a maximal contraction, and that more often fire multiple impulses at the onset of contraction (Griffin and Cafarelli 2005; Van Cutsem et al. 1998).

A number of differences have been observed in the adaptive responses of skeletal muscles to resistance training and to endurance training. For example, endurance training results in adaptive decreases in muscle size and reduced muscle tetanic forces (Fitts and Holloszy 1977; Gallo et al. 2006), whereas resistance training results in muscle hypertrophy and increased muscle tetanic forces (Alway et al. 2005). Interestingly, howevever, some of the adaptive responses to endurance training are the same as those to resistance training, such as the increase in contractile speed that is induced by both forms of training (Alway et al. 2005; Fitts and Holloszy 1977). Surprisingly, although both types of training also result in increased proportions of *slower* myofiber types (type I and type IIA) and the associated myosin heavy chain isoforms, at the expense of the fastest myofiber types (type IID[X] in humans, cats, and horses and type IIB in rodents) and myosin heavy chain isoforms, endurance trained and resistance trained muscles both contract *more quickly* than untrained muscles, demonstrating that trained myofibers contract more effeciently than untrained myofibers (Baldwin and Haddad 2001; Pette 1998; Serrano et al. 2000). In rodents, training sometimes also increases the muscle content of type IId(x) myosin heavy chain, leading to even larger decreases in type IIb myosin heavy chain (Baldwin and Haddad 2001; Demirel et al. 1999).

1.1.2 The effects of various chronic electrical stimulation patterns reveal the neuromuscular bases for establishing muscle speed, force, and fatigue resistance

Long-term electrical stimulation of the muscle nerve or of the muscle at the motor point is another important experimental approach to understanding activity-dependent muscle

plasticity. The advantage of electrical stimulation is that it permits precise control of frequency, block duration (i.e., the total percentage of the day during which electrical impulses are delivered to the muscle regardless of frequency), and total daily number of neuromuscular impulses. Further, this can be done without interfering with endogenous neuromuscular activity if the stimulation is delivered at a low (i.e., tonic) frequency, although higher frequencies of applied stimulation may interfere with native patterns of neuromuscular activity or cause pain (Pette and Vrbova 1999).

Chronic electrical stimulation studies have demonstrated that the electrical impulses delivered by the motoneuron are not the extent of motoneurons' influence on the muscles they innervate, because motoneurons also provide trophic support to muscles (Davis and Kiernan 1981). However, it has been estimated that at least 60% of normal muscle properties are due to neuromuscular electrical impulses (Davis and Kiernan 1981), so changes in neuromuscular impulse patterns do result in very large changes in muscle phenotype (Gordon et al. 1997). With respect to the influence of neuromuscular impulses on whole muscle function, the effects of whole muscle nerve electrical stimulation are that: (1) muscle contractile speed is determined principally by the frequency of neuromuscular impulses; (2) muscle force production is inversely determined by the regularity of neuromuscular impulses; (3) muscle fatigue resistance is determined principally by the total daily number of neuromuscular impulses to a muscle (Gordon et al. 1997; Kernell et al. 1987a; Kernell et al. 1987b). That is, an increase in block duration at the same stimulation frequency results in an increase in fatigue resistance, or when the stimulation frequency is increased substantially a much smaller increase in block duration is required for the same increase in fatigue resistance (Gordon et al. 1997). Accordingly, the expression of muscle contractile proteins and of metabolic enzymes is also altered by electrical stimulation. For example, in primarily fast rabbit hindlimb muscles such as the tibialis anterior and the extensor digitorum longus, long-term (> 1 month) stimulation at 10 Hz and in block durations of 40-100% causes large increases in the content of slow type I myosin heavy chain at the expense of fast type IId(x) myosin heavy chain, and causes large increases in oxidative enzyme activities (Hämäläinen and Pette 1997; Simoneau et al. 1993). Similarly, in cat medial gastrocnemius muscles, long-term stimulation at 20 Hz and in a 50% block duration causes transformations of mATPase-identified muscle fibers from primarily fast (types FOG and FG) to completely slow (type SO), and causes a parallel transformation of the physiologically-classified motor units from primarily fast (types FR, FI and FF) to completely slow (type S; (Gordon et al. 1997). In other words, augmented neuromuscular activity significantly alters muscle structure and function. What happens when neuromuscular activity is reduced?

1.2 ELIMINATING AND REDUCING MUSCLE ACTIVITY WITH SPINAL ISOLATION AND SPINAL CORD TRANSECTION

1.2.1 Spinal isolation eliminates muscle activity almost completely

Spinal isolation is an experimental model of reduced muscle activity, in which muscles are paralyzed by completely transecting the spinal cord at two levels and by completely

bilaterally cutting the dorsal roots that enter the cord between these transections. Motoneuron cell bodies located between the transections are completely isolated from descending, afferent, and infraspinal (i.e., ascending from lower segments) inputs and thus their respective muscles, although innervated, experience pronounced reductions in neuromuscular activity, of at least 92% (Roy et al. 2006). The remaining activity is most likely the result of spontaneous firing by the paralyzed motoneurons (Harris RLW and Bennett DJ, unpublished observations). This model was originally introduced in 1943 by Sarah Tower, who demonstrated that muscles paralyzed by spinal isolation undergo substantial degeneration, including myofiber atrophy and disproportionate increases in connective tissue (Tower 1937). In fact, spinal isolation is the best model available so far for the assessment of chronic (> 6 weeks) muscle inactivity, without directly interrupting the innervation of muscles by their motoneurons. As a result, Sarah Tower's pioneering experiments have been followed-up extensively in order to elucidate the role of neuromuscular activity in defining the properties of muscles and their myofibers.

The results of spinal isolation experiments, conducted in the hindlimb muscles of both rats and cats, can be used to summarize the effects on skeletal muscle of a near-complete reduction in muscle activity. Briefly, up to 6 months of spinal isolation consistently results in: (1) whole muscle atrophy; (2) myofiber atrophy; (3) a transformation in the myofiber distribution from slower, more fatigue-resistant myofiber types (e.g., slow oxidative) to faster, more fatigable myofiber types (e.g., fast oxidative-glycolytic and fast glycolytic); (4) a transformation in the distribution of both myofibrillar (e.g., myosin heavy chain isoforms) and sarcoplasmic (e.g., sarco/endoplasmic reticulum calcium reuptake channels) proteins from slow isoforms to fast isoforms, and the emergence of developmental isoforms of some myofibrillar proteins; (5) a decrease in the oxidative metabolic capacity and an increase in the glycolytic metabolic capacity; (6) a decrease in peak tetanic forces; (7) an increase in muscle contractile speed; and (8) a loss of muscle fatigue resistance (Graham et al. 1992; Grossman et al. 1998; Jiang et al. 1991; Pierotti et al. 1991; Roy et al. 2000; Roy et al. 1992; Roy et al. 2002a; Roy et al. 2002b; Talmadge et al. 1996; Zhong et al. 2002).

While it is interesting to examine the effects on muscle physiology of completely eliminating neuromuscular activity, spinal isolation does not have any direct relevance to normal central nervous system injury conditions in mammals. The effects of spinal isolation are perhaps most useful as a background for understanding other diseases and experimental models in which muscle activity is altered, in particular, spinal cord transection. What are the differences between the effects of these two models?

1.2.2 Muscle properties are better preserved following spinal cord transection than following spinal isolation

Spinal isolation results in a reduction in muscle activity of *at least* 92% compared to normal (Roy et al. 2006). In contrast, spinal cord transection results in a reduction in muscle activity of *at most* 75% compared to normal (Alaimo et al. 1984). The difference in the extent to which these injury conditions reduce muscle activity is critical to their impact on muscle properties: although the results of these two forms of paralysis are

similar, the effects of spinal cord transection are generally not so severe. Specifically, whole muscle atrophy, myofiber atrophy, myofiber type transformations, myofibrillar and sarcoplasmic protein isoform transformations, changes in metabolic enzymes, decreases in peak tetanic forces, increases in muscle contractile speed, and losses of muscle fatigue resistance are all less marked following spinal cord transection than following spinal isolation (Baldwin et al. 1984; Jiang et al. 1990; Lovely et al. 1990; Roy and Acosta 1986; Roy et al. 1999; Roy et al. 1998; Talmadge et al. 2002; Talmadge et al. 1996; Talmadge et al. 1999, 1995). In fact, unlike spinal isolation, spinal cord injury does not result in the appearance of developmental myosin heavy chain isoforms in the paralyzed myofibers (Talmadge et al. 1996), the emergence of which indicates that paralyzed myofibers are regenerating (Kern et al. 2004). This suggests that muscle degeneration occurring due to spinal isolation is more severe than that occurring due to spinal cord transection, and possibly even that spinal isolation induces the repair of muscle tissue by invading satellite cells. Overall, the comparison between these two models demonstrates that although spinal cord injury and spinal cord transection have been described as conditions of muscle disuse (Dupont-Versteegden et al. 1998; Houle et al. 1999; Rochester et al. 1995a; Rochester et al. 1995b), they are instead examples of reduced muscle activity, the results of which are less severe than those of the near-complete neuromuscular silence observed after spinal isolation.

1.3 NORMAL MUSCLE PROPERTIES CAN BE PRESERVED OR RESTORED AFTER INJURY BY USING INTERVENTIONS THAT GENERATE MUSCLE ACTIVITY

What happens when paralysis that reduces neuromuscular activity, such as spinal cord transection or spinal isolation, is combined with an intervention that augments neuromuscular activity, such as training or electrical stimulation? In fact, this question has been investigated extensively. For example, passive cyclical stretch of the muscles paralyzed by spinal isolation fails to counteract the deleterious effects of muscle inactivity (Roy et al. 1992), but electrical stimulation of the paralyzed muscles, which results in the generation of static muscle force, does attenuate some of the deleterious effects, especially when the muscle is held in either an isometric or a lengthened position, positions that generate load on the myofibers (Roy et al. 2002a; Zhong et al. 2002). Interestingly, when passive cyclical stretch is applied after spinal cord transection, when reflex pathways are intact and the cyclical exercise thus induces some muscle activity and generates some resistance or loading, normal myofiber type proportions and myofiber sizes are partially restored (Dupont-Versteegden et al. 1998). These interventions emphasize that muscle structure and function are determined by electromechanical activity, and not by mechanical activity alone (or by electrical activity alone).

1.3.1 Exercise promotes recovery of paralyzed muscles in a muscle- and training-dependent manner

With particular reference to the changes that are observed in the contractile and myofiber phenotypes of muscles paralyzed by spinal cord transection in animals, various

interventions have been tested that demonstrate the benefits both of exercise training and of electrical stimulation. Exercise programs that emphasize body mass support and/or locomotor-like behaviour have proven particularly effective in promoting recovery of muscle contractile properties and myofiber properties following spinal cord transection. For example, in the primarily slow cat soleus (> 95% slow myofibers), post-transection training protocols that involve several months of daily standing (i.e., static body mass support) or several months of daily stepping on a treadmill (i.e., dynamic body mass support) promote substantial recovery of: muscle and myofiber size; muscle tetanic force; muscle contractile speed; muscle fatigue resistance; proportions of mATPase-classified myofibers; and myosin heavy chain protein isoform distributions (Roy et al. 1998). Similarly, in the primarily fast (> 67% fast myofibers) cat medial gastrocnemius, stand and step training promote recovery of: muscle size; muscle tetanic force; muscle fatigue resistance; myofiber proportions; and myosin heavy chain distributions (Roy et al. 1999). There is no change in contractile speed of the medial gastrocnemius with spinal cord transection, so no recovery was measured (Roy et al. 1999).

These summaries of the training effects for hindlimb extensors after spinal cord transection in the cat ignore the fact that different magnitudes of recovery for the various parameters measured are observed with stand and step training. In the soleus, which is generally considered a postural muscle, the degree of recovery is actually better with step (i.e., dynamic or locomotor) training than with stand (i.e., static or postural) training, even if these differences are not statistically significant (Roy et al. 1998). Moreover, following spinal cord transection soleus muscle contractile speed recovers toward normal levels with stand training but not with step training, while soleus myosin heavy chain isoform distributions recover toward normal proportions with step training but not with stand training (Roy et al. 1998). Similarly, in the medial gastrocnemius, stand training is substantially more effective in promoting recovery of muscle size and of muscle tetanic force, while step training is substantially more effective in promoting recovery of fatigue resistance, myofiber type proportions, and myosin heavy chain distributions (Roy et al. 1999). In fact, in the medial gastrocnemius after spinal cord transection fatigue resistance declines even further with stand training than with no training at all (Roy et al. 1999). These results suggest that a training paradigm that applies an appropriate combination of both dynamic or locomotor-like tasks and static or postural tasks might achieve the best overall results in the recovery of muscle structure and function after spinal cord injury.

1.3.2 Human muscles recover with exercise following long-term spinal cord injury

Training interventions also have been applied successfully in the clinical setting to promote substantial recovery both of muscle fatigue resistance and of myofiber type distributions in muscles paralyzed by spinal cord injuries in humans (Mohr et al. 1997; Stein et al. 1992). Consistent with the findings in animals models, training paradigms that compare dynamic and static exercise or that compare exercise programs providing levels of resistance to the paralyzed musculature reveal that these training differences yield variable results (Crameri et al. 2004; Hartkopp et al. 2003). Specifically, electrically stimulated unloaded dynamic cycling exercise and electrically stimulated isometric exercise against a static load both promote similar isometric force recovery in paralyzed

vastus lateralis muscles, but only static exercise results in a clear recovery of both myofiber type proportions and of myofiber sizes (Crameri et al. 2004). Similarly, electrically stimulated static resistance exercise in paralyzed wrist extensor muscles improves muscle fatigue resistance regardless of the load applied, but only larger loads assist in the recovery of muscle force generation (Hartkopp et al. 2003). As already mentioned above for passive cycling exercise after spinal cord transection or spinal isolation in animals, these findings emphasize that muscle and myofiber properties are determined by a combination of electrical and mechanical activity as opposed to only electrical or only mechanical activity.

In summary, following spinal cord transection in adult cats and following spinal cord injury in humans, the results of exercise and stimulation interventions demonstrate that training has variable effects depending both on the training paradigm used and on the particular muscle assessed after training. In other words, whether or not activity after training is considered successful in promoting muscle recovery is dependent upon the desired outcome. Moreover, also judging from the results of electrical stimulation studies, it appears likely that a detailed analysis of activity in a normal muscle or group of muscles must be performed in numerous individuals in order to determine what, on average, are the pattern of activity, the amount of activity, and the associated loading or forces routinely required during training over the long term in order to maintain or recover the best compromise among muscle force, speed, and fatigue resistance.

1.4 SPASTICITY MAY PROMOTE RECOVERY AFTER SPINAL CORD INJURY BY GENERATING ACTIVITY IN PARALYZED MUSCLES

Importantly, while training after spinal cord injury clearly assists in the maintenance or restoration of the properties of paralyzed muscles and their constituent myofibers, some paralyzed muscles demonstrate remarkably normal properties *without* training, even many years after injury. Specifically, in some long-term spinal cord injured individuals, the paralyzed vastus lateralis muscle contains near-normal proportions of type I myosin heavy chain, and this is associated with normal-like fatigue resistance and slow contractile properties (Gerrits et al. 2003). Similarly, there is a case report on a long-term spinal cord injured individual demonstrating nearly 100% type I myosin heavy chain in the paralyzed tibialis anterior muscle, a proportion even greater than that normally observed in unparalyzed muscles (~70%), and this unusual myofiber distribution is associated with slow contractile properties and a high resistance to fatigue (Hartkopp et al. 1999). It has been suggested that such unexpected adaptations in muscle properties after long-term spinal cord injury are associated with muscle activity due to spasticity (Hartkopp et al. 1999). Indeed, some recovery or preservation of muscle contractile properties is observed in spinal cord injured individuals with documented spasticity, and the degree of recovery or preservation is quantitatively well-correlated with the severity of the spasticity (Hidler et al. 2002; Thomas 1997; Thomas and Ross 1997; Zijdewind and Thomas 2001). What is spasticity after spinal cord injury, and why might it be associated with adaptations in muscle properties that resemble those to exercise and stimulation?

1.4.1 Spasticity after spinal cord injury in humans is characterized by velocity-dependent hypertonus, hyperreflexia, and involuntary spasms

Spasticity is a neuromuscular disorder that occurs as a result of spinal cord injury and several other diseases or traumas, including stroke (Satkunam 2003). Although these diseases and traumas result in spasticity symptoms that are similar in some respects (Satkunam 2003), the underlying mechanisms and the appropriate treatments are not identical (Faist et al. 1999). Spasticity due to spinal cord injury, or spinal spasticity, is the focus of this overview.

The most basic neuromuscular component of spinal spasticity is the α-motoneuron/intrafusal myofiber/Ia afferent circuit responsible for the generation of the monosynaptic stretch reflex. In this reflex, stretch of the muscle activates the muscle spindles, resulting in firing of the Ia afferents, which synapse directly with motoneurons; thus Ia afferent firing in turn activates these motoneurons, resulting in a muscle contraction that counteracts the stretch. Following spinal cord injury the hyperexcitability of this stretch reflex is largely responsible for the most often cited definition of spinal spasticity: "Spasticity is a motor disorder characterized by a velocity-dependent increase in tonic stretch reflexes (muscle tone) with exaggerated tendon jerks, resulting from hyperexcitability of the stretch reflex," (Lance 1980).

Recently, it has been suggested that the first part of the above definition is one of three major components of the spastic syndrome, namely, intrinsic tonic spasticity, which refers to the hyperexcitability of stretch reflexes in response to maintained or tonic stretch (Adams and Hicks 2005; Decq 2003). The velocity-dependence of spastic hypertonus is derived from the fact that the muscle spindles that sense muscle stretch are sensitive both to changes in the length of the muscle, and also to the rate at which muscle length changes. In other words a sustained, static stretch of a spastic muscle evokes a sustained, length-dependent reflex contraction, resulting in considerable muscle tone. Additionally, the faster a spastic muscle is stretched during passive dynamic manipulation of a paralyzed limb, the greater the magnitude of the velocity-dependent spastic hypertonia observed in response to this manipulation (Ashby and McCrea 1987; Kuhn and Macht 1948). Thus, hypertonus is observed in response to muscle stretch that is sustained, that is evoked slowly over periods of many seconds, or that is evoked as quickly as the muscle can be passively manipulated.

The second major component of the spastic syndrome, namely, intrinsic phasic spasticity, refers to hyperexcitability of stretch reflexes in response to phasic stimulation of muscle spindles (Adams and Hicks 2005; Decq 2003), for example, brief ankle extensor stretch reflexes in response to ballistic taps of the Achilles tendon. Clonus, a rapidly oscillating (≤ 10 Hz) muscle contraction most often observed as vibration about the ankle joint due to activity in the ankle extensor muscles (Ashby and McCrea 1987; Pierrot-Deseilligny and Burke 2005), is also a manifestation of intrinsic phasic spasticity resulting in part from repetetive activation of the stretch reflex (Adams and Hicks 2005; Wallace et al. 2005). In other words, both tonic and phasic intrinsic spasticity involve the length- and

velocity-dependent stretch reflex loop, and this reflex manifests differently in spasticity based upon the exact way in which the muscle or its tendons are stimulated.

The third major component of the spastic syndrome is extrinsic spasticity, which refers to hyperexcitability of reflexes that occur in response to perturbations external to the muscle itself. For example, in response to noxious stimuli of cutaneous, subcutaneous, and joint receptors, (as well as muscular mechanoreceptors that feedback via slowly-conducting, non-primary afferents), flexor reflex afferents mediate polysynaptic signals involved in flexion withdrawal, and this withdrawal is greatly exaggerated in spasticity (Kuhn and Macht 1948; Sandrini et al. 2005; Wu et al. 2006). Extrinsic spasticity, which is missing from the definition cited above, is the source of much continuing debate over the exact nature of spasticity: some investigators suggest that such hyperrexcitable flexor reflexes are not part of spasticity at all (Sheean 2002). However, for many years flexor spasms and reflexes have been as much a part of the clinical picture of the motor pathophysiology described after spinal cord injury as has the largely extensor-based intrinsic spasticity described above, even though extensor tone and reflexes predomintate (Kuhn and Macht 1948).

Hypertonus and hyperreflexia resulting from spasticity can have a variety of negative impacts on the quality of life of individuals living with spinal cord injury, including inhibition of residual motor behaviours such as locomotion, reaching, and grasping, and thus it is usually treated with one or a combination of physical or pharmacological therapies (Adams and Hicks 2005). However, as described above, spasticity may have some benefit for paralyzed muscles after spinal cord injury because, evidently, spasticity is capable of generating a great deal of muscle activity (Hidler et al. 2002; Thomas 1997; Thomas and Ross 1997; Zijdewind and Thomas 2001). What is the source of this activity?

1.4.2 The neurophysiological basis of spasticity involves altered motoneuronal excitability

Normally, motoneurons in the spinal cord receive facilitatory support from descending monoaminergic sources (Lee and Heckman 1999). These facilitatory inputs are particularly important in the activation of motoneuronal persistant inward currents (PICs) that mediate regenerative membrane potentials, called plateau potentials, and self-sustained firing (Harvey et al. 2006b). Evidently, such neuromodulatory inputs are lost following a complete spinal cord transection (Harvey et al. 2006b) and thus, acutely, there is a profound reduction in motoneuronal excitability below a complete spinal cord lesion (Bennett et al. 2001b). However, descending monoaminergic inputs also inhibit dorsal horn interneurons that are involved in polysynaptic reflex excitation of motoneurons (Jankowska et al. 2000) and these inhibitory inputs are also lost after injury. Thus acute complete spinal cord transection permits facilitation of motor output by eliminating the inhibition of polysynaptic reflexes, but transection also limits the ability of motoneurons to respond to such excitation by terminating some of their most prominent facilitatory inputs. The net effect is that, immediately after complete spinal cord injury, in addition to loss of voluntary control and sensation (i.e., paralysis) reflexes

are profoundly depressed and spasticity is not observed but instead takes weeks or months to appear, a condition called spinal shock (Bennett et al. 1999; Bennett et al. 2004; Kuhn and Macht 1948).

If descending inhibition of excitatory motor reflex pathways is eliminated but motoneuron excitability via PICs is preserved by lesioning *only* the descending pathways that carry monoaminergic inputs to the dorsal horn, spastic-like behaviour is observed acutely after injury (Heckman 1994). Moreover, by using conditioning nociceptive stimuli acutely after transection it is possible to generate sufficient background motoneuronal activity that reflex activity can actually be evoked, even when motoneuron excitability is depressed at this early stage of spinal shock (Bennett et al. 2004). This acute reflex excitability is mediated by long-lasting polysynaptic activity (Bennett et al. 2004), suggesting that it emerges due to the disinhibition of dorsal horn interneurons, as described above.

Importantly, it is now well-established that with time after complete sacral spinal cord transections in rats, sacrocaudal motoneurons become supersensitive to monoamines that are present in small amounts below the lesion, and thus PICs re-emerge and motoneuronal excitability returns (Harvey et al. 2006a, b; Li and Bennett 2003). It has been demonstrated that these sacrocaudal motoneuron PICs are responsible for the generation of the spastic reflexes observed in the segmental tail muscles of chronic sacral spinal rats (Bennett et al. 2001a; Bennett et al. 2004), and there is strong evidence that the same adaptive motoneuronal mechanisms (i.e., supersensitivity to monoamines leading to PIC and plateau potential generation) underlie the long-lasting spasms observed in human spasticity (Gorassini et al. 2004). Therefore, a key neurophysiological basis for the development of spasticity with time after spinal cord injury is a chronic change in motoneuronal supersensitivity to monoamines. This return of motoneuronal excitability ultimately leads to the generation of prolonged involuntary muscle activity (Bennett et al. 2004; Gorassini et al. 2004), and hence possibly to the preservation of muscle contractile properties and myofiber type distributions, despite paralysis (Gerrits et al. 2003; Hartkopp et al. 1999; Hidler et al. 2002; Thomas 1997; Thomas and Ross 1997; Zijdewind and Thomas 2001).

1.5 RESIDUAL MUSCLE ACTIVITY AFTER PARALYSIS HAS CLINICAL AND EXPERIMENTAL IMPLICATIONS

The possibility that spasticity generates considerable activity in muscles that are otherwise paralyzed raises an interesting question: what happens when a paralyzed muscle remains active? As stated above, paralysis is the loss of sensation and voluntary control, and this is the definition that will be used for the purposes of this thesis. A residual degree of motor and sensory function often follows partial spinal cord injury in humans, which is considered positive from a functional perspective, but spasticity can interfere with this function, which is considered undesirable from a functional perspective (Adams and Hicks 2005). If spasticity actually generates enough activity in paralyzed muscles to promote normal-like myofibers and contractile properties in those muscles but

it also interferes with the function of those muscles, then how should spasticity be treated? Obviously the therapy should be selected not only based upon the negative impact of spasticity on muscle function in individuals with spinal cord injuries (Adams and Hicks 2005) but also based upon the potential benefit of spasticity in assisting in the recovery of normal-like properties in long-term paralyzed muscles.

An associated issue is the question of how conflicting influences on muscle activity might interact in experimental models. An excellent example of this is in the long-term electrical stimulation studies described above. As mentioned, stimulation can be applied chronically without interfering in endogenous muscle activity or causing pain (Pette and Vrbova 1999). However, does the endogenous muscle activity affect the outcome of stimulation? Kernell and colleagues attempted to eliminate the possible effects of endogenous neuromuscular activity on stimulated hindlimb muscles in the cat by unilaterally hemisecting (HS) and deafferenting (DA) those hindlimbs, without damaging the ventral roots to those muscles and without damaging the descending or afferent inputs to the contralateral limbs (Kernell et al. 1987a; Kernell et al. 1987b). In other words, these cats had one hindlimb in which muscles were paralyzed, even though the efferent motoneuronal output to the muscles was intact, because the major descending and afferent inputs were eliminated ipsilaterally. These paralyzed muscles were stimulated via the muscle nerves to determine the chronic effects on muscles of specific electrical inputs. Interestingly, however, in this model the unstimulated paralyzed muscles, examined as controls, exhibited limited changes in contractile properties: their contractile force and speed were unaltered, but they became more fatigable (Kernell et al. 1987a; Kernell et al. 1987b). It is tempting to speculate that even though this model of hindlimb paralysis obviously reduced muscle activity substantially, resulting in reduced fatigue resistance, some residual activity promoted the mainenance of contractile force and speed.

1.6 OBJECTIVE AND HYPOTHESES

The goal of this thesis is to investigate myofibrillar and contractile properties in the tail muscles of adult chronic sacral spinal rats with spasticity and in the paralyzed hindlimb muscles of adult cats with HSDA injuries. These two models are explored in parallel because preliminary examinations of the paralyzed muscles in these animals suggested that their properties are surprisingly similar. Specifically, in spastic rat tail muscles after long-term spinal cord transection, muscle twitches are longer and larger than in normal muscles. Further, the myofiber type proportions classified according to contractile protein expression are preserved compared to in normal tail muscles, and all myofiber types recover completely or partially from atrophy that is observed early after injury. Similarly, in cat hindlimb muscles after long-term HSDA, contractile speed, tetanic force, and myosin heavy chain contractile protein distributions are all preserved compared to in normal muscles. However, in both models, the paralyzed muscles become substantially more fatigable. By comparison, spinal isolation, described above, leads to a near-complete elimination of muscle activity, resulting in considerable atrophy increases in contractile speed, and slow-to-fast myofiber type transformations. Thus it seems

reasonable to speculate that, as observed in adult chronic sacral spinal rats with spasticity and in adult cats with HSDA injuries, if contractile properties and myofiber types are normal or slower than normal, there must some muscle activity present.

Based upon these preliminary results, it was hypothesized that following complete sacral spinal cord transection in adult rats or following complete unilateral lumbar HSDA in adult cats, the properies of the long-term paralyzed muscles would provide evidence that some muscle acitivity remains or recovers following these interventions. Specifically, it was anticipated that in paralyzed muscles compared to in control muscles, single motor unit and/or whole muscle contractile properties, myofiber histochemistry, and metabolic enzyme activities would demonstrate a recovery from size and strength atrophy and a recovery from slow-to-fast transformations in the contractile phenotype, but a loss of fatigue resistance and a transformation to a more glycolytic metabolism.

The purpose of the subsequent chapters is to report studies that test these hypotheses. In the experiments described, the tail muscles of chronic spinal rats with spasticity were assessed using analyses of contractile properties, myofiber histochemistry, and quantitative EMG measurements of muscle activity. These spastic tail muscles were compared to those of normal adult rats and to those of adult rats with sacrocaudal spinal isolation. In addition, medial gastrocnemius muscles of cats paralyzed by HSDA were assessed using physiological characterization of both the whole muscle and individual motor units, myofiber histochemistry, and biochemical measurements of enzyme activities. These paralyzed medial gastronemius muscles were compared to the unparalyzed medial gastrocnemius muscles of normal control cats.

1.8 REFERENCES FOR CHAPTER 1

Adams MM, and Hicks AL. Spasticity after spinal cord injury. *Spinal Cord* 43: 577-586, 2005.

Alaimo MA, Smith JL, Roy RR, and Edgerton VR. EMG activity of slow and fast ankle extensors following spinal cord transection. *J Appl Physiol* 56: 1608-1613, 1984.

Alway SE, Siu PM, Murlasits Z, and Butler DC. Muscle hypertrophy models: applications for research on aging. *Can J Appl Physiol* 30: 591-624, 2005.

Ashby P, and McCrea DA. Neurophysiology of spinal spasticity. In: *Handbook of the Spinal Cord*, edited by Davidoff RA. New York: Marcel Dekker, Inc., 1987, p. 119-143.

Baldwin KM, and Haddad F. Effects of different activity and inactivity paradigms on myosin heavy chain gene expression in striated muscle. *J Appl Physiol* 90: 345-357, 2001.

Baldwin KM, Roy RR, Sacks RD, Blanco C, and Edgerton VR. Relative independence of metabolic enzymes and neuromuscular activity. *J Appl Physiol* 56: 1602-1607, 1984.

Bennett DJ, Gorassini M, Fouad K, Sanelli L, Han Y, and Cheng J. Spasticity in rats with sacral spinal cord injury. *J Neurotrauma* 16: 69-84, 1999.

Bennett DJ, Li Y, Harvey PJ, and Gorassini M. Evidence for plateau potentials in tail motoneurons of awake chronic spinal rats with spasticity. *J Neurophysiol* 86: 1972-1982, 2001a.

Bennett DJ, Li Y, and Siu M. Plateau potentials in sacrocaudal motoneurons of chronic spinal rats, recorded in vitro. *J Neurophysiol* 86: 1955-1971, 2001b.

Bennett DJ, Sanelli L, Cooke CL, Harvey PJ, and Gorassini MA. Spastic long-lasting reflexes in the awake rat after sacral spinal cord injury. *J Neurophysiol* 91: 2247-2258, 2004.

Crameri RM, Cooper P, Sinclair PJ, Bryant G, and Weston A. Effect of load during electrical stimulation training in spinal cord injury. *Muscle Nerve* 29: 104-111, 2004.

Davis HL, and Kiernan JA. Effect of nerve extract of atrophy of denervated or immobilized muscles. *Exp Neurol* 72: 582-591, 1981.

Decq P. Pathophysiology of spasticity. *Neuro-Chirurgie* 49: 163-184, 2003.

Demirel HA, Powers SK, Naito H, Hughes M, and Coombes JS. Exercise-induced alterations in skeletal muscle myosin heavy chain phenotype: dose-response relationship. *J Appl Physiol* 86: 1002-1008, 1999.

Dupont-Versteegden EE, Houle JD, Gurley CM, and Peterson CA. Early changes in muscle fiber size and gene expression in response to spinal cord transection and exercise. *Am J Physiol Cell Physiol* 275: C1124-1133, 1998.

Faist M, Ertel M, Berger W, and Dietz V. Impaired modulation of quadriceps tendon jerk reflex during spastic gait: differences between spinal and cerebral lesions. *Brain* 122 (Pt 3): 567-579, 1999.

Fitts RH, and Holloszy JO. Contractile properties of rat soleus muscle: effects of training and fatique. *Am J Physiol* 233: C86-91, 1977.

Gallo M, Gordon T, Syrotuik D, Shu Y, Tyreman N, MacLean I, Kenwell Z, and Putman CT. Effects of long-term creatine feeding and running on isometric functional measures and myosin heavy chain content of rat skeletal muscles. *Pflugers Arch* 452: 744-755, 2006.

Galvani L, and Giovanni A. *Commentary on the effect of electricity on muscular motion; a translation of Luigi Galvani's De viribus electricitatis in motu musculari commentarius, by Robert Montraville Green.* Cambridge, Massachusetts: Elizabeth Licht, 1953, p. 97.

Gerrits HL, Hopman MT, Offringa C, Engelen BG, Sargeant AJ, Jones DA, and Haan A. Variability in fibre properties in paralysed human quadriceps muscles and effects of training. *Pflügers Arch* 445: 734-740, 2003.

Gorassini MA, Knash ME, Harvey PJ, Bennett DJ, and Yang JF. Role of motoneurons in the generation of muscle spasms after spinal cord injury. *Brain* 127: 2247-2258, 2004.

Gordon T, Tyreman N, Rafuse VF, and Munson JB. Fast-to-slow conversion following chronic low-frequency activation of medial gastrocnemius muscle in cats. I. Muscle and motor unit properties. *J Neurophysiol* 77: 2585-2604, 1997.

Graham SC, Roy RR, Navarro C, Jiang B, Pierotti D, Bodine-Fowler S, and Edgerton VR. Enzyme and size profiles in chronically inactive cat soleus muscle fibers. *Muscle Nerve* 15: 27-36, 1992.

Griffin L, and Cafarelli E. Resistance training: cortical, spinal, and motor unit adaptations. *Can J Appl Physiol* 30: 328-340, 2005.

Grossman EJ, Roy RR, Talmadge RJ, Zhong H, and Edgerton VR. Effects of inactivity on myosin heavy chain composition and size of rat soleus fibers. *Muscle Nerve* 21: 375-389, 1998.

Hämäläinen N, and Pette D. Coordinated fast-to-slow transitions of myosin and SERCA isoforms in chronically stimulated muscles of euthyroid and hyperthyroid rabbits. *J Muscle Res Cell Motil* 18: 545-554, 1997.

Hartkopp A, Andersen JL, Harridge SD, Crone C, Gruschy-Knudsen T, Kjaer M, Masao M, Ratkevicius A, Quistorff B, Zhou S, and Biering-Sorensen F. High expression of MHC I in the tibialis anterior muscle of a paraplegic patient. *Muscle Nerve* 22: 1731-1737, 1999.

Hartkopp A, Harridge SD, Mizuno M, Ratkevicius A, Quistorff B, Kjaer M, and Biering-Sorensen F. Effect of training on contractile and metabolic properties of wrist extensors in spinal cord-injured individuals. *Muscle Nerve* 27: 72-80, 2003.

Harvey PJ, Li X, Li Y, and Bennett DJ. 5-HT2 receptor activation facilitates a persistent sodium current and repetitive firing in spinal motoneurons of rats with and without chronic spinal cord injury. *J Neurophysiol* 96: 1158-1170, 2006a.

Harvey PJ, Li X, Li Y, and Bennett DJ. Endogenous monoamine receptor activation is essential for enabling persistent sodium currents and repetitive firing in rat spinal motoneurons. *J Neurophysiol* 96: 1171-1186, 2006b.

Heckman CJ. Alterations in synaptic input to motoneurons during partial spinal cord injury. *Med Sci Sports Exerc* 26: 1480-1490, 1994.

Hidler JM, Harvey RL, and Rymer WZ. Frequency response characteristics of ankle plantar flexors in humans following spinal cord injury: relation to degree of spasticity. *Ann Biomed Eng* 30: 969-981, 2002.

Houle JD, Morris K, Skinner RD, Garcia-Rill E, and Peterson CA. Effects of fetal spinal cord tissue transplants and cycling exercise on the soleus muscle in spinalized rats. *Muscle Nerve* 22: 846-856, 1999.

Jankowska E, Hammar I, Chojnicka B, and Heden CH. Effects of monoamines on interneurons in four spinal reflex pathways from group I and/or group II muscle afferents. *The European journal of neuroscience* 12: 701-714, 2000.

Jiang B, Roy RR, and Edgerton VR. Enzymatic plasticity of medial gastrocnemius fibers in the adult chronic spinal cat. *Am J Physiol* 259: C507-514, 1990.

Jiang BA, Roy RR, Navarro C, Nguyen Q, Pierotti D, and Edgerton VR. Enzymatic responses of cat medial gastrocnemius fibers to chronic inactivity. *J Appl Physiol* 70: 231-239, 1991.

Kern H, Boncompagni S, Rossini K, Mayr W, Fano G, Zanin ME, Podhorska-Okolow M, Protasi F, and Carraro U. Long-term denervation in humans causes degeneration of both contractile and excitation-contraction coupling apparatus, which is reversible by functional electrical stimulation (FES): a role for myofiber regeneration? *J Neuropathol Exp Neurol* 63: 919-931, 2004.

Kernell D, Donselaar Y, and Eerbeek O. Effects of physiological amounts of high- and low-rate chronic stimulation on fast-twitch muscle of the cat hindlimb. II. Endurance-related properties. *J Neurophysiol* 58: 614-627, 1987a.

Kernell D, Eerbeek O, Verhey BA, and Donselaar Y. Effects of physiological amounts of high- and low-rate chronic stimulation on fast-twitch muscle of the cat hindlimb. I. Speed- and force-related properties. *J Neurophysiol* 58: 598-613, 1987b.

Kuhn RA, and Macht MB. Some manifestations of reflex activity in spinal man with particular reference to the occurrence of extensor spasm. *Bull Johns Hopkins Hosp* 84: 43-75, 1948.

Lance JW. The control of muscle tone, reflexes, and movement: Robert Wartenberg Lecture. *Neurology* 30: 1303-1313, 1980.

Lee RH, and Heckman CJ. Enhancement of bistability in spinal motoneurons in vivo by the noradrenergic alpha1 agonist methoxamine. *J Neurophysiol* 81: 2164-2174, 1999.

Li Y, and Bennett DJ. Persistent sodium and calcium currents cause plateau potentials in motoneurons of chronic spinal rats. *J Neurophysiol* 90: 857-869, 2003.

Lovely RG, Gregor RJ, Roy RR, and Edgerton VR. Weight-bearing hindlimb stepping in treadmill-exercised adult spinal cats. *Brain Res* 514: 206-218, 1990.

Mohr T, Andersen JL, Biering-Sorensen F, Galbo H, Bangsbo J, Wagner A, and Kjaer M. Long-term adaptation to electrically induced cycle training in severe spinal cord injured individuals. *Spinal Cord* 35: 1-16, 1997.

Pette D. Training effects on the contractile apparatus. *Acta Physiol Scand* 162: 367-376, 1998.

Pette D, and Vrbova G. What does chronic electrical stimulation teach us about muscle plasticity? *Muscle Nerve* 22: 666-677, 1999.

Pierotti DJ, Roy RR, Bodine-Fowler SC, Hodgson JA, and Edgerton VR. Mechanical and morphological properties of chronically inactive cat tibialis anterior motor units. *J Physiol* 444: 175-192, 1991.

Pierrot-Deseilligny E, and Burke D. The pathophysiology of spasticity and parkinsonian rigidity. In: *The Circuitry of the Human Spinal Cord: Its Role in Motor Control and Movement Disorders*. Cambridge: Cambridge University Press, 2005, p. 556-599.

Rochester L, Barron MJ, Chandler CS, Sutton RA, Miller S, and Johnson MA. Influence of electrical stimulation of the tibialis anterior muscle in paraplegic subjects. 2. Morphological and histochemical properties. *Paraplegia* 33: 514-522, 1995a.

Rochester L, Chandler CS, Johnson MA, Sutton RA, and Miller S. Influence of electrical stimulation of the tibialis anterior muscle in paraplegic subjects. 1. Contractile properties. *Paraplegia* 33: 437-449, 1995b.

Roy RR, and Acosta L, Jr. Fiber type and fiber size changes in selected thigh muscles six months after low thoracic spinal cord transection in adult cats: exercise effects. *Exp Neurol* 92: 675-685, 1986.

Roy RR, Kim JA, Grossman EJ, Bekmezian A, Talmadge RJ, Zhong H, and Edgerton VR. Persistence of myosin heavy chain-based fiber types in innervated but silenced rat fast muscle. *Muscle Nerve* 23: 735-747, 2000.

Roy RR, Pierotti DJ, Flores V, Rudolph W, and Edgerton VR. Fibre size and type adaptations to spinal isolation and cyclical passive stretch in cat hindlimb. *J Anat* 180 (Pt 3): 491-499, 1992.

Roy RR, Talmadge RJ, Hodgson JA, Oishi Y, Baldwin KM, and Edgerton VR. Differential response of fast hindlimb extensor and flexor muscles to exercise in adult spinalized cats. *Muscle Nerve* 22: 230-241, 1999.

Roy RR, Talmadge RJ, Hodgson JA, Zhong H, Baldwin KM, and Edgerton VR. Training effects on soleus of cats spinal cord transected (T12-13) as adults. *Muscle Nerve* 21: 63-71, 1998.

Roy RR, Zhong H, Hodgson JA, Grossman EJ, Siengthai B, Talmadge RJ, and Edgerton VR. Influences of electromechanical events in defining skeletal muscle properties. *Muscle Nerve* 26: 238-251, 2002a.

Roy RR, Zhong H, Khalili N, Kim SJ, Higuchi N, Monti RJ, Grossman E, Hodgson JA, and Edgerton VR. Is spinal cord isolation a good model of muscle disuse? *Muscle Nerve* 2006.

Roy RR, Zhong H, Monti RJ, Vallance KA, and Edgerton VR. Mechanical properties of the electrically silent adult rat soleus muscle. *Muscle Nerve* 26: 404-412, 2002b.

Sandrini G, Serrao M, Rossi P, Romaniello A, Cruccu G, and Willer JC. The lower limb flexion reflex in humans. *Progress in neurobiology* 77: 353-395, 2005.

Satkunam LE. Rehabilitation medicine: 3. Management of adult spasticity. *CMAJ* 169: 1173-1179, 2003.

Serrano AL, Quiroz-Rothe E, and Rivero JL. Early and long-term changes of equine skeletal muscle in response to endurance training and detraining. *Pflugers Arch* 441: 263-274, 2000.

Sheean G. The pathophysiology of spasticity. *Eur J Neurol* 9 Suppl 1: 3-9; dicussion 53-61, 2002.

Simoneau JA, Kaufmann M, and Pette D. Asynchronous increases in oxidative capacity and resistance to fatigue of electrostimulated muscles of rat and rabbit. *J Physiol* 460: 573-580, 1993.

Stein RB, Gordon T, Jefferson J, Sharfenberger A, Yang JF, de Zepetnek JT, and Belanger M. Optimal stimulation of paralyzed muscle after human spinal cord injury. *J Appl Physiol* 72: 1393-1400, 1992.

Talmadge RJ, Roy RR, Caiozzo VJ, and Edgerton VR. Mechanical properties of rat soleus after long-term spinal cord transection. *J Appl Physiol* 93: 1487-1497, 2002.

Talmadge RJ, Roy RR, and Edgerton VR. Myosin heavy chain profile of cat soleus following chronic reduced activity or inactivity. *Muscle Nerve* 19: 980-988, 1996.

Talmadge RJ, Roy RR, and Edgerton VR. Persistence of hybrid fibers in rat soleus after spinal cord transection. *Anat Rec* 255: 188-201, 1999.

Talmadge RJ, Roy RR, and Edgerton VR. Prominence of myosin heavy chain hybrid fibers in soleus muscle of spinal cord-transected rats. *J Appl Physiol* 78: 1256-1265, 1995.

Thomas CK. Contractile properties of human thenar muscles paralyzed by spinal cord injury. *Muscle Nerve* 20: 788-799, 1997.

Thomas CK, and Ross BH. Distinct patterns of motor unit behavior during muscle spasms in spinal cord injured subjects. *J Neurophysiol* 77: 2847-2850, 1997.

Tower SS. Function and structure in the chronically isolated lumbo-sacral spinal cord of the dog. *J Comp Neurol* 67: 109-131, 1937.

Van Cutsem M, Duchateau J, and Hainaut K. Changes in single motor unit behaviour contribute to the increase in contraction speed after dynamic training in humans. *J Physiol* 513 (Pt 1): 295-305, 1998.

Wallace DM, Ross BH, and Thomas CK. Motor unit behavior during clonus. *J Appl Physiol* 99: 2166-2172, 2005.

Wu M, Hornby TG, Kahn JH, and Schmit BD. Flexor reflex responses triggered by imposed knee extension in chronic human spinal cord injury. *Exp Brain Res* 168: 566-576, 2006.

Zhong H, Roy RR, Hodgson JA, Talmadge RJ, Grossman EJ, and Edgerton VR. Activity-independent neural influences on cat soleus motor unit phenotypes. *Muscle Nerve* 26: 252-264, 2002.

Zijdewind I, and Thomas CK. Spontaneous motor unit behavior in human thenar muscles after spinal cord injury. *Muscle Nerve* 24: 952-962, 2001.

CHAPTER 2: Tail muscles become slow but fatigable in chronic sacral spinal rats with spasticity[1]

2.1 INTRODUCTION

Spinal cord injury has long been recognized to reduce the level of neuromuscular activity in skeletal muscles innervated below the level of the lesion and thus alter their physiological and histological properties (Shields 2002; Talmadge et al. 1995). Such a decrease in neuromuscular activity typically results in atrophy of skeletal muscles and slow-to-fast transformation in myosin heavy chain isoform expression (Burnham et al. 1997; Lieber et al. 1986a; Talmadge et al. 1995). These changes render muscles smaller, faster, weaker, and more fatigable (Lieber et al. 1986b; Talmadge et al. 2002). These effects occur in all hindlimb muscles but are somewhat larger in predominantly slow muscles such as the soleus (Davey et al. 1981; Lieber et al. 1986a; Lieber et al. 1986b). Importantly, interventions such as functional electrical stimulation and exercise, which restore normal-like activity levels, have been found to minimize (counteract) such changes or restore muscle properties to normal (Hartkopp et al. 2003; Kernell et al. 1987a; Kernell et al. 1987b; Rochester et al. 1995; Roy et al. 1999; Roy et al. 1998).

In humans and a few animal models, spinal cord injury results in a spasticity syndrome that includes hyperreflexia, hypertonus, and muscle spasms (Bennett et al. 2004; Fujimori et al. 1968; Heckman 1994; Kuhn and Macht 1948; Lance and Burke 1974; Ritz et al. 1992; Taylor et al. 1997). This spastic neuromuscular activity after spinal cord injury should, in principle, result in activity-dependent modification of muscle contractile properties (slowing and improved resistance to fatigue), just like exercise training or electrical stimulation does, as described above. However, contractile properties have mainly been studied in animal models of chronic spinal cord injury where no clear spasticity develops (Davey et al. 1981; Roy et al. 1999; Roy et al. 1998) or where spasticity in the muscle studied is not reported in detail (Lieber 2002; Lieber et al. 1986b; Mayer et al. 1984). Thus, an important question that remains is how spastic neuromuscular activity influences the properties of muscles innervated below the level of a spinal cord lesion.

The segmental tail muscles of adult rats develop a clear spasticity syndrome, with pronounced spasms, beginning 2 weeks after a complete transection at the sacral level (Bennett et al. 2004). This tail spasticity resembles that observed in human individuals with long-term spinal cord injury (Bennett et al. 1999; Bennett et al. 2004) and can be detected in segmental tail motor units of awake chronic spinal rats in the form of prolonged muscle spasms that last many seconds, and hypertonus associated with motor unit firing that lasts from minutes to hours (Bennett et al. 2001). Recently, we have performed 24-hour intramuscular EMG recordings revealing a dramatic reduction in muscle activity with acute injury compared to normal, and a recovery to approximately

---

[1] A version of this chapter has been published. Harris RLW, Bobet J, Sanelli L, and Bennett DJ. *J Neurophysiol* 95: 1124-1133, 2006.

normal activity levels due to spasms (active whenever the animal moves or tail contact is made) after chronic injury with spasticity (unpublished data). Thus, in this study, we examined the contractile properties of whole segmental tail muscles *in vivo* in the same chronic sacral spinal cord injured rats used previously to characterize reflex behavior and the time course of the development of spasticity (Bennett et al. 2004), and in uninjured control rats. We hypothesized that the overall muscle contractile speed and fatigability should decrease, or at least be preserved in spastic muscles, compared to normal, in support of the idea that pronounced spastic muscle activity can counter the classic effects of reduced activity due to paralysis following SCI (conversion to more fatigable, faster properties), described above (Shields 2002; Talmadge et al. 1995). Parts of this work have previously been reported in abstract form (Stephens et al. 1999).

2.2 MATERIALS AND METHODS

2.2.1 Spinal cord transection

A complete spinal cord transection was made at the S_2 sacral level in female Sprague-Dawley rats at approximately 2 months of age (adult rats), under sodium pentobarbital anesthesia (58 mg/kg body mass). These rats were drawn from a population of rats used in an earlier study (Bennett et al. 2004) and within 2-3 months, as previously documented, dramatic spasticity developed in the tail muscles and continued indefinitely (mean spasticity rating = 4/5; see Bennett et al. 1999, 2004 for details of the chronic spinal cord transection and spasticity assessment). At approximately 8 months post-injury (10.0 months mean age, n = 5), the contractile properties of muscles from chronic spinal rats with spasticity were studied and compared to those of muscles from age-matched control rats (9.7 months mean age, old normal rats, n = 5) and from younger control rats close to the age at which the transection was made (3.0 months mean age, young normal rats, n = 8; see Table 2-1). The latter group was used to control for the possibility that the normal changes in muscle properties with age may be arrested by spinal cord injury (Talmadge et al. 1995). However, there was no reason to expect, *a priori*, that a large age effect would be observed between animals at the transection age and normal animals at the final age of the chronic spinal rats, since ageing studies have revealed few differences in muscle contractile properties between adult animals of these ages (Ansved and Larsson 1989). All experimental procedures were carried out according to guidelines of the Canadian Council for Animal Care and with the approval of the University of Alberta Animal Welfare and Policy Committee.

2.2.2 Tail muscle and nerve preparation for recording

For recording muscle properties, chronic spinal rats with spasticity and young and old normal rats were anesthetized with 58 mg/kg sodium pentobarbital, the dose being topped up as required. A longitudinal incision approximately 8 cm long was made in the skin on the left ventrolateral side of the tail, from the fourteenth caudal vertebra (Ca14) to the base of the tail near the origin of the caudal nerve trunk supplying the muscle. The 14th ventrolateral segmental muscle was exposed, and the fascia covering the muscle was cleared, taking care not to damage the dorsolateral vein. The distal end of the muscle was

Table 2-1

Experimental (chronic spinal rats) and control (young and old normal rats) animals used in assessing segmental tail muscles in chronic spinal cord-injured rats.

Group	n	Age (months)	Mass (g)	Wet tail muscle mass (mg)	Tail muscle-to-body mass ratio (mg/kg)
young normal rats	8	3.0 ± 0.6	299 ± 21	13.7 ± 2.4	45.6 ± 8.5
old normal rats	5	9.7 ± 1.1 †	386 ± 36 †	17.6 ± 2.3 †	45.9 ± 11.5
chronic spinal rats	5	10.0 ± 1.7 †	415 ± 74 †	13.4 ± 1.9 *	33.2 ± 7.7 *†

A * indicates significant difference from old normal rats, and a † indicates significant difference from young normal rats ($P < 0.05$).

gently separated from the underlying bone and connective tissue with fine forceps. 3-0 surgical silk was threaded under the muscle and securely knotted around the tendon at the muscle's distal tip. To ensure that the suture did not slip, the knot was also glued (RP 1500 [super glue]; Adhesive Systems, Frankfort IL). Then, the muscle and tendon were cut completely from the bone at that end. The 3-0 suture was connected at its loose end to a combination muscle puller/force transducer (Cambridge Technologies model 300B servomotor). At the base of the tail, the nerve supplying the Ca14 segmental muscle was freed for 3-5 cm. The entire tail, including the exposed nerve and muscle, was bathed in mineral oil with the skin flaps around the incision pinned back to a silicone epoxy base at the bottom of the bath, and maintained at 35°C with radiant heat. The nerve was placed across the two leads of a bipolar stimulating electrode connected to a variable rate and voltage stimulator (Grass Instruments SD10), and the nerve was crushed with forceps 2 mm rostral to the electrode. The stimulation intensity was usually set supramaximal to a full muscle twitch, unless otherwise stated in the RESULTS.

2.2.3 Contractions

Initially, the muscle was lengthened slowly during repeated maximal twitch contractions until maximal isometric twitch force was produced, and contractile properties were recorded with the muscle set at this optimal length. Any force present at rest at this length was assumed to be passive and was subtracted from all subsequent trials. Force was sampled at 1000 Hz using a digital data acquisition system (Axoscope; Axon Instruments, Union City CA). Evaluation of muscle contractile properties was performed with a broad range of contractions including single supramaximal twitches, tetani evoked by two-second-long supramaximal stimulus trains at 200 Hz, twitches before and after a brief fused tetanus (200 Hz), and unfused and fused tetani at stimulation frequencies of 10 Hz to 200 Hz. Additionally, we inferred motor unit twitch responses using discrete, stepwise increments in stimulus intensity, as detailed in the RESULTS. To assess muscle fatigability, the muscle was stimulated supramaximally at 40 Hz for 300 ms once per second for 100 s (Burke et al. 1973). The fatigue index was then calculated as the ratio of the peak force in the 100^{th} second to the peak force in the 1^{st} second, where both these values were measured relative to the baseline force prior to the 1^{st} contraction.

2.2.4 Analyses

Analyses of contractions were performed with Clampfit (Axon Instruments, Union City CA), SigmaPlot (SPSS, Chicago IL), Excel (Microsoft, Redwood CA), and custom programs prepared with MATLAB (MathWorks, Natick MA). All data are reported as group means and standard deviations. A Student's *t*-test was used to determine statistical significance at the 95% confidence level ($P < 0.05$).

2.3 RESULTS

2.3.1 Body and muscle masses of normal and chronic spinal rats.

Both chronic spinal rats and age-matched old normal rats had significantly greater total body mass than did young normal rats (Table 2-1). The wet mass of the tail muscles from chronic spinal rats was significantly less than old normal rats, but not different from young normal rats (Table 2-1). Tail muscle mass was not significantly different between young and old normal rats when normalized to body mass (muscle-to-body mass ratios), but chronic spinal rats had muscle-to-body mass ratios that were significantly lower than in young and old normal rats (27.7% less than old normal rats; Table 2-1). As differences in body size are accounted for in this ratio, the change in relative mass reflects considerable atrophy of the tail muscles after injury.

2.3.2 Tail muscles of chronic spinal rats have slower and larger twitches than tail muscles of normal rats

The tail muscle twitch force generated during a supramaximal electrical stimulation of the nerve is shown for a typical old normal rat with dashed lines in Figures 1A and B. Young normal rats and old normal rats were not significantly different in either time to peak twitch (Figure 2-1C) or mean half-rise time (Figure 2-1D). By contrast, in chronic spinal rats, supramaximal nerve stimulation evoked twitches that were substantially prolonged relative to those in old normal rats (Figure 2-1A, B, solid lines). That is, the time to peak twitch in chronic spinal rats was significantly longer than in young and old normal rats (48.9% larger than old normal rats; Figure 2-1C), as was the half-rise time (150.0% larger than old normal rats; Figure 2-1D).

Young normal rats had, on average, 32.7% lower twitch force than old normal rats (significantly lower peak twitch; Figure 2-1E), as expected for a much smaller muscle (Table 2-1). However, the twitch force normalized to the muscle mass was not significantly different between young and old normal rats (Figure 2-1F). Interestingly, the absolute peak twitch force was significantly larger in spastic muscles than in normal muscles (85.2% and 39.5% greater, respectively, than young and old normal rats; Figure 2-1E). Further, twitch force normalized to muscle mass was almost doubled in spastic muscles from chronic spinal rats compared to muscles from young normal rats (88.0% increase, significant difference) and old normal rats (81.1% increase, significant difference; Figure 2-1F). Thus, spastic muscles contracted more slowly and generated more force in a twitch.

2.3.3 Motor unit twitches were enhanced in chronic spinal rats

Discrete, stepwise increases in stimulus intensity elicited large, discrete muscle twitch force increments (e.g., from "a" to "b" in Figure 2-2A and B) that were the result of the recruitment of new units. Thus, by subtracting the means of successive, discrete twitch levels as the force increased, it was possible to infer the twitches of individual motor units (Tam et al. 2001). No doubt some of these subtractions may have contained multiple motor unit twitches, but given that these muscles have 12 or fewer motor units

Figure 2-1

Twitch properties of the 14th ventrolateral segmental tail muscle of old normal rats and of rats with spasticity after chronic sacral spinal cord injury, in response to supramaximal stimulation pulses. Representative twitches from normal (---) and chronic spinal (—) animals show that peak twitch force is much greater in chronic spinal animals (A). When these twitches are normalized to peak twitch force, it is clear that contraction and relaxation are both prolonged in spastic tail muscles from chronic spinal animals (B), and not just larger. Time to peak twitch (C) is the time required to achieve peak twitch force beginning at the onset of force production. The twitch half-rise time (D) is the time required to achieve half of peak force (see 0.5 on vertical scale of B) beginning at the onset of force production. Twitch force (E) is taken as the absolute maximal twitch force, and force : mass ratio (F) is the ratio of twitch force to muscle mass. In this and subsequent figures, white bars are normal animals and black bars are chronic spinals. A * represents significant difference from old normal rats and a † represents significant difference from young normal rats in this and subsequent figures ($P < 0.05$). Values shown are means ± standard deviations.

Figure 2-1

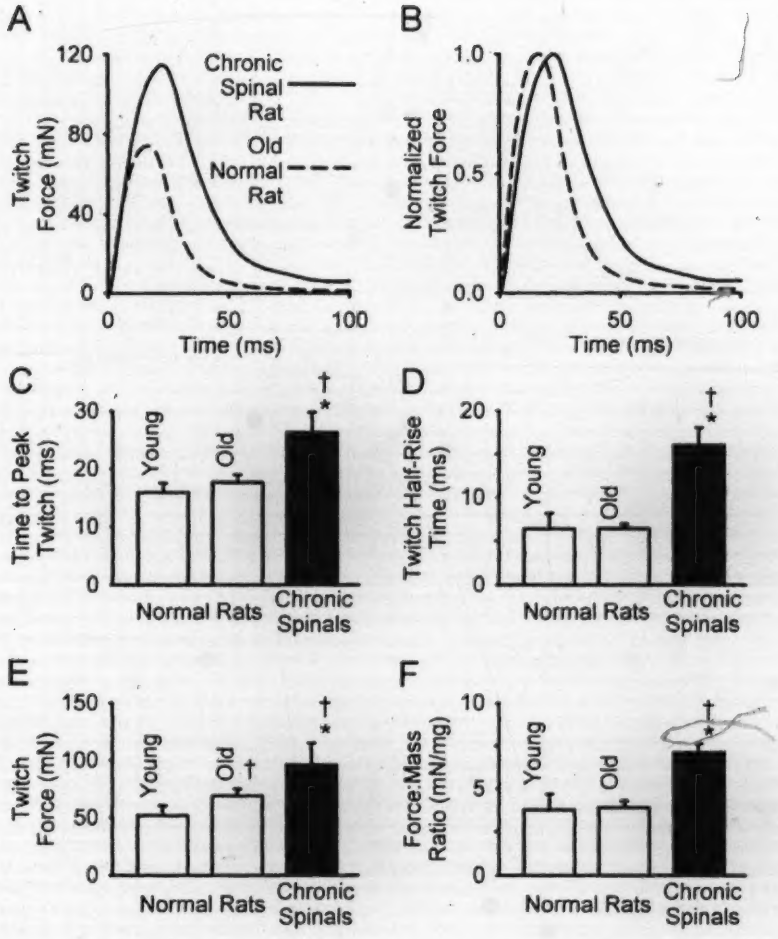
A
120
80
40
0
Twitch Force (mN)
Chronic Spinal Rat
Old Normal Rat
0
50
100
Time (ms)
B
1.0
0.5
0.0
Normalized Twitch Force
0
50
100
Time (ms)
C
30
20
10
0
Time to Peak Twitch (ms)
Young
Old
†
*
Normal Rats
Chronic Spinals
D
20
10
0
Twitch Half-Rise Time (ms)
Young
Old
†
*
Normal Rats
Chronic Spinals
E
150
100
50
0
Twitch Force (mN)
Young
Old †
†
*
Normal Rats
Chronic Spinals
F
10
5
0
Force:Mass Ratio (mN/mg)
Young
Old
†
*
Normal Rats
Chronic Spinals

Figure 2-2

Representative traces from both old normal (A) and chronic spinal (B) rats demonstrate that twitch contractions of segmental tail muscles can be separated into the twitches of their constituent motor units. With nerve stimulation of slowly increasing intensity, discrete increases in twitch force were seen (a through g in A, and a through h in B), representing successive recruitment of individual motor units. Means of successive motor unit twitches that make up the muscle twitch were subtracted as indicated to reveal the constituent motor units. For example, c-b=1 in A and d-c=1 in B. The motor units are arranged from fastest (1) to slowest (6 or 7) twitch contraction time. Note that the slowest units in the chronic spinals reached their peak force approximately 50 ms after the force onset, while the faster units completed their twitch by this time. Thus, the twitch force at 50 ms (TT_{50}), normalized to the peak twitch force, demonstrates the overall "slowness" of a tail muscle (C; also see text). Bar graph format as in Figure 2-1. Significance accepted at $P < 0.05$.

Figure 2-2

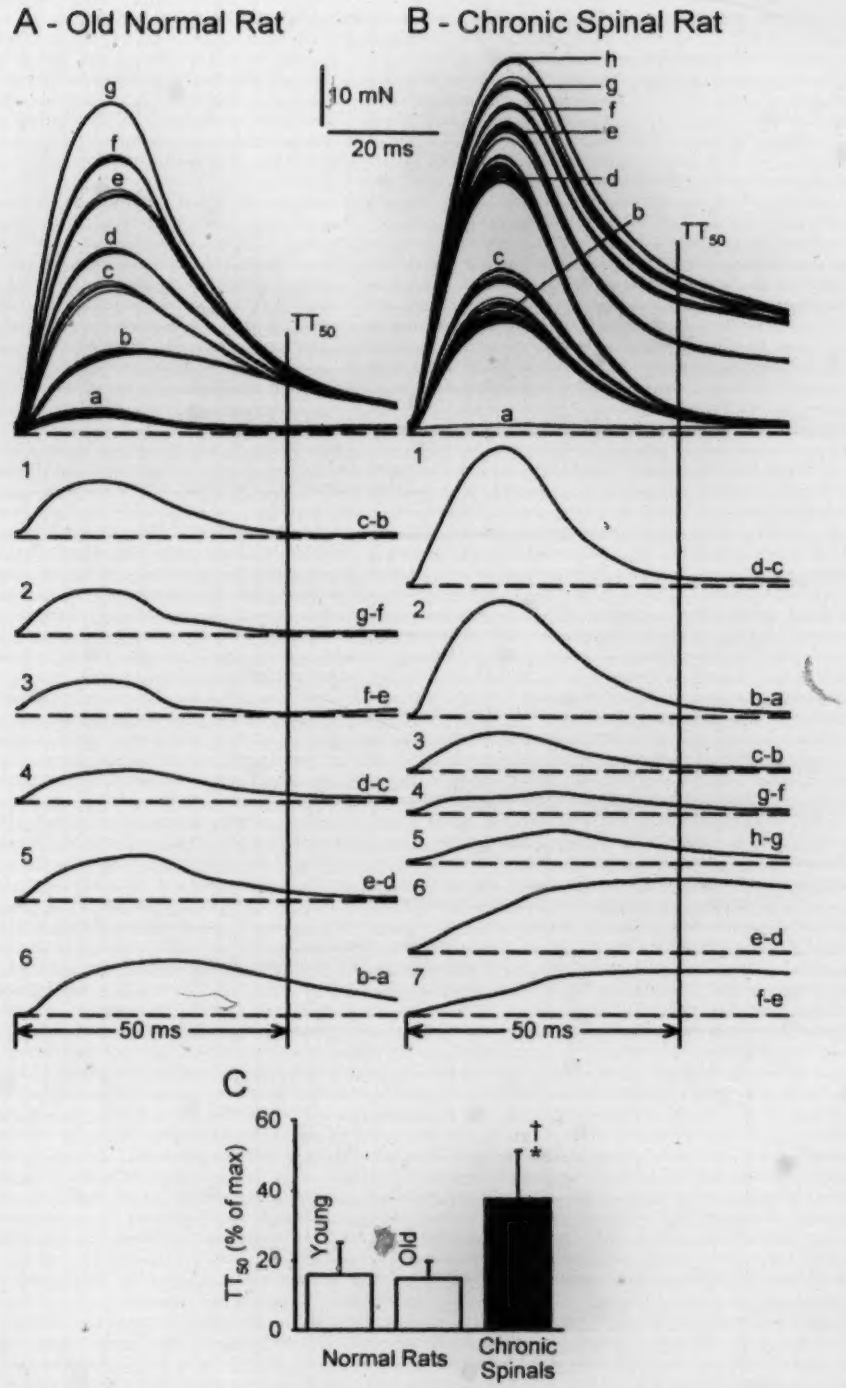
A - Old Normal Rat
B - Chronic Spinal Rat
10 mN
20 ms
TT50
50 ms
C
TT50 (% of max)
Young
Old
Normal Rats
Chronic Spinals

(Steg 1964), most subtractions likely reflected a single motor unit twitch (Figure 2-2; see also Tam et al. 2001). The low number of motor units (≤ 12) in the segmental tail muscles made this analysis possible, despite occasional motor unit alternation (Wang et al. 2004). When stimulating the nerve, two factors determine the recruitment order: the size and the random distribution of axons in the nerve. Because of this random element, the closest axons rather than the largest were often recruited first, and thus the larger, faster units were not always recruited first (e.g., "a" in Figure 2-2A and B).These motor unit profiles revealed fast and slow motor unit twitches in both normal and injured animals. The fastest motor unit twitches made up the majority of the force in both normal and chronic spinal animals, with a time to peak of approximately 15 ms (see Figure 2-2A, B), consistent with previous findings (Steg 1964). Conveniently, these fast twitches ended almost completely within 50 ms, whereas the slower motor unit twitches had a time to peak force of about approximately 30 ms in normal rats and of approximately 50 ms in chronic spinal rats.

Thus, the twitch force measured at 50 ms and normalized to peak force (TT_{50}) was a useful measure of the total contribution of the slower motor units to the twitch contraction (Figure 2-2), since the major fast component had ended by that time. This TT_{50} was not significantly different between young normal rats and old normal rats (Figure 2-2C). However, TT_{50} in chronic spinal animals was significantly greater on average than in both young normal rats (137.3% larger) and old normal rats (153.4% larger; Figure 2-2A, B, C). This tripling of TT_{50} in whole muscle after injury suggests an overall slowing of some of the motor units that contribute to the twitch in spastic tail muscles.

2.3.4 The absolute rate of rise of twitch force is not lower in chronic spinal rats; it just takes longer to develop the larger peak force

The absolute rates of rise (Figure 2-3A) and decay (Figure 2-3B) of twitch force (determined from the derivative of the twitch) for chronic spinal rats were not significantly different from those for young or old normal rats. However, we normalized twitch rate to peak twitch force, and this normalized maximum rate of rise of twitch force in chronic spinal rats was significantly lower than in normal rats (35.0% lower in chronic spinal rats than in old normal rats; Figure 2-3C), as was the normalized maximum rate of twitch force decay (40.1% lower than in old normal rats; Figure 2-3D). This was simply due to the longer-lasting rise and fall of the twitch in spastic tail muscles, because it rose to a larger peak amplitude at the same absolute speed. These results may be consistent with reduced rates of buffering and sequestration of free myoplasmic calcium following stimulation, allowing longer periods of Ca^{2+} availability and, thus, greater, longer force production in chronic spinal rats, as detailed in the DISCUSSION.

2.3.5 Tetani and post-tetanic twitch properties of tail muscles

Despite the larger twitches seen following chronic sacral spinal cord injury, the absolute peak tetanic force (supramaximal stimulation at 200 Hz) was significantly reduced in spastic muscles relative to that in old normal control muscles (38.1% smaller in chronic

Figure 2-3

Maximum rates of twitch rise and of twitch decay determined from the derivative of the twitch. The absolute max rise rate (A) is the maximum rate of rise of twitch force development in the twitch, and the absolute max decay rate (B) is the maximum rate of muscle relaxation following peak twitch force. The normalized rise (C) and decay (D) rates are the rates of rise and decay of the twitch normalized to peak force. Bar graph format as in Figure 2-1. Significance accepted at $P < 0.05$.

Figure 2-3

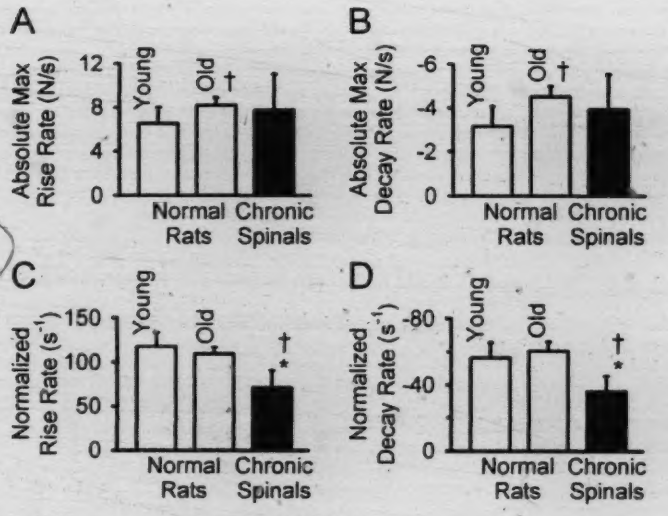
A
Absolute Max Rise Rate (N/s)
12
8
4
0
Young
Old
†
Normal Rats
Chronic Spinals
B
Absolute Max Decay Rate (N/s)
-6
-4
-2
0
Young
Old
†
Normal Rats
Chronic Spinals
C
Normalized Rise Rate (s-1)
150
100
50
0
Young
Old
†
*
Normal Rats
Chronic Spinals
D
Normalized Decay Rate (s-1)
-80
-40
0
Young
Old
†
*
Normal Rats
Chronic Spinals

spinal rats than in old normal rats; Figure 2-4A, B, C). However, the peak tetanic force in chronic spinal rats was not significantly reduced relative to that in young normal rats (Figure 2-4C). When normalized to muscle mass to account for changes due to muscle atrophy, the tetanic force was not significantly different among tail muscles of chronic spinal rats, old normal rats, and young normal rats (Figure 2-4D). Importantly, tetanus half-rise time was not significantly different across groups (Figure 2-4E), but the tetanus half-fall time was significantly prolonged in spastic muscles relative to normal muscles (53.8% longer than in old normal rats; Figure 2-4F).

Segmental tail muscle twitches in both normal and chronic spinal animals were potentiated immediately following tetani (relative to the prior twitches; Figure 2-4A, B, G). This post-tetanic potentiation was not significantly different in young normal rats and old normal rats (Figure 2-4G). Twitches of chronic spinal rats' tail muscles potentiated significantly less than did those of young and old normal rats (9.2% lower PTP than in old normal rats; Figure 2-4G), consistent with a transition toward slower muscle properties, since slower muscles typically have lower post-tetanic potentiation (Davey et al. 1981), or even exhibit post-tetanic depression of twitch (Stephens and Stuart 1975).

Young normal rats had twitch-to-tetanus ratios that were not significantly different from old normal rats (4.3% difference; Figure 2-4H). The twitch-to-tetanus ratio was much larger in chronic spinal rats than in young and old normal rats (chronic spinal rats 104.0% larger than old normal rats, significant difference; Figure 2-4H), as similarly observed by Lieber and colleagues (1986) in paralyzed hindlimb muscles after SCI compared to normal muscles. Thus, relative to tetani, chronic spinal tail muscles have larger twitches than do normal rats, consistent with the increased twitch force but decreased tetanic force observed here.

2.3.6 Chronic spinal tail muscles fuse more easily

When the tail nerve was stimulated with 300-ms trains of increasing frequencies (10-200 Hz), the tetanic muscle force production was initially low and unfused at low frequencies, and then became larger and more fused at higher stimulation frequencies. When the tetanic force production at each frequency was normalized to the maximum, fused tetanic force (at 200 Hz), on average, this normalized tetanic force was nearly identical at all frequencies in young and old normal rats (not significantly different; open circles and squares overlay in Figure 2-5A). However, the normalized tetanic force production was significantly larger in chronic spinal rats (Figure 2-5A, closed circles) at all frequencies up to 70 Hz, compared to in young and old normal rats. Also, the stimulation frequency required to achieve the half-maximal tetanic force, F_{50}, was significantly lower for muscles of chronic spinal rats compared to those of normal rats (39.0% lower; Figure 2-5B). Thus, in chronic spinal rats with spasticity, tetani became fused and reached maximum tetanic force production at lower frequencies than in normal rats. This is in contrast to the higher fusion frequency observed for non-spastic hindlimb muscles after SCI (Lieber et al. 1986b) but, again, is consistent with a slowing of the spastic muscles.

Figure 2-4

Representative tetani and their relationships to twitch contractions are shown for old normal rats (A) and chronic spinal rats (B). Tetani were elicited with supramaximal stimulation at 200 Hz for 500 ms. Twitches were produced by single, supramaximal stimulation pulses delivered 1200 ms before and 1200 ms after the onset of tetanus. In A and B, twitch before and twitch after are shown on an enlarged scale to the right of the full-scale traces. Tetanic force (C) is the peak force achieved during a single tetanus, and normalized tetanus (D) is the ratio of tetanic force to muscle mass. Note that tetanic force production is significantly smaller in tail muscles from chronic spinal rats (C). However, when the ratio of tetanic force to muscle mass is calculated, the decrease in tetanic force with spinal cord injury appears to be accounted for by muscle mass atrophy (D). Tetanus half-rise time (E) is the time required to reach half of the peak tetanic force. Tetanus half-fall time (F) is the time required after the end of tetanic stimulation for muscle force to be reduced by half. Post-tetanic potentiation (G) is the ratio of the peak twitch force after a tetanus to the peak twitch force before a tetanus. Twitch:tetanus ratio (H) is the ratio of the peak force of the non-potentiated twitch (twitch before) to the peak force of the tetanus. Bar graph format as in Figure 2-1. Significance accepted at $P < 0.05$.

Figure 2-4

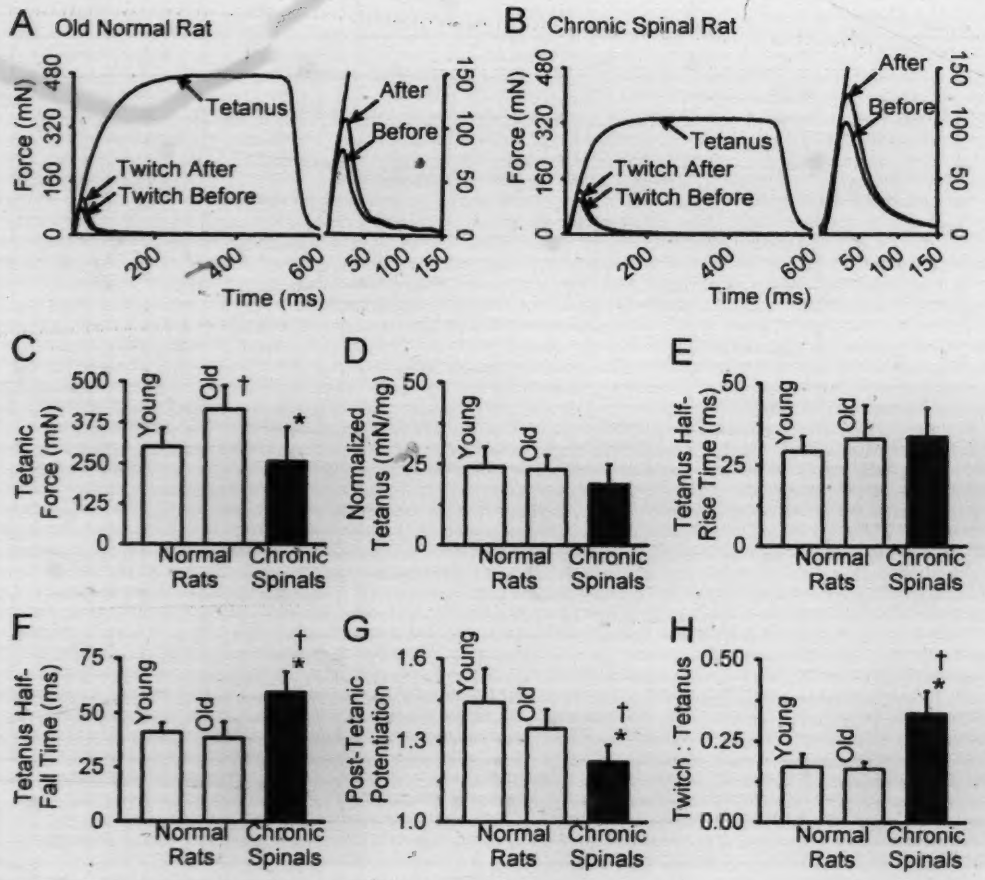
A Old Normal Rat
Force (mN)
0 160 320 480
Tetanus
Twitch After
Twitch Before
After
Before
0 50 100 150
200 400 600
50 100 150
Time (ms)
B Chronic Spinal Rat
Force (mN)
0 160 320 480
Tetanus
Twitch After
Twitch Before
After
Before
0 50 100 150
200 400 600
50 100 150
Time (ms)
C
Tetanic Force (mN)
500
375
250
125
0
Young
Old
†
*
Normal Rats
Chronic Spinals
D
Normalized Tetanus (mN/mg)
50
25
0
Young
Old
Normal Rats
Chronic Spinals
E
Tetanus Half-Rise Time (ms)
50
25
0
Young
Old
Normal Rats
Chronic Spinals
F
Tetanus Half-Fall Time (ms)
75
50
25
0
Young
Old
†
*
Normal Rats
Chronic Spinals
G
Post-Tetanic Potentiation
1.6
1.3
1.0
Young
Old
†
*
Normal Rats
Chronic Spinals
H
Twitch : Tetanus
0.50
0.25
0.00
Young
Old
†
*
Normal Rats
Chronic Spinals

Figure 2-5

Fusion properties of segmental tail muscles. (A) Forces developed during supramaximal tetanic stimuli (300 ms) at frequencies from 10-200 Hz are shown for chronic spinal rats (closed circles, error bars upward), old normal rats (open circles, error bars downward), and young normal rats (open squares, error bars upward). Note that the symbols for old normal rats largely overlay those for young normal rats as the values for these groups are nearly identical. Values are normalized to the maximum tetanic force at 200 Hz. (B) F_{50} is the frequency required to reach half-maximal tetanic force (0.50 on vertical scale in A). The force frequency curve for each animal was fit to a sigmoidal function ($r^2 \geq 0.9$ for all sigmoidal fits), and then F_{50} was calculated for each animal using its sigmoidal function. In chronic spinal rats relative to normal rats, F_{50} is achieved at a significantly lower stimulation frequency. Bar graph format as in Figure 2-1. Significance accepted at $P < 0.05$.

Figure 2-5

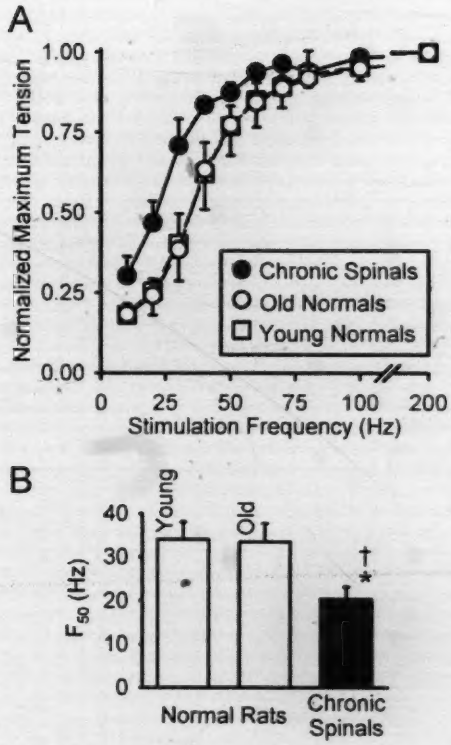
A
Normalized Maximum Tension
1.00
0.75
0.50
0.25
0.00
0
25
50
75
100
200
Stimulation Frequency (Hz)
Chronic Spinals
Old Normals
Young Normals
B
F_{50} (Hz)
40
30
20
10
0
Young
Old
†
*
Normal Rats
Chronic Spinals

2.3.7 Chronic spinal tail muscles are fatigable

Fatigability of segmental tail muscles was measured by producing 300-ms tetanic contractions (each with supramaximal stimulation at 40 Hz), repeated once per second for 100 s (see also MATERIALS AND METHODS and Figure 2-6). Overall, during these repeated contractions, the muscles of chronic spinal rats, compared to normal rats, reached a maximum tetanic force after fewer contractions (~9 contractions in chronic spinal rat, shown in Figure 2-6B inset, compared to ~17 contractions in old normal rat, shown in Figure 2-6A inset). However, the tetanic force then dropped more quickly (after fewer contractions) and reached a lower steady-state tetanic force by the 100th contraction (insets in Figures 6A and B), indicating that the chronic spinal muscles were more fatigable.

To quantify the fatigability, the fatigue index was calculated as the ratio of the maximum steady state tetanic force produced in the 100th contraction to the maximum steady-state tetanic force produced in the 1st contraction (both forces were measured relative to the baseline force prior to the first contraction; see Figure 2-6A and B). On average, the fatigue index was not significantly different in young and old normal rats (Figure 2-6C). However, the fatigue index was significantly lower in chronic spinal rats than in young (71.5% lower) and old (61.5% lower) normal rats (Figure 2-6C). Thus, the muscles of chronic spinal rats were more fatigable than were those of normal rats.

In tail muscles from spastic animals relative to those from normal animals there was also a much greater rise in the baseline force prior to the 100th contraction, indicating that the muscle remained more contracted between contractions. This rise in baseline force is consistent with contractures resulting from compromised metabolic capacity (Layzer 1986). This larger baseline rise in chronic spinal rats tended to increase the force measured on the 100th contraction and thus resulted in an underestimation of muscle fatigue as measured by the fatigue index.

2.4 DISCUSSION

The results demonstrate that, in rats following chronic sacral spinal cord injury and spasticity, the segmental tail muscles undergo substantial changes in contractile properties. We suggest that some of these changes result from an increase in muscle activity due to the prominent spasticity in these muscles (Bennett et al. 2004); that is, there is a slowing of the twitch, a marked increase in peak twitch force, a slowing of relaxation from tetanus, a decrease in fusion frequency, and a decrease in post-tetanic potentiation that are all consistent with the contractile phenotype of a classically slower muscle (Davey et al. 1981; Lieber et al. 1986b; Stephens and Stuart 1975). This slowing is similar to that seen in general with increased activity (Hartkopp et al. 2003; Roy et al. 1999; Roy et al. 1998), and thus is consistent with the idea that the spastic activity influences muscle contraction and relaxation, and likely exerts its influence especially on the low-threshold motor units that are more often very active in spasms. In contrast, these muscles of spastic rats also become more fatigable, produce less tetanic force, have increased twitch-to-tetanus ratios, and are atrophied in mass.

Figure 2-6

Fatigue with repeated contractions. Muscles were fatigued by producing 300-ms tetanic contractions (each with supramaximal stimulation at 40 Hz), repeated once per second for 100 s. Representative traces show the 1st and 100th tetani of the test for segmental tail muscles in old normal rats (A) and chronic spinal rats (B), and insets demonstrate the ongoing change in peak tetanic force over 100 sweeps. Note that the peak force in repeated 40-Hz trains potentiates slightly before declining, as shown in the insets of A and B, and declines more in chronic spinal rats. Note also that the force scales in A and B differ. To quantify the fatigability, the fatigue index (C) was calculated as the ratio of the tetanic force produced in the 100th contraction to the tetanic force produced in the 1st contraction. Both forces were measured relative to the baseline force prior to the first contraction. Bar graph format as in Figure 2-1. Significance accepted at $P < 0.05$.

Figure 2-6

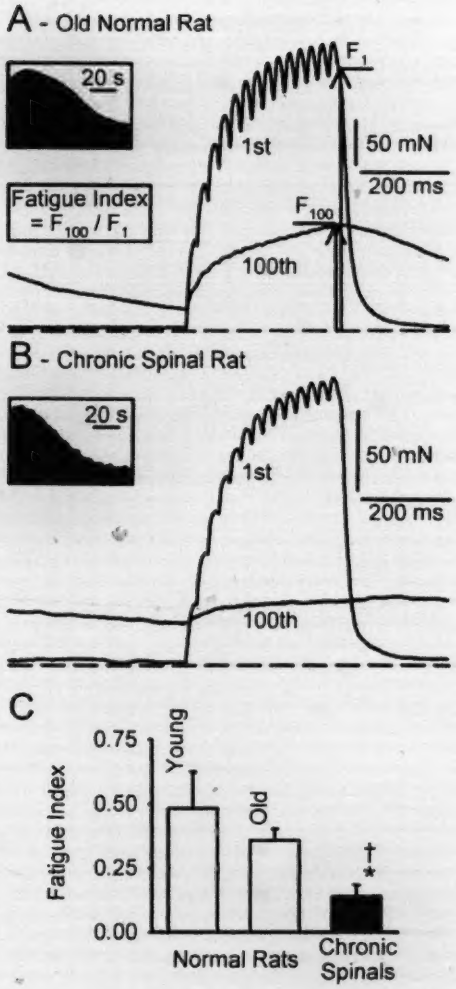
A - Old Normal Rat
20 s
F1
1st
50 mN
200 ms
Fatigue Index
= F100 / F1
F100
100th
B - Chronic Spinal Rat
20 s
1st
50 mN
200 ms
100th
C
Fatigue Index
0.75
0.50
0.25
0.00
Young
Old
†
*
Normal Rats
Chronic
Spinals

2.4.1 Spastic muscle activity depends on the model and muscle examined

The finding that spasticity is associated with slower muscle contractile properties is particularly striking when compared to spinal cord-injured muscle in other studies where spasticity is not observed (Davey et al. 1981; Lieber et al. 1986b; Roy et al. 1999; Roy et al. 1998), again suggesting that spasticity promotes slower muscle contractile properties. That is, following complete spinal cord transections that do not lead to spasticity, there is a classical slow-to-fast myofiber type conversion and muscle atrophy, which result in a faster, more fatigable, and weaker muscle. In these classical studies, the slow type-I and fast fatigue resistant type-IIA myofibers are markedly reduced and converted to fast fatigable type-IID/X and type-IIB myofibers (Burnham et al. 1997; Lieber et al. 1986a; Talmadge et al. 1995). Thus, the slowing and increased twitch size that we see in spastic tail muscles compared to in normal tail muscles is even more remarkable compared to in non-spastic muscles after spinal cord injury, which have faster, weaker contractile properties than normal.

It might be argued that the tail muscles are peculiar in their response to spinal cord injury and activity-related changes (spasticity), especially considering that we did not examine the impact on contractile properties of spinal cord injury *without* spasticity. Indeed, several comprehensive studies of the soleus or medial gastrocnemius in cats with complete spinal cord transections are in constrast to our own findings, demonstrating clear slow-to-fast transformations in contractile speed and myofiber type in conjunction with increased fatigability (Cope et al. 1986; Mayer et al. 1984; Munson et al. 1986). Unfortunately, however, these studies either do not report spasticity (Cope et al. 1986; Munson et al. 1986) or do not report in detail the degree of spastic muscle activity (Mayer et al. 1984) in the specific muscles examined, and thus the conclusions they draw regarding mechanisms underlying spasticity must be treated with caution.

In contrast, the tail muscles studied in the current paper have been well documented to be spastic (Bennett et al. 2004) and, in particular, the same rats were used in the current study as in the Bennett et al. (2004) study. Further, our recent unpublished 24-hour EMG recordings indicate that tail muscle activity drops dramatically compared to normal with acute injury, and with long-term injury and spasticity muscle activity recovers to as much as in the normal rats (though always linked to spasms as opposed to voluntary movements). Thus, it is likely that the changes in contractile properties seen in the current paper are related to these changes in spastic muscle activity. Furthermore, similar changes in muscle properties (slowing with increased fatigability) have been seen in human muscles that are spastic after long-term spinal cord injury (Hidler et al. 2002; Thomas 1997; Zijdewind and Thomas 2003), and thus the changes we see are not peculiar to the rat tail muscle. Moreover, our recent immunohistochemical findings (Harris et al. 2007) reveal that following spinal cord injury, spasticity indeed plays a central role in regulating myofiber type. Specifically, early after injury, tail myofibers identified by immunohistochemistry atrophy dramatically and undergo a transformation toward a faster, more fatigable myofiber distribution, and these changes occur in association with flaccid paralysis, prior to the development of full spasticity, consistent with other studies of SCI without spasticity (Lieber et al. 1986a; Talmadge et al. 1995).

Furthermore, with long-term full spasticity (as in chronic spinal rats in the current paper) the opposite occurs: myofibers hypertrophy and undergo a recovery toward slower isoforms (Harris et al. 2007). All myofibers recover completely from atrophy, with the exception of the dominant type-IID/X myofibers, which partially recover (Harris et al. 2007), consistent with the total muscle mass atrophy described here, and consistent with the idea that the higher threshold units recruited less frequently by spasticity should exhibit fewer activity-dependent adaptations. Ultimately, after long-term injury and spasticity, myofiber size and proportions recover nearly completely to normal (Harris et al. 2007). Consequently, spasticity does indeed preserve myofiber properties over the long term after SCI by countering early atrophy and transformations due to reduced activity, ultimately normalizing the myofiber phenotype and morphology.

In the DISCUSSION below, we suggest possible mechanisms that might explain these changes in contractile properties seen in spastic muscles. As we have just mentioned, with long-term injury and spasticity, the myosin heavy chain-identified myofiber distribution is well preserved compared to normal (Harris et al. 2007) and therefore does *not* account for the slowing of the muscle that we have observed with long-term injury. Thus, we explore the hypothesis that the prolonged and larger twitches seen in these muscles might be due to decreased intracellular calcium buffering and sequestering that is known to be influenced by increased activity, and is associated with longer and larger twitches (Green et al. 1984; Schwaller et al. 1999).

2.4.2 Myofiber type changes with injury

Rat segmental tail muscles have been studied in detail previously only by Steg (1964), who assessed some mechanical and electrophysiological properties of their motor units. The motor unit composition in segmental tail muscles reported by Steg was approximately 67% fast, 25% intermediate, and 8% slow (Steg 1964). Our recent data from immunohistochemical staining of myosin heavy chain isoforms are consistent with this distribution. We have found that rat segmental tail muscles are composed of predominantly fast myofiber types: fatigue intermediate type-IID/X myofibers constitute approximately 65-70% of the muscle; the remaining myofibers are slow non-fatigable type-I (10-20%) and fast fatigue resistant type-IIA (10-20%), and there is a near absence of fast fatigable type-IIB myofibers (Harris et al. 2007).

With long-term spinal cord injury, we have found that spastic tail muscles exhibit very few changes in myofiber proportions compared to age-matched normal rats, as already mentioned. Specifically, the dominant fast fatigue intermediate type-IID/X myofiber proportion increases slightly with long-term injury in spastic muscles (approximately 10% increase), and there is a small loss of slow non-fatigable type-I myofibers (Harris et al. 2007). However, from a functional perspective, these changes are small in relation to the initial large changes in myofiber types prior to the development of spasticity (see above), where type-I and type-IIA myofiber proportions are halved and type-IID/X proportions are increased accordingly. Further, these changes are very small in relation to the large losses of slow and fatigue resistant myofibers and the proportional increases in faster, more fatigable myofibers seen following spinal cord injury that is *not* associated

with spasticity (Burnham et al. 1997; Lieber et al. 1986a; Talmadge et al. 1995). Thus, the relatively small changes in myofiber types seen in spastic tail muscles are consistent with the possibility that the spastic activity preserves the myofiber type distribution.

2.4.3 Factors that influence fatigue after injury

The large increase in spastic tail muscle fatigability observed in the current study cannot be attributed to the small increase in fast fatigue intermediate type-IID/X myofibers we have observed in these same muscles (Harris et al. 2007). Metabolic factors likely play a role, given the very large change in fatigability (>50% reduction in fatigue index). For example, poor blood circulation to the tail, as might be expected due to reduced autonomic tone associated with spinal cord injury (Johnson et al. 1998; Yu 1998), might ultimately lead to compromised ATP availability during our 100-s-long fatigue tests. Perhaps this also would account for the contractures that build up over the course of these tests. A number of other metabolic factors can influence muscle fatigability, including plasma membrane density of Na^+,K^+-ATPase (Fowles et al. 2002), creatine phosphate availability (Hartkopp et al. 2003), and concentration or activity of key oxidative enzymes such as succinate dehydrogenase and cytochrome C oxidase (Haller et al. 1991; Hambrecht et al. 1997); these factors may play a role in the fatigue of spastic muscles.

2.4.4 Factors that don't influence twitch duration and size after injury

The slowing/prolongation of the muscle twitch after injury *cannot* be accounted for by changes in myofiber types because the proportion of slow type-I myofibers does not increase in spastic tail muscles following chronic spinal cord injury (Harris et al. 2007). Further, the increased twitch size after chronic injury and long-term spasticity cannot be accounted for by changes in myofibers because there are only small changes in myofiber distributions, with an increase in the type-IID/X myofibers of only 10%, which is countered by some atrophy in the type-IID/X myofibers (Harris et al. 2007). Altered pennation angle can affect muscle force production, but this usually occurs in conjunction with myofiber hypertrophy (Aagaard et al. 2001); instead of hypertrophy, we saw a moderate atrophy of muscle in spastic chronic spinal rats compared to normal rats. Changes in muscle stiffness can also affect muscle force production; this force-stiffness interaction is dependent to a large extent on myofiber type composition (Malamud et al. 1996; Mirbagheri et al. 2001). However, we have found that stiffness does not change with injury in spastic tail muscles (unpublished observations) and, again, that myofiber type composition does not change much in spastic chronic spinal rats (Harris et al. 2007). Finally, changes due to muscle maturation over the 8 months of the current experiments are also unlikely to account for changes in contractile properties, as we saw no major changes in old age-matched normal rats compared to young normal rats, consistent with limited changes in contractile properties observed over this age range by Ansved and Larsson (1989).

2.4.5 Possible changes in intracellular calcium buffering and sequestering

One possibility that might account for many of the mechanical changes seen in spastic tail muscle is impaired myoplasmic calcium buffering (e.g., by parvalbumin) and/or

decreased calcium sequestering into the sarcoplasmic reticulum (Jiang et al. 1996). Such changes would result in calcium staying in the myoplasm longer during a twitch (Schwaller et al. 1999). Thus, force generation would be *prolonged* and the twitch force would reach a *larger* peak until calcium was sequestered into the sarcoplasmic reticulum. This scenario appears consistent with the prolonged and much larger twitches seen in spastic muscles. The concept that the decay of myoplasmic calcium is a major factor in determining twitch duration and amplitude has support in a number of other experimental systems where Ca^{2+} handling is rate limiting (Allen and Westerblad 1995; Choisy et al. 2001; Raymackers et al. 2000; Schwaller et al. 1999; Stein et al. 1982). In contrast, calcium decay should not affect the absolute maximum rate of rise of force during a twitch or a tetanus, so impaired calcium handling due to spinal cord injury should not affect these parameters, consistent with our observations. Also, during maximal repetitive stimulation yielding a tetanus, there should be no lack of free calcium regardless of the calcium buffering/sequestering; thus, the rise in force during a tetanus and the maximal tetanic force should not be affected by myoplasmic calcium handling, apparently consistent with our results. Certainly, the spastic tail muscle atrophied and produced *less* (not more) tetanic force, but it is compelling that the tetanic force normalized by the muscle mass is not different between normal and spastic muscles, and that the rate of rise of tetanic force did not change. Ultimately, this should lead to a larger twitch–to-tetanus ratio, as also observed here. Further, the decay of tetanic force is significantly slower in spastic muscles, again implying poor post-tetanus calcium handling (Raymackers et al. 2000). Thus, in general, with the exception of changes in fatigue, all changes in the muscle twitch and tetanus in spinal cord-injured rats with spasticity may be consistent with a compromised myoplasmic calcium buffering/sequestering system that occurs without major changes in contractile proteins (myosin heavy chain-identified myofiber proportions; Schwaller et al. 1999; Raymackers et al. 2000).

The spastic activity following spinal cord injury may produce a decrease in myoplasmic calcium buffering in the same way that electrical stimulation and exercise have been shown to decrease calcium buffering and sequestering in the hindlimb muscles of rats (Green et al. 1984; Huber and Pette 1996). Specifically, endurance training in rats induces a decrease in myoplasmic parvalbumin content (Green et al. 1984), a protein which normally serves to buffer calcium from troponin C until it is sequestered by the sarcoplasmic reticulum (Jiang et al. 1996). Training also markedly decreases the concentration of the SR Ca^{2+}-ATPase that pumps calcium into the sarcoplasmic reticulum during sequestration (Green et al. 1984). Additionally, when parvalbumin is eliminated in parvalbumin knockout mice, the twitch is of *increased duration* and *increased peak amplitude* (Schwaller et al. 1999) and relaxation from tetanus is *slower* (Raymackers et al. 2000), remarkably consistent with our own observations in spastic muscles. The opposite effect is observed for twitch contractions following transgenic overexpression of parvalbumin in mice; in these mice, in contrast to our own findings, twitch contraction and relaxation are faster, and tetani fuse and reach maximum tetanic force at higher frequencies than in normal mice (Chin et al. 2003).

Importantly, myosin heavy chain-identified myofiber types are *not* changed in parvalbumin-knockout mice (Schwaller et al. 1999) or in mice overexpressing

parvalbumin (Chin et al. 2003), and changes in parvalbumin and SR Ca^{2+}-ATPase occurred well in advance of altered myosin ATPase-identified myofiber types over 15 weeks of intensive exercise (Green et al. 1984). These data emphasize that calcium handling proteins such as parvalbumin and the SR Ca^{2+}-ATPase can be altered *independently* of myofiber type transformations. Again, this appears consistent with our results in segmental tail muscles of chronic spinal rats, in which the twitch properties change as though calcium buffering might be compromised, with little change in myosin heavy chain-identified myofiber distribution.

Other investigators have found injury-induced or humoral changes in calcium handling with results similar to those seen in spastic tail muscles. For example, 7-day denervation causes reduced calcium uptake into the sarcoplasmic reticulum in rat fast fatigable type-IIB myofibers and is associated with slowing of twitches and increased peak twitch (Germinario et al. 2002). Likewise, the opposite effects are seen in the soleus of hyperthyroid rats in which calcium re-uptake by the SR is increased (Fitts et al. 1980).

2.4.6 Summary

Overall, spastic tail muscles from chronic spinal rats are more fatigable than tail muscles from normal rats, likely due to changes in metabolic factors, rather than changes in myosin heavy chain-identified myofiber types. The spastic muscles also have considerably slower contractile properties than normal muscles, including prolonged twitch contraction and relaxation, slower relaxation from tetanus, and lower fusion frequencies. Together with larger twitches, these results may be most consistent with altered intracellular calcium handling. Surprisingly, the slowing of active spastic muscle after long-term spinal cord injury is *not* associated with increased slow type-I myofibers (Harris et al. 2007).

Importantly, slowing of muscle with spinal cord injury and spasticity is not unprecedented in humans. That is, human triceps surae and thenar muscles that are spastic after long-term spinal cord injury have considerably slower contraction speeds compared to those in uninjured humans (Hidler et al. 2002; Thomas 1997; Zijdewind and Thomas 2003). This effect is notably spasticity-dependent, with the most severe spasticity resulting in the most enhanced slow properties (Hidler et al. 2002). Thus, spastic muscle activity is associated with preserved or even enhanced slow contractile properties.

2.5 REFERENCES FOR CHAPTER 2

Aagaard P, Andersen JL, Dyhre-Poulsen P, Leffers AM, Wagner A, Magnusson SP, Halkjaer-Kristensen J, and Simonsen EB. A mechanism for increased contractile strength of human pennate muscle in response to strength training: changes in muscle architecture. *J Physiol* 534: 613-623, 2001.

Allen D and Westerblad H. The effects of caffeine on intracellular calcium, force and the rate of relaxation of mouse skeletal muscle. *J Physiol* 487: 331-342, 1995.

Ansved T and Larsson L. Effects of ageing on enzyme-histochemical, morphometrical and contractile properties of the soleus muscle in the rat. *J Neurol Sci* 93: 105-124, 1989.

Bennett DJ, Gorassini M, Fouad K, Sanelli L, Han Y, and Cheng J. Spasticity in rats with sacral spinal cord injury. *J Neurotrauma* 16: 69-84, 1999.

Bennett DJ, Li Y, Harvey PJ, and Gorassini M. Evidence for plateau potentials in tail motoneurons of awake chronic spinal rats with spasticity. *J Neurophysiol* 86: 1972-1982, 2001.

Bennett DJ, Sanelli L, Cooke CL, Harvey PJ, and Gorassini MA. Spastic long-lasting reflexes in the awake rat after sacral spinal cord injury. *J Neurophysiol* 91: 2247-2258, 2004.

Burke RE, Levine DN, Tsairis P, and Zajac FE, 3rd. Physiological types and histochemical profiles in motor units of the cat gastrocnemius. *J Physiol* 234: 723-748, 1973.

Burnham R, Martin T, Stein R, Bell G, MacLean I, and Steadward R. Skeletal muscle fibre type transformation following spinal cord injury. *Spinal Cord* 35: 86-91, 1997.

Chin ER, Grange RW, Viau F, Simard AR, Humphries C, Shelton J, Bassel-Duby R, Williams RS, and Michel RN. Alterations in slow-twitch muscle phenotype in transgenic mice overexpressing the Ca2+ buffering protein parvalbumin. *J Physiol* 547: 649-663, 2003.

Choisy S, Divet A, Huchet-Cadiou C, and Leoty C. Sarcoplasmic reticulum Ca(2+) content affects 4-CmC and caffeine contractures of rat skinned skeletal muscle fibers. *Jpn J Physiol* 51: 661-669, 2001.

Cope TC, Bodine SC, Fournier M, and Edgerton VR. Soleus motor units in chronic spinal transected cats: physiological and morphological alterations. *J Neurophysiol* 55: 1202-1220, 1986.

Davey DF, Dunlop C, Hoh JF, and Wong SY. Contractile properties and ultrastructure of extensor digitorum longus and soleus muscles in spinal cord transected rats. *Aust J Exp Biol Med Sci* 59: 393-404, 1981.

Fitts RH, Winder WW, Brooke MH, Kaiser KK, and Holloszy JO. Contractile, biochemical, and histochemical properties of thyrotoxic rat soleus muscle. *Am J Physiol Cell Physiol* 238: C14-20, 1980.

Fowles JR, Green HJ, Tupling R, O'Brien S, and Roy BD. Human neuromuscular fatigue is associated with altered Na+-K+-ATPase activity following isometric exercise. *J Appl Physiol* 92: 1585-1593, 2002.

Fujimori B, Shimamura M, Kato M, Yamauchi T, Aoki M, and Tanji J. Studies on the mechanisms of spasticity and rigidity following spinal lesions and ischaemia. *Proc Aust Assoc Neurol* 5: 35-39, 1968.

Geminario E, Esposito A, Megighian A, Midrio M, Biral D, Betto R, and Danieli-Betto D. Early changes of type 2B fibers after denervation of rat EDL skeletal muscle. *J Appl Physiol* 92: 2045-2052, 2002.

Green HJ, Klug GA, Reichmann H, Seedorf U, Wiehrer W, and Pette D. Exercise-induced fibre type transitions with regard to myosin, parvalbumin, and sarcoplasmic reticulum in muscles of the rat. *Pflügers Arch* 400: 432-438, 1984.

Haller RG, Henriksson KG, Jorfeldt L, Hultman E, Wibom R, Sahlin K, Areskog NH, Gunder M, Ayyad K, Blomqvist CG, and et al. Deficiency of skeletal muscle succinate dehydrogenase and aconitase. Pathophysiology of exercise in a novel human muscle oxidative defect. *J Clin Invest* 88: 1197-1206, 1991.

Hambrecht R, Fiehn E, Yu J, Niebauer J, Weigl C, Hilbrich L, Adams V, Riede U, and Schuler G. Effects of endurance training on mitochondrial ultrastructure and fiber type distribution in skeletal muscle of patients with stable chronic heart failure. *J Am Coll Cardiol* 29: 1067-1073, 1997.

Harris RLW, Putman CT, Rank MM, Sanelli L, and Bennett DJ. Spastic tail muscles recover from myofiber atrophy and myosin heavy chain transformations in chronic spinal rats. *J Neurophysiol* 97: 1040-1051, 2007.

Hartkopp A, Harridge SD, Mizuno M, Ratkevicius A, Quistorff B, Kjaer M, and Biering-Sorensen F. Effect of training on contractile and metabolic properties of wrist extensors in spinal cord-injured individuals. *Muscle Nerve* 27: 72-80, 2003.

Heckman CJ. Alterations in synaptic input to motoneurons during partial spinal cord injury. *Med Sci Sports Exerc* 26: 1480-1490, 1994.

Hidler JM, Harvey RL, and Rymer WZ. Frequency response characteristics of ankle plantar flexors in humans following spinal cord injury: relation to degree of spasticity. *Ann Biomed Eng* 30: 969-981, 2002.

Huber B and Pette D. Dynamics of parvalbumin expression in low-frequency-stimulated fast-twitch rat muscle. *Eur J Biochem* 236: 814-819, 1996.

Jiang Y, Johnson JD, and Rall JA. Parvalbumin relaxes frog skeletal muscle when sarcoplasmic reticulum Ca(2+)-ATPase is inhibited. *Am J Physiol Cell Physiol* 270: C411-417, 1996.

Johnson RL, Gerhart KA, McCray J, Menconi JC, and Whiteneck GG. Secondary conditions following spinal cord injury in a population-based sample. *Spinal Cord* 36: 45-50, 1998.

Kernell D, Donselaar Y, and Eerbeek O. Effects of physiological amounts of high- and low-rate chronic stimulation on fast-twitch muscle of the cat hindlimb. II. Endurance-related properties. *J Neurophysiol* 58: 614-627, 1987a.

Kernell D, Eerbeek O, Verhey BA, and Donselaar Y. Effects of physiological amounts of high- and low-rate chronic stimulation on fast-twitch muscle of the cat hindlimb. I. Speed- and force-related properties. *J Neurophysiol* 58: 598-613, 1987b.

Kuhn RA and Macht MB. Some manifestations of reflex activity in spinal man with particular reference to the occurrence of extensor spasm. *Bull Johns Hopkins Hosp* 84: 43-75, 1948.

Lance JW and Burke D. Mechanisms of spasticity. *Arch Phys Med Rehabil* 55: 332-337, 1974.

Layzer RB. *Myology*. New York: McGraw-Hill, 1986, p. 1907-1922.

Lieber RL. *Skeletal Muscle Structure, Function, & Plasticity: The Physiological Basis of Rehabilitation*. Baltimore MD, Philadelphia PA: Lippincott Williams & Wilkins, 2002, p. 240-242.

Lieber RL, Friden JO, Hargens AR, and Feringa ER. Long-term effects of spinal cord transection on fast and slow rat skeletal muscle. II. Morphometric properties. *Exp Neurol* 91: 435-448, 1986a.

Lieber RL, Johansson CB, Vahlsing HL, Hargens AR, and Feringa ER. Long-term effects of spinal cord transection on fast and slow rat skeletal muscle. I. Contractile properties. *Exp Neurol* 91: 423-434, 1986b.

Malamud JG, Godt RE, and Nichols TR. Relationship between short-range stiffness and yielding in type-identified, chemically skinned muscle fibers from the cat triceps surae muscles. *J Neurophysiol* 76: 2280-2289, 1996.

Mayer RF, Burke RE, Toop J, Walmsley B, and Hodgson JA. The effect of spinal cord transection on motor units in cat medial gastrocnemius muscles. *Muscle Nerve* 7: 23-31, 1984.

Mirbagheri MM, Barbeau H, Ladouceur M, and Kearney RE. Intrinsic and reflex stiffness in normal and spastic, spinal cord injured subjects. *Exp Brain Res* 141: 446-459, 2001.

Munson JB, Foehring RC, Lofton SA, Zengel JE, and Sypert GW. Plasticity of medial gastrocnemius motor units following cordotomy in the cat. *J Neurophysiol* 55: 619-634, 1986.

Raymackers JM, Gailly P, Schoor MC, Pette D, Schwaller B, Hunziker W, Celio MR, and Gillis JM. Tetanus relaxation of fast skeletal muscles of the mouse made parvalbumin deficient by gene inactivation. *J Physiol* 527 Pt 2: 355-364, 2000.

Ritz LA, Friedman RM, Rhoton EL, Sparkes ML, and Vierck CJ, Jr. Lesions of cat sacrocaudal spinal cord: a minimally disruptive model of injury. *J Neurotrauma* 9: 219-230, 1992.

Rochester L, Chandler CS, Johnson MA, Sutton RA, and Miller S. Influence of electrical stimulation of the tibialis anterior muscle in paraplegic subjects. 1. Contractile properties. *Paraplegia* 33: 437-449, 1995.

Roy RR, Talmadge RJ, Hodgson JA, Oishi Y, Baldwin KM, and Edgerton VR. Differential response of fast hindlimb extensor and flexor muscles to exercise in adult spinalized cats. *Muscle Nerve* 22: 230-241, 1999.

Roy RR, Talmadge RJ, Hodgson JA, Zhong H, Baldwin KM, and Edgerton VR. Training effects on soleus of cats spinal cord transected (T12-13) as adults. *Muscle Nerve* 21: 63-71, 1998.

Schwaller B, Dick J, Dhoot G, Carroll S, Vrbova G, Nicotera P, Pette D, Wyss A, Bluethmann H, Hunziker W, and Celio MR. Prolonged contraction-relaxation cycle of fast-twitch muscles in parvalbumin knockout mice. *Am J Physiol Cell Physiol* 276: C395-403, 1999.

Shields RK. Muscular, skeletal, and neural adaptations following spinal cord injury. *J Orthop Sports Phys Ther* 32: 65-74, 2002.

Steg G. Efferent muscle innervation and rigidity. *Acta Physiol Scand* 61 supplementum 225: 1-53, 1964.

Stein RB, Gordon T, and Shriver J. Temperature dependence of mammalian muscle contractions and ATPase activities. *Biophys J* 40: 97-107, 1982.

Stephens JA and Stuart DG. The motor units of cat medial gastrocnemius. Twitch potentiation and twitch-tetanus ratio. *Pflügers Arch* 356: 359-372, 1975.

Stephens M, Bobet J, Han Y, Sanelli L, and Bennett DJ. Changes in muscle mechanical properties following chronic sacral spinal cord injury in rats. *29th Meeting of the Society for Neuroscience*, Miami Beach, FL, 1999.

Talmadge RJ, Roy RR, Bodine-Fowler SC, Pierotti DJ, and Edgerton VR. Adaptations in mysoin heavy chain profile in chronically unloaded muscles. *Basic and Applied Myology* 5: 117-137, 1995.

Talmadge RJ, Roy RR, Caiozzo VJ, and Edgerton VR. Mechanical properties of rat soleus after long-term spinal cord transection. *J Appl Physiol* 93: 1487-1497, 2002.

Tam SL, Archibald V, Jassar B, Tyreman N, and Gordon T. Increased neuromuscular activity reduces sprouting in partially denervated muscles. *J Neurosci* 21: 654-667, 2001.

Taylor JS, Friedman RF, Munson JB, and Vierck CJ, Jr. Stretch hyperreflexia of triceps surae muscles in the conscious cat after dorsolateral spinal lesions. *J Neurosci* 17: 5004-5015, 1997.

Thomas CK. Contractile properties of human thenar muscles paralyzed by spinal cord injury. *Muscle Nerve* 20: 788-799, 1997.

Wang FC, Gerard P, and Bouquiaux O. [Advantages and limitations of the motor unit number estimation techniques]. *Rev Med Liege* 59 Suppl 1: 38-48, 2004.

Yu D. A crash course in spinal cord injury. *Postgrad Med* 104: 109-106, 119, 1998.

Zijdewind I and Thomas CK. Motor unit firing during and after voluntary contractions of human thenar muscles weakened by spinal cord injury. *J Neurophysiol* 89: 2065-2071, 2003.

CHAPTER 3: Spastic tail muscles recover from myofiber atrophy and myosin heavy chain transformations in chronic spinal rats[1]

3.1 INTRODUCTION

Following spinal cord injury (SCI, transection or partial injury), reduced neuromuscular activity leads to myofiber atrophy in muscles innervated below the level of the lesion (Dupont-Versteegden et al. 1998; Lotta et al. 1991), especially when muscle activity is further reduced by spinal cord transections combined with bilateral deafferentation (i.e., spinal isolation; Roy et al. 2000). These muscles typically also undergo transformations in myofiber types and isoforms of the associated myosin heavy chain (MyHC) proteins from slower, fatigue-resistant myofibers to faster, more fatigable myofibers (Dupont-Versteegden et al. 1998; Hartkopp et al. 2003; Lieber et al. 1986a; Roy et al. 2000). Consequently, faster, weaker, and more fatigable muscle contractile properties often result (Cope et al. 1986; Hartkopp et al. 2003; Lieber et al. 1986b; Roy et al. 1999; Roy et al. 2002b).

Interestingly, exercise or muscle activity induced by electrical stimulation attenuates or reverses such detrimental changes in muscle properties following SCI (Dupont-Versteegden et al. 1998; Hartkopp et al. 2003; Kern et al. 2004; Murphy et al. 1999; Roy et al. 1992; Roy et al. 1999; Roy et al. 2002a; Shields and Dudley-Javoroski 2006). That is, generating muscle activity after SCI interrupts the slow-to-fast myofiber transformations and atrophy, and ultimately assists in preserving the normal muscle contractile properties.

Importantly, the classical atrophy and slow-to-fast myofiber transformations associated with SCI (described above) are usually seen in muscles that are rendered relatively inactive (i.e., flaccid paralysis) by the injury (Cope et al. 1986; Dupont-Versteegden et al. 1998; Hartkopp et al. 2003; Lieber et al. 1986a). However, in humans and in some animal models, considerable neuromuscular activity sometimes develops after SCI in the form of spasticity, a syndrome that includes hyperreflexia, hypertonus, and long-lasting spasms (Bennett et al. 2004; Fujimori et al. 1968; Heckman 1994; Kuhn and Macht 1948; Lance and Burke 1974; Ritz et al. 1992; Taylor et al. 1997). Furthermore, preservation of slow (Hidler et al. 2002; Thomas and Ross 1997; Zijdewind and Thomas 2003) and fatigue resistant (Hartkopp et al. 2003) muscle contractile properties has been observed in conjunction with spasticity following SCI in humans. Thus, in principle, this spastic muscle activity that develops after SCI may, like exercise or electrical stimulation (discussed above), act to preserve the normal muscle properties, by interrupting the slow-to-fast myofiber transformation and atrophy. The purpose of the current study was to test this idea in a spinal cord transected rat with spasticity, by examining: (1) whether the classical slow-to-fast myofiber transformation and atrophy occur when *spasticity is not present* (early after transection); (2) whether this myofiber transformation and atrophy are reversed to normal as *spasticity subsequently develops* (long-term transection); and (3)

---

[1] A version of this chapter has been published. Harris RLW, Putman CT, Rank MM, Sanelli L, and Bennett DJ. *J Neurophysiol* 97: 1040-1051, 2007.

whether the classical slow-to-fast myofiber transformation and atrophy persist and become worse when *spasticity is eliminated* by a combination of spinal cord transection and bilateral deafferentation below the transection (spinal isolation).

Recently, it has been shown that following sacral spinal cord transection, rats develop a pronounced spastic syndrome in the segmental muscles of the tail over a period of months (chronic spinal rats; Bennett et al. 1999; Bennett et al. 2001; Bennett et al. 2004). This spasticity is associated with large muscle spasms lasting many seconds that are evoked by brief, normally-innocuous sensory inputs to the tail, such as brushing of the tail on the cage bedding during walking; further, there is ongoing spontaneous EMG activity in the muscles lasting for hours at a time (Bennett et al. 2001). In contrast, following spinal cord transections combined with bilateral deafferentation (spinal isolation), the affected muscles exhibit almost no activity (Pierotti et al. 1991). Thus in the current study we used rat models of spinal cord transection and spinal isolation to evaluate changes in muscle properties with and without spasticity after injury.

In sacral spinal rats the tail muscles are flaccid for the first 2 weeks; then spasticity slowly develops, and the muscles become completely spastic 2-3 months post-injury (Bennett et al. 2004). In response to reduced muscle activity after spinal cord transection in other preparations without spasticity, transformations in rat myofiber types generally occur as early as 1 week after SCI (Dupont-Versteegden et al. 1998), but require months to reach a new steady-state (Talmadge et al. 1999). Thus, if spasticity has the effects hypothesized above, following sacral spinal cord transection in the rat the largest effects of the initial period of reduced activity (i.e., paralysis) should be seen a few months after injury, but not too long after activity (i.e., spasticity) begins to develop. Therefore, as a compromise, we selected a time point 3 months post-injury to study the effects of *relative muscle inactivity* on muscle properties (young chronic spinal rats). To study the full effects of *spasticity* in sacral spinal rats, we evaluated the properties of muscles that had been spastic for many months (completely spastic for 4 months at 7 months post-injury; older chronic spinal rats). Finally, in order to compare the effects of spasticity with the effects of *long-term elimination of muscle activity*, we assessed tail muscle properties in rats that had experienced many months of almost complete neuromuscular silence (7 months of spinal isolation; spinal isolated rats).

We specifically chose to evaluate the SCI-induced changes in the ventrolateral segmental muscles of the tail, because motor unit recordings in these muscles have shown that they are very active in the spastic rat, with spontaneous motor unit firing lasting hours at a time, in association with hypertonus, and bursts of even more intense firing associated with spasms (Bennett et al. 2001). In these segmental tail muscles, we evaluated changes in the distributions of myofiber types and sizes, and the associated MyHC protein isoforms, using immunohistochemistry and gel electrophoresis. Importantly, rat segmental tail muscles have both slow and fast motor units (Harris et al. 2006; Steg 1964), which allowed us to study the effects of SCI and spasticity on slow and fast myofiber types, and ultimately to evaluate transformations between these types. Parts of this work have previously been reported in abstract form (Harris et al. 2005).

3.2 MATERIALS AND METHODS

3.2.1 Animal procedures

Adult, female, Sprague-Dawley rats were used in this study with the approval of the University of Alberta Animal Welfare and Policy Committee and in accordance with the guidelines of the Canadian Council for Animal Care. Respectively, two experimental groups of young (n = 5) and older (n = 9) chronic sacral spinal adult rats were sacrificed at 3 and 7 months after spinal cord transection (spinal cord transection at 2 months of age; see INTRODUCTION for rationale). One experimental group of spinal isolated adult rats (n = 7) was sacrificed at 7 months after spinal isolation (isolation at 2 months of age; age-matched to older chronic spinal rats). Two control groups of young (n = 5, sacrificed at 5 months of age) and older (n = 9, sacrificed at 9 months of age) normal adult rats were age-matched to the injured rats. Some of the chronic sacral spinal rats were the same as those used in earlier studies (Bennett et al. 2004), and within 2-3 months, as previously documented (Bennett et al. 2001; Bennett et al. 2004) according to muscle tone, reflexes, and clonus, spasticity developed in the tail muscles and continued indefinitely. In long-term sacral spinal animals the spasticity rating was always 4/5 or 5/5 (see Bennett et al. 1999, 2004 for further details of the spasticity assessment). In contrast, the tail muscles of the spinal isolated rats were completely areflexive, and unresponsive to any external stimuli (spasticity rating = 0/5).

3.2.2 Spinal cord injury

In the chronic spinal rats, spinal cord transection was performed at the S_2 spinal level under sodium pentobarbital anaesthesia (58 mg/kg body mass) as previously described (Bennett et al. 1999) in adult rats (at 2 months of age). Transection at this S_2 level does not impair hindlimb, bladder, or bowel functions; it only affects tail function.

The spinal isolation procedure was adapted from the previously described sacral spinal cord transection method (Bennett et al. 1999) and modified from models of lumbar spinal isolation in rats and cats (Eldridge 1984; Pierotti et al. 1991; Tower 1937). Specifically, at 2 months of age, in addition to the S_2 spinal cord transection, all the dorsal roots caudal to the transection were cut bilaterally. To this end, a more caudal laminectomy was performed to expose the sacral (S) and caudal (Ca) dorsal roots at their entry points to the spinal cord, and the dura mater was incised above these roots. The sacral S_2-S_4 and all caudal dorsal roots were cut bilaterally and intradurally, taking great care not to damaging the sacral spinal cord, 1-2 mm from their points of entry to the cord. Unlike with lumbar spinal isolation a second, more caudal transection is not required with sacrocaudal spinal isolation, because the caudal cord is the end of the spinal cord

3.2.3 24-hour EMG recordings

Recordings were performed in acutely spinalized animals (2 days post-injury at 2 months of age, n = 5), in older chronic spinal (n = 5) and spinal isolated (n = 7) rats, as well as in older normal animals (age-matched to chronic spinal and spinal isolated rats; n = 5). Subcutaneous EMG electrodes were made using ultra miniature stainless steel medical

wire (fluorocarbon-insulated, total diameter 78 μm; Cooner Wire, Chatsworth CA, part #AS-632), which was threaded through 16 cm-long, 22 gauge needles with blunted and smoothed tips. Each 1 mm end of the wire was deinsulated, and the wires and needles were then sterilized.

Electrodes were inserted while animals were under continuous inhalation anaesthesia with halothane (2% in oxygen). The left lateral surface of the tail was marked at the rostral and caudal borders of the 14th segment of the tail, at which segment the 14th ventrolateral intersegmental tail muscle is located. The skin over the lumbar vertebrae was shaved and disinfected, and a 1.5 cm skin incision was made perpendicular to the vertebral column. A blunt sterile needle was inserted at the incision and threaded under the skin until the tip of the needle could be seen subcutaneously 0.5 mm caudal to the 14th tail segment, on the left side. Then the tail was clamped firmly with thumb and forefinger at this level to maintain the electrode wire tip at this position while the needle was carefully removed. Using this method a second subcutaneous electrode was inserted 0.5 mm rostral to the 14th tail segment on the left side in order to permit bipolar recording. A third subcutaneous electrode was inserted above the 3rd tail segment on the right (opposite) side, and this electrode served as the ground. Each wire (electrode) was labelled immediately after insertion.

The three electrodes were wound once in a 1 cm-diameter loop, which was sutured subcutaneously to the fascia at the level of the incision. This loop served as slack, in order to ensure that the electrodes would not move in the event that tension was accidentally exerted on the external portion of the wire. The incision was sutured, with the free end of the electrodes exiting the skin at one end of the skin closure. The external ends of the electrodes were soldered into machine pins connected to 1 m-long insulated and electrically shielded multiconductor wires (Cooner Wire, Chatsworth CA, part #NMUF 1/30-4046 SJ) that led to a digital data acquisition system. These 1 m-long leads were hung from a spring-loaded pulley system, which ensured that no tension was exerted on the wires, and thus the animal experienced no discomfort.

Upon cessation of anaesthesia, the animal was placed in an open-topped cage with standard base dimensions and 75 cm-high walls. Standard bedding was provided, and food and water were provided *ad libitum*. The animal was monitored continuously by the experimenter throughout the 24-hour recording session. The EMG signal was high pass filtered at 100 Hz with a first order filter to remove movement artifact and 60 Hz noise. Then it was rectified and lowpass filtered at 10 Hz, to determine the envelope of the EMG activity. Finally, it was sampled at 20 Hz by a data aquisition system (Axoscope, Axon Instruments, Union City, CA). Lighting was adjusted according to the animal's regular 12-hour light/dark cycle. When the recording session was complete, the animal was either anaesthetized for tail muscle extraction (see below) or euthanized immediately.

Data were analyzed in consecutive 0.5 hour-long bins. For each animal, Clampfit (Axon Instruments, Union City, CA) was used to measure the baseline-adjusted absolute mean

rectified EMG amplitude in each 0.5 hour-long bin. For each animal these 42 measured means were gain-corrected and averaged to calculate the mean 24-hour EMG amplitude.

3.2.4 Muscle preparation and sectioning

At 3 months after injury (young chronic spinal rats) and at 7 months after injury (older chronic spinal rats and spinal isolated rats) in experimental animals or at corresponding ages in age-matched normals (5 months of age and 9 months of age), animals were anaesthetized with sodium pentobarbital (58 mg/kg body mass) and tail muscles were removed. Specifically, a 2.5-cm-long incision on the left lateral side of the tail exposed the 14th ventrolateral segmental tail muscle. This muscle was completely freed from the underlying bone and from surrounding connective tissue along its entire length and removed. The muscle was coated in Tissue Tek Embedding Medium (Sakura Finetek U.S.A. Inc., Torrance CA) in a cryomold, frozen in liquid nitrogen-cooled, melting isopentane, and immediately stored at -80°C until sectioning. Finally, animals were euthanized with an overdose of sodium pentobarbital. Transverse sections (10 μm thick) were cut from the belly of frozen muscles in a -24°C cryostat following 30 minutes of equilibration at this temperature. Sections were mounted on precleaned Colorfrost Plus slides (Fisher Scientific, Pittsburgh, PA) and stored at -80°C until used for immunohistochemical staining.

3.2.5 Immunohistochemical staining of myofibers with antibodies against myosin heavy chain isoforms

Myofibers were assessed by immunohistochemical staining (Putman et al. 2000; Putman et al. 2003). Primary monoclonal antibodies directed against adult rodent myosin heavy chain (MyHC) isoforms were used to identify individual myofiber types in serial sections (Figure 3-1A-Q): slow type I (clone BA-D5, IgG), fast type IIA (clone SC-71, IgG), and fast type IIB (clone BF-F3, IgM). Primary antibodies against cardiac type Iα myofibers (clone F88-12F8.1, IgG) and embryonic myofibers (clone BF-45, IgG) were used for preliminary staining that revealed no positive reactions in tail muscles from control or experimental animals, and thus were not used further. Immunoreactivity was subsequently localized with biotinylated secondary antibodies (Vector Laboratories, Burlingame, CA): goat anti-mouse IgM directed against clone BF-F3, or horse anti-mouse IgG (rat absorbed, affinity purified) directed against all other primary antibodies. Immunohistochemical staining always included negative control tissue sections to which these biotinylated secondary antibodies were applied without prior application of primary antibodies directed against MyHC isoforms. Color development of sections (Putman et al. 1999) was achieved by incubation in a biotin-avidin horseradish peroxidase complex followed by a buffered mixture of diaminobenzidine (DAB) and hydrogen peroxide (Vector Laboratories, Burlingame, CA). Segmental tail muscle sections were accompanied on every slide by a positive control section from mixed extensor digitorum longus (EDL) hindlimb muscles from normal rats in this study (Figure 3-1R-T).

Stained sections were photomicrographed at 160× in grayscale. Myofibers were assessed in photomicrographs for reactions with antibodies and for cross-sectional area using

Figure 3-1

Representative photomicrographs show immunohistochemical staining of rat segmental tail muscles in serial cross sections. A, B, C: young normal rat. D, E, F: young chronic spinal rat. G, H, J: older normal rat. K, L, M: older chronic spinal rat. N, P, Q: older spinal isolated rat. R, S, T: for reference, sections are shown from an unparalyzed control hindlimb extensor digitorum longus (EDL) muscle from a young normal rat. Sample myofibers marked "I" (type I), "IIA" (type IIA), and "IIB" (type IIB) were identified according to their positive staining reaction with the corresponding myosin heavy chain (MyHC) antibody, as indicated (left hand column: type I, clone BA-D5; middle column: type IIA, clone SC-71; right-hand column: type IIB, clone BF-F3). Sample myofibers marked "IID(X)" (type IID(X)) were identified by the absence of staining reactions with these antibodies (see MATERIALS AND METHODS); this "subtraction" method of staining consistently identified type IID(X) myofibers, as determined by direct comparison to staining patterns observed with clone BF-35 against all MyHCs *except* MyHC IId(x). Bar is 50 μm.

Figure 3-1

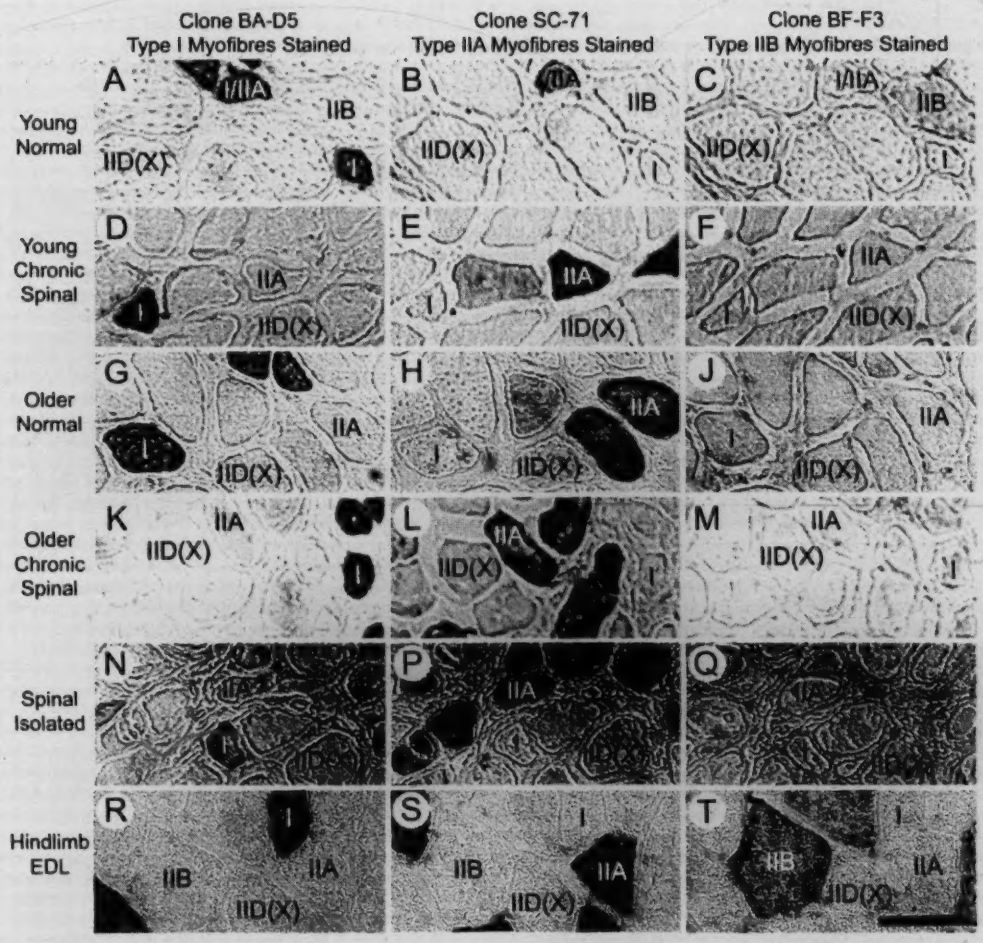
Clone BA-D5
Type I Myofibres Stained
Clone SC-71
Type IIA Myofibres Stained
Clone BF-F3
Type IIB Myofibres Stained
Young Normal
Young Chronic Spinal
Older Normal
Older Chronic Spinal
Spinal Isolated
Hindlimb EDL
A
B
C
D
E
F
G
H
J
K
L
M
N
P
Q
R
S
T
I
IIA
IIB
IID(X)

custom designed image analysis software (Putman et al. 2000). An average of 284±147 myofibers per section was analysed, ensuring adequate myofiber numbers for statistical analyses of myofiber proportions and sizes (McGuigan et al. 2002). Type I, type IIA, and type IIB myofibers were identified by positive staining reactions with the corresponding primary monoclonal antibodies (see above). The absence of staining reactions with this series of antibodies was used to identify type IID(X) (also called type IID, type IID/X, or type IIX) myofibers (Putman et al. 2003). Although this "subtraction" method for the identification of type IID(X) myofibers previously has been reliably applied in rodent hindlimb skeletal muscle using the same antibodies (Rosenblatt and Parry 1992), we wanted to validate the reliability of this approach for the characterization of rat tail muscles. Thus in 10 animals we also used limited quantities of a primary antibody that stains all myofibers *except* type IID(X) myofibers (clone BF-35, IgG). Then, in each animal, we compared the total number of myofibers that could be identified as type IID(X) according to both classifications. When the values obtained from each method were assessed with a paired Student's *t* test across all 10 animals, they were not significantly different ($P > 0.05$); thus we employed the subtraction method for all subsequent analyses.

For each muscle, the number of myofibers expressing a given MyHC isoform was reported as a proportion of the total number of myofibers in that muscle. The cross-sectional area of individual myofibers was calculated by custom designed image analysis software (Putman et al. 2000) using a conversion factor determined from a 1-μm graticule photomicrographed at 160×. The *area density* of each muscle was also determined; that is, the total myofibrillar cross-sectional area that expressed *each isoform* (i.e., the sum of the cross-sectional areas of all myofibers of that type) was reported as a proportion of the total cross-sectional area of *all* the myofibers in that muscle (i.e., the sum of the cross-sectional areas of all the myofibers regardless of type).

3.2.6 Electrophoresis of myosin heavy chain protein isoforms

The relative contents of myosin heavy chain (MyHC) protein isoforms MyHC I, MyHC IIa, MyHC IId(x), and MyHC IIb were determined electrophoretically for each tail muscle (Figure 3-2) as previously described (Putman et al. 2003). Briefly, MyHC protein was extracted from frozen muscle tissue homogenates and separated by SDS-PAGE for 24-hours at 275 V. Gels were silver stained (Oakley et al. 1980). Integrated densitometry (ChemiGenius, GeneSnap™, and GeneTools™, Syngene, Frederick MD) was used to determine individual isoform amounts expressed as relative proportions of the total MyHC protein present in each muscle. A hindlimb medial gastrocnemius muscle sampled from an age-matched control rat in this study was included on each gel as a control for the position of each MyHC protein band (Figure 3-2).

3.2.7 Statistical analyses

All data are reported as means ± standard deviations. Unpaired Student's t tests were used to determine statistical significance between means (SigmaPlot, SPSS, Chicago IL).

Figure 3-2

The relative muscle contents of myosin heavy chain (MyHC) protein isoforms MyHC I, MyHC IIa, MyHC IId(x), and MyHC IIb in protein extracts from whole muscle homogenates were assessed by integrated densitometry following electrophoretic separation of these isoforms on a polyacrylamide gel. Electrophoresis was used to separate MyHC isoforms in segmental tail muscle homogenates, as labelled for representative samples from young normal, young chronic spinal, older normal, older chronic spinal, and older spinal isolated rats. Also, on each gel, a sample extract from a normal rat hindlimb medial gastrocnemius (MG) was used as a positive control to confirm the position of each MyHC band.

Figure 3-2

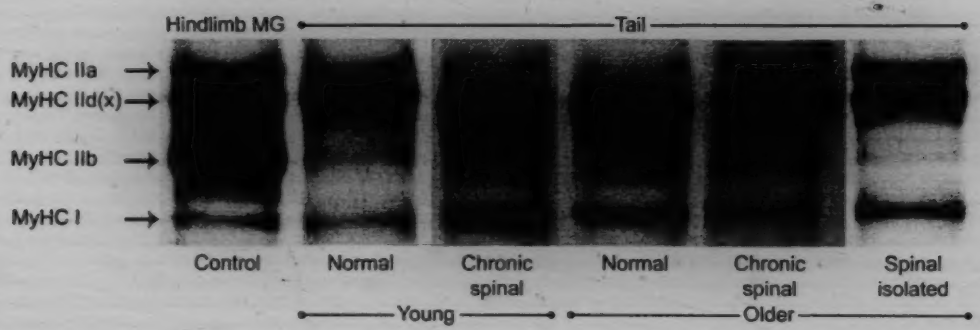
Hindlimb MG
Tail
MyHC IIa
MyHC IId(x)
MyHC IIb
MyHC I
Control
Normal
Chronic spinal
Normal
Chronic spinal
Spinal isolated
Young
Older

Significance was accepted at $P < 0.05$. As required for the t test, normality of the data was verified using a Kolmogorov-Smirnov test ($P < 0.05$).

3.3 RESULTS

3.3.1 Spinal isolation eliminates spasticity

To compare muscle activity in chronic spinal, spinal isolated, and age-matched normal animals, we recorded segmental tail muscle EMG over a 24-hour period in each of these groups of rats (Figure 3-3). In normal rats, daily tail muscle EMG activity was characterized by bursts in association with voluntary movements such as during locomotion (older normal rats, n = 5). These bursts were usually followed by long periods of sustained low-amplitude firing that lasted a few to several minutes in association with maintained postural control of the tail during tasks such as feeding and grooming (Figure 3-3A). In acutely spinalized animals, the tail muscles were virtually silent, exhibiting only rare, low amplitude spontaneous firing that was never sustained (2 days after transection, n = 5; Figure 3-3B), consistent with the flaccid paralysis exhibited by these muscles during the first 2 weeks (Bennett et al. 2004). Even skin stimulation, such as pinch (not shown), could not evoke prolonged spasms. Previously, we have quantified the gradual increase in EMG and reflex evoked muscles spasms that emerge over the first few months after injury (Bennett et al. 2004), and thus this was not repeated here. Relevant to the current study is that muscle properties depend on the activity over the past few months (see INTRODUCTION), and thus muscle properties of young chronic spinal rats suffered the deleterious effects of inactivity early after injury.

Compared to in acute spinal rats, the tail muscles in older chronic spinal animals exhibited a large and significant increase in 24-hour EMG activity (n = 5). There was continuous low-level EMG activity (lasting hours at a time), interspersed with intense EMG activity lasting for several seconds (e.g., at arrow in Figure 3-3C) and associated with tail spasms (i.e., coiling; also see Bennett et al. 1999). This EMG activity and these spasms were evoked by sensory inputs, such as dragging of the tail on the ground during walking and bending/pressing on the tail when the animal sat or slept on it. The EMG activity observed in chronic spinal animals (n = 5) tended to be larger in magnitude than that observed in age-matched normal animals (n = 5), but there was no significant difference between these groups in the tail EMG amplitude averaged over 24-hours (Figure 3-3E). This indicated that muscle activity in chronic spinals was close to that in normals, though abnormally spasm-like in nature.

In the spinal isolated animals, daily EMG activity was similar to that in acutely transected animals, with little or no activity, except for the occasional, brief low-amplitude spontaneous bursts (n = 7; Figure 3-3D). These brief EMG bursts were completely centrally generated, because they could not be evoked by any kind of direct tail stimulation (e.g., pinching, not shown). In summary, acute spinal rats (n = 5) and older spinal isolated rats exhibited no spasticity, and their mean 24-hour EMG amplitudes were significantly lower than both normal and chronic spinal rats (Figure 3-3E).

Figure 3-3

A-D: Representative tail muscle EMG records taken from 24-hour EMG recording sessions. The left-hand column shows typical 10 minute-long records of rectified tail muscle EMG that was recorded from old normal (n = 5; A), acute spinal (n = 5; B), old chronic spinal (n = 5; C), and old spinal isolated (n = 7; D) animals. Note that there is ongoing large-amplitude activity in the normal and chronic spinal animals, while no large-amplitude or continuous activity is observed in acute spinal or spinal isolated animals. In the right-hand column, records on an expanded scale show 30 s-long detail of the activity associated with normal behaviour in normal animals (A), associated with spasticity in chronic spinal animals (C), and associated with the nominal bursts occasionally observed in acutely spinalized (B) and spinal isolated (D) animals. Arrows in the left-hand column indicate t = 0 in the right-hand column. E: the mean 24-hour EMG amplitude is shown for each group (see MATERIALS AND METHODS for calculation). * indicates a significant difference compared to normal. Significant differences were accepted at $P < 0.05$.

Figure 3-3

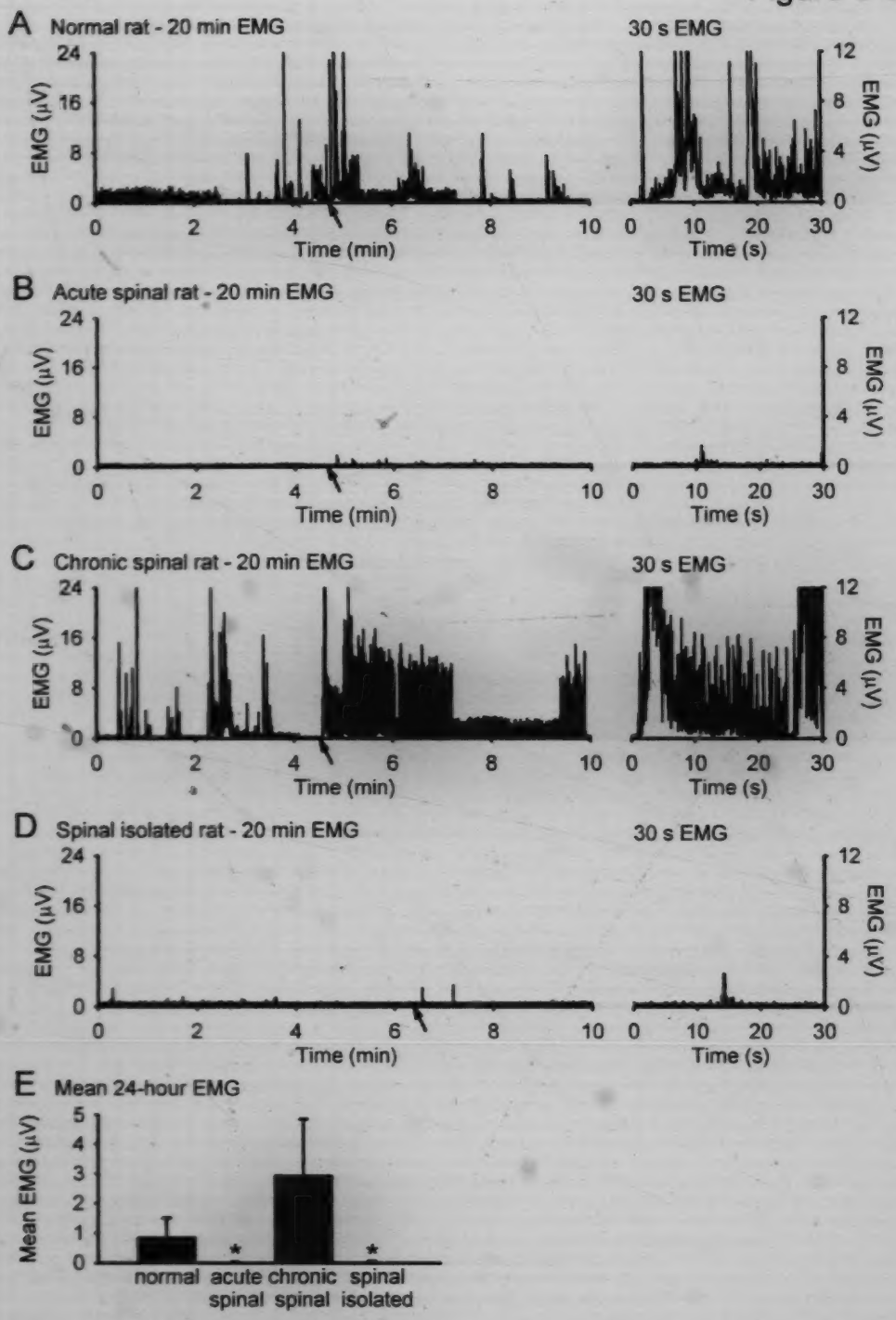
A
Normal rat - 20 min EMG
30 s EMG
EMG (μV)
Time (min)
Time (s)
B
Acute spinal rat - 20 min EMG
30 s EMG
C
Chronic spinal rat - 20 min EMG
30 s EMG
D
Spinal isolated rat - 20 min EMG
30 s EMG
E
Mean 24-hour EMG
Mean EMG (μV)
normal
acute spinal
chronic spinal
spinal isolated

3.3.2 Myofiber composition is not affected by differences in the ages of the rats studied

The segmental tail muscles of normal rats were of mixed myofiber distribution (Figure 3-1A-C, G-J). In young normal rats (5 months of age, n = 5), we observed myofiber proportions of 15.9±3.5% slow type I, 18.7±10.7% fast type IIA, 60.8±12.6% fast type IID(X), and very little fast type IIB (2.3±1.3%; Figure 3-4A-D). Hybrid type I/IIA myofibers were negligible (1.5±1.7%, not significantly different from zero). In older normals (9 months of age, n = 9), the distribution of myofibers was not significantly different from that in young normals (Figure 3-4A-D), and thus there was no age effect observed between our two normal groups, which were age-matched to our young and older chronic spinal rats. As a positive control, we assessed the mixed fast twitch hindlimb extensor digitorum longus muscle (Figure 3-1R-T), which displayed a myofiber distribution (not shown, n = 5) of 10.1±3.8% type I, 25.1±1.9% type IIA, 28.5±4.1% type IID(X), 28.3±2.6% type IIB, and 8.0±2.0% hybrid type I/IIA. These values were similar to previous descriptions of extensor digitorum longus myofiber proportions (Bamford et al. 2003; Dupont-Versteegden et al. 1998; Putman et al. 2000).

3.3.3 Transformation toward a faster myofiber composition early after spinal cord transection is reversed by prolonged spasticity

After sacral spinal cord transection in adult rats, segmental tail muscles demonstrated flaccid paralysis for 2 weeks, and then over the subsequent 2-3 months these muscles gradually developed complete spasticity. Thus, young chronic spinal rats (3 months post-injury) had experienced a 3-month period of relatively reduced tail muscle activity, whereas older chronic spinal rats (7 months post-injury) had experienced a long-term augmentation of tail muscle activity due to 4 months of complete spasticity. A transformation toward a faster myofiber type distribution was associated with this latter period of relative inactivity in young chronic spinal rats. Specifically, in young chronic spinal rats (n = 5), the proportion of slow type I tail myofibers was significantly lower than in age-matched young normals (n = 5; Figure 3-4A), while the proportion of fast type IID(X) myofibers (the dominant myofiber type) was significantly higher than in young normals (Figure 3-4C). The mean proportions of type IIA and type IIB myofibers did not change significantly. This type I to type IID(X) myofiber transformation was reversed with the 4 months of complete spasticity experienced by the older chronic spinal rats. Specifically, in older chronic spinal rats (n = 9), proportions of both slow type I myofibers (Figure 3-4A) and fast type IID(X) myofibers (Figure 3-4C) were not significantly different from those in age-matched older normals (n = 9). In summary, in young chronic spinal rats, a transformation toward faster myofiber types was associated with reduced activity and was apparent in tail muscles after 3 months of injury, whereas older chronic spinal rats that were injured for 7 months and completely spastic for 4 months exhibited a recovery from reduced activity-associated alterations in myofiber types. Hybrid myofibers did not emerge after 3 or 7 months of spinal cord transection.

A slow-to-fast myofiber type transformation was associated with the 7 months of near-elimination of muscle activity after spinal isolation. Specifically, in spinal isolated rats (n = 7) there were a significant decrease in the proportion of type I myofibers (Figure 3-4A)

Figure 3-4

A-D: the mean proportion of each myofiber type is shown for young normals (n = 5) and young chronic spinal rats (n = 5; white bars), older normals (n = 9) and older chronic spinal rats (n = 9; black bars), and older spinal isolated rats (n = 7; grey bars), as determined from immunohistochemical staining of frozen muscle sections (cf. Figure 3-1; values of "n" supplied here apply in all subsequent figures). E-H: also shown are percent changes (see RESULTS for calculation) in myofiber type proportions in young chronic spinal rats relative to age-matched young normals (YC, white bar), in older chronic spinal rats relative to age-matched older normals (OC, black bar), and in older spinal isolated rats (SI, grey bar) relative to age-matched normals. A, E: slow type I. B, F: fast type IIA. C, G: fast type IID(X). D, H: fast type IIB. Please note that in A, B, and D the y-axis extends to 60%, whereas in C the y-axis extends to 100%. *Note*: the following statisical symbols apply here and in the subsequent Figures 5 and 7. * represents a significant difference between each chronic experimental group and its age-matched normal group (A-D), or a significant difference from zero in the percent change of an injured experimental group relative to its age-matched normal group (E-H). ‡ represents a significant difference between the old spinal isolated group and the old chronic spinal group (A-D) and between the percent changes in these groups relative to their age-matched old normal group (SI vs. OC in E-H). Significant differences were accepted at $P < 0.05$.

Figure 3-4

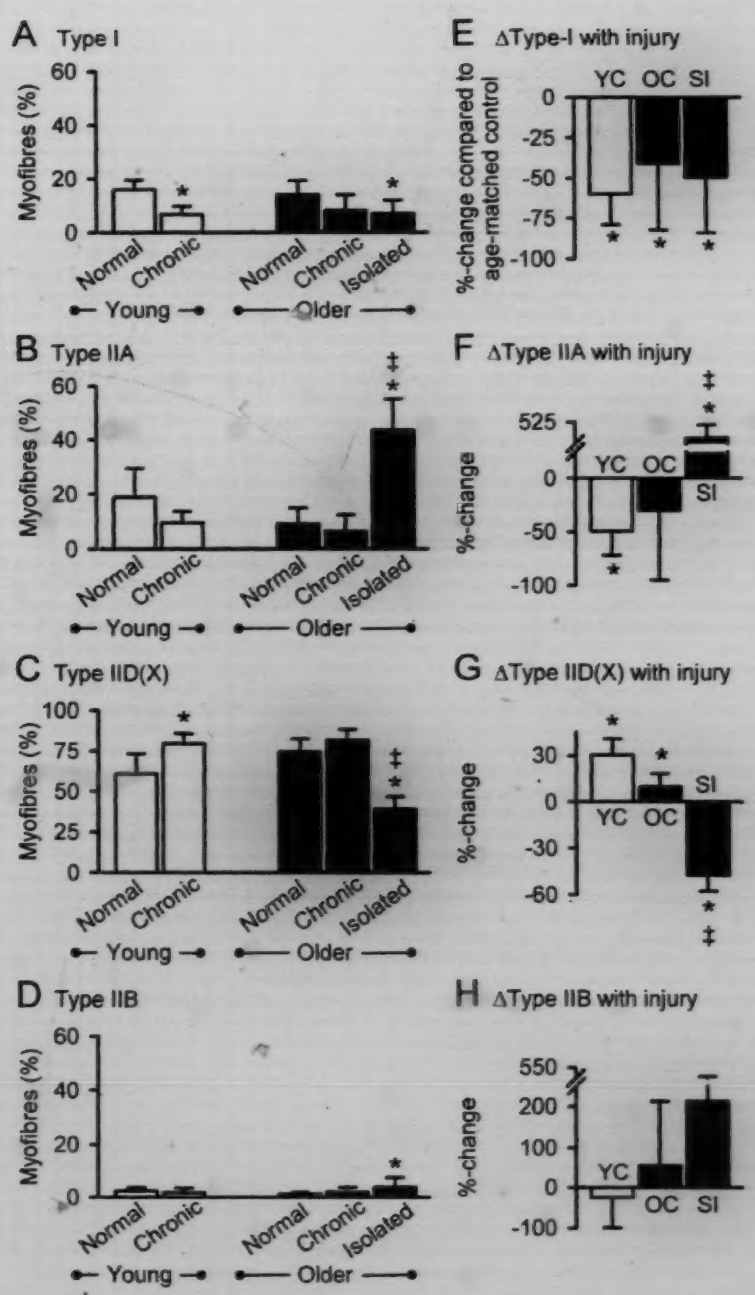
A Type I
Myofibres (%)
60
40
20
0
Normal
Chronic
Normal
Chronic
Isolated
Young
Older
B Type IIA
Myofibres (%)
C Type IID(X)
Myofibres (%)
100
75
50
25
D Type IIB
Myofibres (%)
E ΔType-I with injury
%-change compared to age-matched control
YC OC SI
0
-25
-50
-75
-100
F ΔType IIA with injury
%-change
525
G ΔType IID(X) with injury
%-change
30
-30
-60
H ΔType IIB with injury
%-change
550
200
100

and significant increases in the proportions of both type IIA and type IIB myofibers (Figure 3-4B, D). Interestingly, there was also a significant reduction in the proportion of the normally dominant type IID(X) myofibers (Figure 3-4C), which apparently transformed to type IIA myofibers (Figure 3-4B) for unknown reasons. Also, in spinal isolated rats a small proportion of hybrid type I/IIA myofibers emerged (coexpressing both MyHC I and MyHC IIa isoforms, not shown; 4.5±3.4%, significantly different from 0).

Mean myofiber proportions were not significantly different in young normals, compared to in older normals, consistent with previous evidence that there should be no differences in myofiber proportions among adult animals of these ages (Ansved and Larsson 1989). However, there tended to be a discrepancy between these two groups for type IIA and type IID(X) myofibers (Figure 3-4B, C). Thus, despite the absence of a significant age effect between these normal groups, we wanted to account for the potentially confounding effects of age on altered myofiber proportions. To this end, the percent change in myofiber proportion (Y) for each young chronic spinal rat was computed relative to the mean myofiber proportion (Z) in age-matched young normal rats (see Figure 3-4E-H, white bars); that is, the percent change = $(Y - Z) / Z \times 100\%$. Likewise, myofiber proportions from older chronic spinal rats (Figure 3-4E-H, black bars) and from spinal isolated rats (Figure 3-4E-H, grey bars) were expressed as percent changes with respect to age-matched old normals. In young chronic spinal rats, the mean percent changes in myofiber proportions relative to in young normal rats were large and significantly different from zero, with a -60.0±19.1% decrease in type I, a -49.7±22.3% decrease in type IIA, and a +30.5±10.3% increase in type IID(X) myofiber proportions with injury (Figure 3-4E, F, G). In older chronic spinal rats with spasticity these percent changes in myofiber proportions tended to be much smaller in magnitude compared to in young chronic spinal rats; specifically, the percent change in type IIA myofibers was reduced so much that it was no longer significantly different from zero (Figure 3-4F), indicating a substantial recovery of type IIA proportions in spastic tail muscles. Furthermore, in older chronic spinal rats with spasticity the percent change in type IID(X) was only +9.7±8.6%, which was significantly smaller than the percent change in type IID(X) for young chronic spinal rats (+30.5±10.3%, Figure 3-4G). In contrast, in spinal isolated rats there was a +376.3±124.9% increase in the type IIA myofiber proportion relative to normal and there was a -47.5±2.3% decrease in the type IID(X) myofiber proportion, and these values were both significantly different from zero and significantly different from the changes observed for old chronic spinal rats. This demonstrates a much different effect associated the with long-term increased muscle activity due to spasticity after chronic spinal cord transection, compared to the long-term near-elimination of activity after chronic spinal isolation. In all injured groups, the large variability in the percent changes in type IIB myofiber proportions (Figure 3-4H) occurred because these myofibers were so infrequently observed (Figure 3-4D).

Overall, the observed myofiber distributions and changes due to SCI suggest that muscles initially exhibiting flaccid paralysis (young chronic spinal rats) demonstrated a modest transformation toward faster myofibers, and muscles experiencing a long-term near-elimination of activity (older spinal isolated rats) demonstrated a persistence of this slow-

to-fast myofiber type transformation. However, 4 months of complete spasticity (older chronic spinal rats) resulted in a partial re-establishment of the normal distribution of myofiber types.

3.3.4 Tail myofiber size is not affected by differences in the ages of the rats studied

The mean cross-sectional area of all the myofibers that were assessed in segmental tail muscles from young normals (n = 5) was 1474±714 μm^2 (min = 270 μm^2, max = 5604 μm^2). Myofibers from older normals (n = 9) were of similar size (mean = 1615±797 μm^2, min = 135 μm^2, max = 5049 μm^2), and the mean sizes of individual myofiber types were not significantly different from young normals (Figure 3-5A-D); thus, there was no effect of age on tail myofiber size in normal adult rats. In normal hindlimb extensor digitorum longus muscles from these same animals, the mean cross-sectional area of myofibers was 2096±972 μm^2 (min = 463 μm^2, max = 7407 μm^2), similar to that reported previously (Dupont-Versteegden et al. 1998; Lieber et al. 1986a). Consistent with previous assessments of myofibers from a wide selection of rat skeletal muscles of various locations and serving a variety of functions (Bamford et al. 2003; Delp and Duan 1996), both tail muscles and hindlimb extensor digitorum longus muscles demonstrated mean myofiber cross-sectional areas ranked type I < type IIA < type IID(X) < type IIB.

3.3.5 Myofibers atrophy early after spinal cord transection but recover with prolonged spasticity

Tail muscles exhibited significant myofiber atrophy early after spinal cord transection (young chronic spinal rats, n = 5; for all myofibers: mean = 683±250 μm^2, min = 118 μm^2, max = 1805 μm^2). Specifically, slow type I, fast type IIA, fast type IID(X), and fast type IIB tail myofibers in young chronic spinal rats were all significantly atrophied compared to in young normals (Figure 3-5A-D). However, 4 months of complete tail muscle spasticity was associated with a substantial recovery from myofiber atrophy (older chronic spinal rats, n = 9; for all myofibers: mean = 1054±514 μm^2, min = 101 μm^2, max = 3710 μm^2). Specifically, the type I, type IIA, and type IIB myofibers in older chronic spinal rats recovered from atrophy in that they were significantly larger than in young chronic spinal rats and were not significantly smaller than in older normals (Figure 3-5A, B, D). Type IID(X) myofibers also recovered in older chronic spinal rats in that they were significantly larger than in young chronic spinal rats, although they remained significantly smaller than in older normals (Figure 3-5C). Interestingly, the type IID(X) myofibers are the dominant myofiber type in this muscle and, with the exception of the infrequently observed type IIB myofibers, are likely to be in the highest threshold motor units and thus least active during spasticity. This partial recovery from atrophy of type IID(X) myofibers is also consistent with previous observations that following periods of reduced muscle activity, the predominant myofiber type tends to exhibit the greatest atrophy (Ohira et al. 2002).

In contrast to the recovery of myofiber size observed with spasticity, there was no recovery from atrophy with long-term near-elimination of muscle activity after spinal isolation (spinal isolated rats, n = 7; for all myofibers: mean = 508±328 μm^2, min = 53

Figure 3-5

A-D: the mean cross-sectional area of each myofiber type for young normals and young chronic spinal rats (white bars), older normals and older chronic spinal rats (black bars), and older spinal isolated rats (grey bars) is shown in units of cross-sectional area (μm^2), as determined from immunohistochemical staining of frozen muscle sections (cf. Figure 3-1). E-H: also shown are percent changes (see RESULTS for calculation) in myofiber cross-sectional area in young chronic spinal rats relative to in age-matched young normal rats (YC, white bar), in older chronic spinal rats relative to in age-matched older normals (OC, black bar), and in older spinal isolated rats relative to in age-matched normals (SI, grey bar). Format, statistical symols, and values of "n" are the same as that in the previous Figure 3-4. Significant differences were accepted at $P < 0.05$.

Figure 3-5

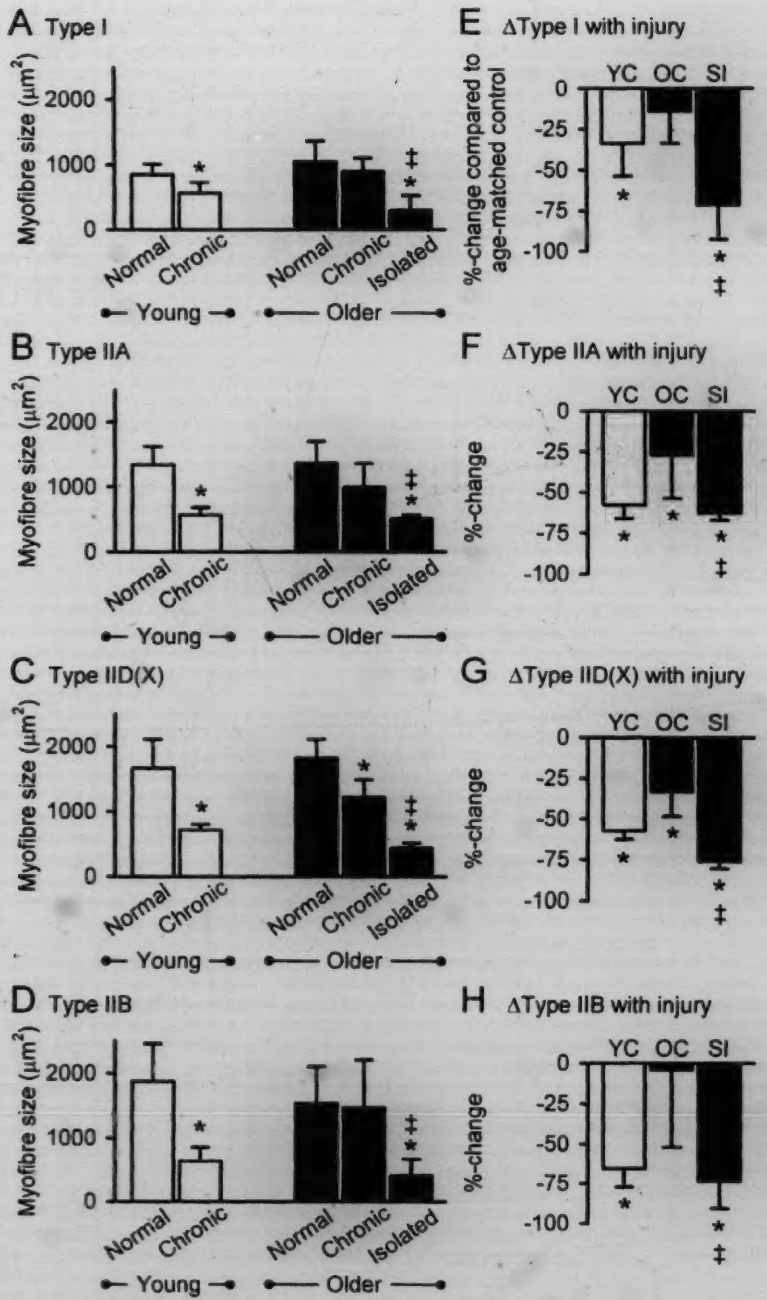
A Type I
Myofibre size (μm²)
2000
1000
0
Normal
Chronic
Normal
Chronic
Isolated
Young
Older
B Type IIA
C Type IID(X)
D Type IIB
E ΔType I with injury
%-change compared to age-matched control
YC
OC
SI
0
-25
-50
-75
-100
F ΔType IIA with injury
%-change
G ΔType IID(X) with injury
H ΔType IIB with injury

μm^2, max = 2302 μm^2). Specifically, myofibers of all types in spinal isolated rats were atrophied compared to in age-matched old normal and old chronic spinal rats (Figure 3-5A-D). These data indicate that reduced muscle activity is associated with tail myofiber atrophy 3 months after spinal cord transection, and this association of reduced muscle activity with myofiber atrophy is also apparent 7 months after spinal isolation. In contrast, prolonged spasticity after spinal cord transection is apparently associated with a persistent increase in muscle activity that promotes recovery of myofiber size via compensatory hypertrophy.

We wanted to account for the potentially confounding effects of age on altered myofiber cross-sectional areas; to this end, the percent changes in myofiber sizes in injured rats were computed relative to age matched normal rats, as also done for myofiber proportions (see above). In young chronic spinal rats, these percent changes in myofiber size were large and significantly different from zero, with decreases of -33.9±19.9% for type I, -57.7±8.5% for type IIA, -57.6±5.3% for type IID(X), and -65.8±11.5% for type IIB myofibers (Figure 3-5E-H), again suggesting considerable atrophy compared to in young normal rats. Myofibers recovered from this atrophy in older chronic spinal rats with spasticity; specifically, the percent changes in the sizes of type I and of type IIB myofibers were no longer significantly different from zero (Figure 3-5E, H). Moreover, the percent changes in the sizes of type IIA and type IID(X) myofibers from older chronic spinal rats relative to normal were reduced to -27.1±26.8% and -33.6±15.1%, respectively (Figure 3-5F, G), significantly less than the percent changes for atrophied type IIA and type IID(X) myofibers in young chronic spinal rats relative to normal (-57.7±8.5% and -57.6±5.3% respectively). In contrast, in spinal isolated rats the percent changes (decreases) in cross-sectional area for all myofiber types were both significantly different from zero and significantly larger than the relatively small percent decreases observed in old chronic spinal rats relative to normal (Figure 3-5E-H).

Myofiber cross-sectional areas were further analyzed for normal and injured rats by separating myofibers into bins 500 μm^2 in size, as shown in Figure 3-6 (i.e., 1-500 μm^2, 501-1000 μm^2, and so on, up to 3501-4000 μm^2; the top of each range is specified on the x-axis throughout Figure 3-6, and all bins are listed in the Figure 3-6 caption). Since myofibers with cross-sectional areas greater than 4000 μm^2 were observed in very low proportions, axes extend only to 4000 μm^2 (Figure 3-6).

Tail myofiber size distributions were broadly right-skewed with peaks at 1001-1500 μm^2 in both young and older normals (Figure 3-6A and B). Overall in these normal rats, the majority of myofibers were less than 1500 μm^2, although very few myofibers were observed in the smallest 1-500 μm^2 bin. No large differences due to age were apparent in older normals (Figure 3-6B) compared to in young normals (Figure 3-6A).

In young chronic spinal rats compared to in young normals, the distribution of myofiber sizes narrowed substantially, becoming more bell-shaped and shifting leftward, with the peak at 501-1000 μm^2 and the majority of myofibers less than 1000 μm^2 (Figure 3-4C). In older chronic spinal rats, although the peak of the distribution remained at 501-1000 μm^2, the proportion of myofibers in this bin was much smaller than in young chronic

Figure 3-6

The mean myofiber cross-sectional areas shown in Figure 3-5 are detailed according to size distributions in the following bins of 500 μm^2 each: 1-500 μm^2, 501-1000 μm^2, 1001-1500 μm^2, 1501-2000 μm^2, 2001-2500 μm^2, 2501-3000 μm^2, 3001-3500 μm^2, and 3501-4000 μm^2. A: young normals, white bars. B: older normals, black bars. C: young chronic spinal rats, white bars. D: older chronic spinal rats that had complete spasticity for 4 months, black bars. E: older spinal isolated rats that had near-elimination of muscle activity for 7 months, grey bars. See Figure 3-4 caption for values of "n." Inset values show minimum, maximum, and mean myofiber size for each group (standard deviations are found in the text of the RESULTS).

Figure 3-6

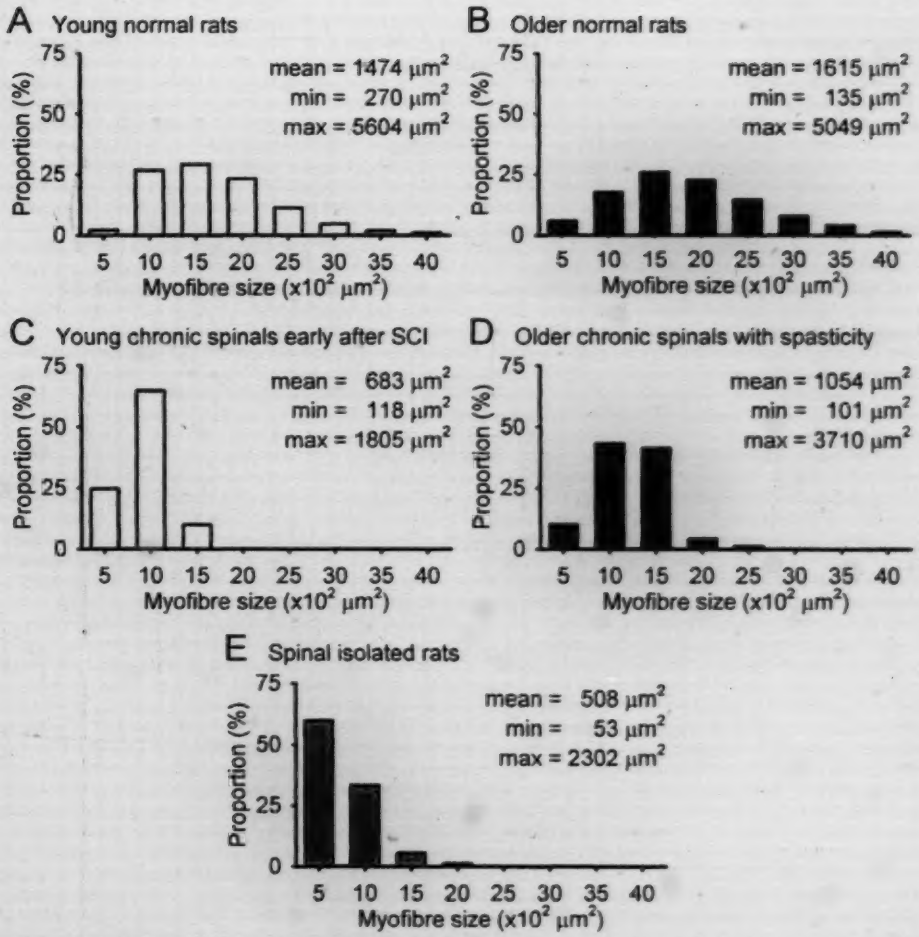
A Young normal rats
mean = 1474 μm²
min = 270 μm²
max = 5604 μm²
B Older normal rats
mean = 1615 μm²
min = 135 μm²
max = 5049 μm²
C Young chronic spinals early after SCI
mean = 683 μm²
min = 118 μm²
max = 1805 μm²
D Older chronic spinals with spasticity
mean = 1054 μm²
min = 101 μm²
max = 3710 μm²
E Spinal isolated rats
mean = 508 μm²
min = 53 μm²
max = 2302 μm²
Proportion (%)
0
25
50
75
5 10 15 20 25 30 35 40
Myofibre size (x10² μm²)

spinal rats, and the distribution was recovered closer to normal (peak shifted back toward the right) with increased numbers of larger myofibers; specifically, the proportion of myofibers that were 1001-1500 μm^2 more than quadrupled in older chronic spinals compared to in young chronic spinals (Figure 3-6C, D). In contrast, the myofiber size distribution for spinal isolated rats was sharply right-skewed compared to chronic spinal rats, and the majority of myofibers were less than 500 μm^2 (Figure 3-6E).

Interestingly, a relatively large population of very small myofibers appeared early after injury in young chronic spinal rats (~25% of myofibers 1-500 μm^2; Figure 3-6C). Yet associated with 4 months of complete spasticity in older chronic spinal rats, hypertrophy resulted in a substantial decrease in the number of these very small myofibers (~10% of myofibers 1-500 μm^2; Figure 3-6D). However, in spinal isolated rats, these small myofibers accounted for ~65% of all myofibers (Figure 3-6E). In all injured rats, these small myofibers appeared in every myofiber type, but did not express embryonic myosin heavy chain (MyHC) and had normal morphological appearance, indicating that they were neither newly formed nor necrotic.

3.3.6 Electrophoretically-determined MyHC isoform content and computed area density are stable with long-term spinal cord transection and spasticity

The proportions of MyHC isoforms were assessed by gel electrophoresis (Figure 3-2). When young normals (n = 5) were compared to older normals (n = 9), there were no significant age-related differences in the relative muscle contents of MyHC I, MyHC IIa, MyHC IId(x), or MyHC IIb as assessed by integrated densitometry following gel electrophoresis (Figure 3-7A-D). Likewise, comparing young chronic spinal rats (n = 5) to young age-matched normals there were no significant differences early after injury in the relative contents of MyHC I, MyHC IId(x), or MyHC IIb proteins (Figure 3-7A, C, D), but there was a significant decrease in the relative content of MyHC IIa protein (Figure 3-7B). Comparing older chronic spinal rats (n = 9) to age-matched older normals there were no significant differences after prolonged spasticity in the relative contents of MyHC I, MyHC IIa, MyHC IId(x), or MyHC IIb proteins (Figure 3-7A-D). Comparing spinal isolated rats (n = 7) to both age-matched old normals and old chronic spinal rats there was a significant increase in the relative content of MyHC IIa (Figure 3-7B) and a significant decrease in the relative content of MyHC IId(x) (Figure 3-7C), as similarly observed for the proportion of myofibers expressing these isoforms (Figure 3-4), but there were no changes in the relative contents of either MyHC I or MyHC IIb (Figure 3-7A, D).

The MyHC isoform contents determined from gel electrophoresis correspond to the combined influence of both myofiber proportion and myofiber cross-sectional area. Specifically, MyHC isoform contents correspond to the *area density*, which is defined as the total myofibrillar cross-sectional area expressing each isoform in a given muscle, reported as a proportion of the total cross-sectional area of all the myofibers in that muscle (Fry et al. 1994; Hansen et al. 2004). Mathematically, the area density of a given MyHC isoform (or myofiber type) is equivalent to the *product* of the myofiber proportion of that type (Figure 3-4A-D) and the mean cross-sectional area of that myofiber type

Figure 3-7

A-D: the relative muscle content of each myosin heavy chain (MyHC) isoform is shown for young normals and young chronic spinal rats (white bars), older normals and older chronic spinal rats (black bars), and older spinal isolated rats (grey bars), as determined by integrated densitometry following electrophoretic separation of these MyHC isoforms on a polyacrylamide gel (cf. Figure 3-2). E-H: the area densities of the corresponding MyHC isoforms are shown as computed from immunohistochemical staining of frozen muscle sections (see RESULTS for calculation). A, E: MyHC I. B, F: MyHC IIa. C, G: MyHC IId(x). D, H: MyHC IIb. The values of "n" and formats for A-D and for E-H are the same as that for Figure 3-4A-D, except that in 7B and 7F the vertical scale extends to 75%. Significant differences were accepted at $P < 0.05$.

Figure 3-7

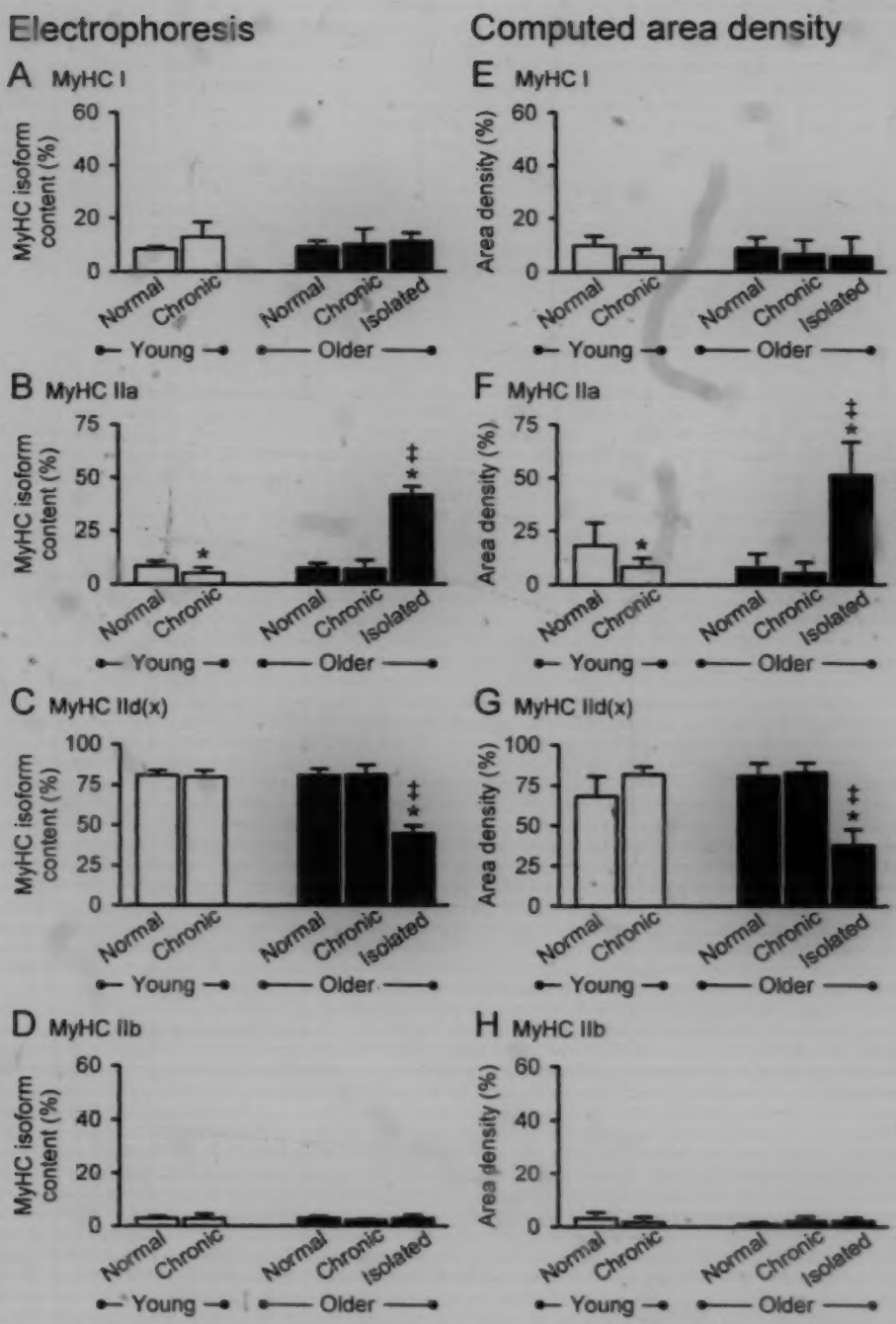
Electrophoresis
Computed area density
A MyHC I
E MyHC I
B MyHC IIa
F MyHC IIa
C MyHC IId(x)
G MyHC IId(x)
D MyHC IIb
H MyHC IIb
MyHC isoform content (%)
Area density (%)
Normal
Chronic
Isolated
Young
Older

(Figure 3-5A-D), *normalized* to the mean cross-sectional area of all myofibers. As with electrophoresis, immunohistochemical stains showed no significant changes in these computed area densities for MyHC I or MyHC IIb with age or injury (Figure 3-7E, H); however, as also observed with electrophoresis, in young chronic spinal rats (n = 5) compared to in young normals (n = 5) the MyHC IIa area density was decreased (Figure 3-7F), and in spinal isolated rats (n = 7) compared to in both age-matched old normals (n = 9) and old chronic spinal rats (n = 9) the MyHC IIa area density was increased and the MyHC IId(x) area density was decreased (Figure 3-7F, G).

3.4 DISCUSSION

3.4.1 Spasticity promotes recovery from myofiber atrophy after chronic spinal cord transection

Our results from adult rats with sacral spinal cord transection demonstrate that early after spinal cord transection, tail myofibers are atrophied relative to age-matched normals, likely due to flaccid paralysis during the early period after spinal cord transection. Following long-term spasticity in older chronic spinal rats tail myofibers recover from this atrophy. This myofiber size recovery is nearly complete for all myofiber types with the exception of the type IID(X) myofibers, which, interestingly, should represent the highest threshold motor units and thus be the least active during spasticity. This recovery is due to spastic muscle activity; because when spasticity is eliminated by cutting the dorsal roots bilaterally in addition to transecting the cord (spinal isolation), atrophy then only further increases with time after injury. These results are consistent with previous findings indicating that following long-term SCI recovery from myofiber atrophy occurs with exercise-induced muscle activity (Crameri et al. 2004; Dupont-Versteegden et al. 1998; Roy et al. 1999; Roy et al. 1998). Previously, we have shown that spastic tail muscle activity results from a spontaneous recovery of motoneuron excitability following injury, combined with exaggerated reflex-evoked synaptic inputs to motoneurons (Bennett et al. 2004) and thus, ultimately, muscle properties are indirectly linked to changes in motoneuron properties.

3.4.2 Spasticity opposes transformation of myofiber types after chronic spinal cord transection

Our results also demonstrate that, early after spinal cord transection, tail muscles in young chronic spinal rats undergo a modest transformation in their myofiber types toward faster MyHC isoforms compared to in young normal rats, with smaller proportions of slow type I myofibers and larger proportions of fast type IID(X) myofibers, consistent with the classic effects of reduced muscle activity (Roy et al. 2000; Talmadge et al. 1999). Again, after 4 months of complete spasticity in older chronic spinal rats, these proportions recover to no different from in age-matched older normal rats. The magnitudes of transformation in young chronic spinal rats and of recovery in older chronic spinal rats are small due to the already high proportion of fast type IID(X) myofibers in normal rats. However, the relative changes in type I and type IIA myofiber proportions early after injury are very large (reduced to approximately half of young

normal). Again, this recovery is due to spastic muscle activity, since eliminating spasticity in the spinal isolated animals eliminates the recovery and only further augments the slow-to-fast myofiber type transformation.

Unexpectedly following spinal isolation, within the fast type II myofiber population, there is a large decrease in the proportion of type IID(X) myofibers and a large increase in the proportion of type IIA myofibers, which is not consistent with observations of other muscles after spinal isolation (Roy et al. 2000), but which may be associated with altered muscle loading (see below). Associated with this there is an emergence of type IIB and hybrid type I/IIA myofibers that were very low in number or absent in all other conditions. There is also an emergence of many more very small myofibers, which are neither regenerating (no embryonic MyHC) nor necrotic (normal morphology). Thus this seems to be a stable tail muscle phenotype after long-term sacral spinal isolation in the adult rat.

3.4.3 Recovery of myofiber types and myofiber morphology resembles the effects of exercise

It is well-documented that, in the absence of muscle activity, myofibers often transform robustly toward faster, more fatigable types and undergo considerable atrophy (Roy et al. 2002a). Early after spinal cord transection and after long-term spinal isolation in our rats, reduced muscle activity results in a similar atrophy and decrease in type I myofiber type proportions, as seen in our results.

It is also well-documented that following SCI (in animals and humans), cauda equina injuries (in humans), and spinal isolation (in animals), reflex-generated exercise or direct electrical stimulation of muscle nerves induces recovery from myofiber atrophy in both primarily slow and primarily fast muscles, and also opposes transformations in myofiber types toward faster isoforms (Dupont-Versteegden et al. 1998; Hartkopp et al. 2003; Kern et al. 2004; Murphy et al. 1999; Roy et al. 1999; Roy et al. 2002a; Shields and Dudley-Javoroski 2006). Thus the recovery of myofiber sizes and proportions in chronic spinal rats with long-term spasticity resembles the effects of training interventions that provide muscle activity following central nervous system lesions in animals and humans. Consistent with previous evidence, the recovery we observe in both myofiber types and myofiber size is not associated with changes in myofibers due to age (Ansved and Larsson 1989; Putman et al. 2001), as described in the RESULTS, and *is* associated with spasticity because the recovery is eliminated when spasticity is eliminated by sectioning the dorsal roots in addition to transecting the spinal cord (spinal isolation). Taken together, our histochemical and 24-hour EMG results from older chronic spinal rats *and* their age-matched older spinal isolated rats demonstrate that spasticity provides sufficient muscle activity to promote the recovery from reduced activity-dependent changes early after injury.

The mechanical consequences of the histological changes we observed in myofibers should be that, early after injury, the muscles are weaker, faster, and more fatigable, as seen in previous investigations (Cope et al. 1986; Hartkopp et al. 2003; Lieber et al.

1986b; Roy et al. 1999). Furthermore, with long-term injury and spasticity, compared to the earlier deleterious adaptations, muscles should recover their force-generating capability, become slower, and become less fatigable, consistent with previous investigations in humans that indicate a role for spasticity in preserving slower muscle contractile properties (Hartkopp et al. 1999; Hidler et al. 2002; Thomas 1997; Zijdewind and Thomas 2003). The actual changes in tail muscle contractile properties in chronic spinal rats with long-term spasticity, which include a slowing of muscle contractile speed and an increase in muscle twitch force, but losses of fatigue-resistance and of tetanic force, are explored in a companion study (Harris et al. 2006).

3.4.4 Rat segmental tail muscles can be reliably assessed with routine immunohistochemical staining and gel electrophoresis

Our study is the first to report myofiber type composition, MyHC isoform distributions, and myofiber size in the segmental tail muscles of the rat. The prominent features of these muscles are: small myofibers, a high proportion of type IID(X) myofibers, and a conspicuous absence of both type IIB and hybrid myofibers (approximately 15% type I, 15% type IIA, 67.5% type IID(X), 2.5% type IIB, and no hybrids). In contrast, hindlimb muscles such as the extensor digitorum longus (EDL, stained as positive control in our study) often have: larger myofibers, fewer type IID(X) myofibers, and numerous type IIB and hybrid myofibers (approximately 10% type I, 25% type IIA, 30% type IID(X), 30% type IIB, and 5% hybrids for EDL in this study).

Importantly, the close agreement of our immunohistochemical and electrophoretic methods shows that tail myofibers can be reliably assessed by immunohistochemistry, and this is especially important for type IID(X) myofibers, which we quantified indirectly by counting myofibers that are not immunostained (subtraction method). Further validation of our methodology for assessing rat segmental tail muscles is derived from the close agreement between the results of our subtraction method and those of our immunostaining with clone BF-35 (a monoclonal primary antibody that labels all MyHC isoforms *except* MyHC IId(x); see MATERIALS AND METHODS) in the identification of type IID(X) myofibers, as well as from the close agreement of our histochemical evaluation of the positive control hindlimb EDL muscle with that performed in previous studies (Bamford et al. 2003; Delp and Duan 1996; Dupont-Versteegden et al. 1998; Lieber et al. 1986a; Putman et al. 2000).

Although hybrid myofibers are often present in muscles transforming both to slower and to faster distributions of myosin heavy chain (MyHC) isoforms and myofibers (Putman et al. 2001; Talmadge et al. 1999), there are no hybrid type I/IIA or hybrid type IIA/B myofibers in normal rat tail muscles or following spinal cord transection alone. The lack of hybrid myofibers in tail muscles in this study is not a result of limitations in our methodology since we observe the expected number of hybrid myofibers in the normal hindlimb EDL muscle, which is used as a positive control. Moreover, a small but significant proportion of hybrid type I/IIA myofibers does emerge in tail muscles following spinal isolation. This is consistent with the idea that the sacrocaudal spinal isolation (sacral spinal cord transection combined with bilateral sacrocaudal

deafferentation) results in a drastic long-term reduction of neuromuscular activity among tail motor units, just as a more rostral lumbar spinal isolation (bilateral lumbar deafferentation between transections at low thoracic and high sacral levels) dramatically reduces muscle activity in rats and cats (Pierotti et al. 1991; Roy et al. 2000). No antibody specific for MyHC IId(x) was available; thus, it is not known if there are hybrid tail myofibers coexpressing the MyHC IId(x) isoform (e.g., type IIA/D(X) or type IID(X)/B myofibers).

3.4.5 Altered muscle loading may influence tail myofiber type proportions after spinal isolation

The ventrolateral segmental tail muscles are small intervertebral flexor muscles with only approximately 12 motor units each and, in the normal animal, these muscles primarily provide intervertebral postural stability during activation of the tail by much larger muscles located at the base of the tail (Brink and Pfaff 1980; Steg 1964). Thus, it is likely that the unique functional demands of the segmental tail muscles lead to their myofiber composition, including the high proportion of type IID(X) myofibers.

In older chronic spinal rats compared to in age-matched older normals, there is no change in the proportion of type IID(X) myofibers (or in the proportions of any other myofiber types) in the long-term spastic muscles. This suggests that the daily intermittent load these muscles must bear during spasms (i.e., ventroflexion; see also Bennett et al. 1999, 2004) is similar to the daily load experienced by normal, unparalyzed segmental tail muscles, and this is supported by the fact that tail muscles from these two groups of animals experience similar amounts of average daily EMG activity. On the other hand, tail muscles experience little daily EMG activity following spinal isolation (rare and low-amplitude spontaneous bursts), and thus the daily contractile activity of tail muscles in spinal isolated animals is likely negligible.

Following spinal isolation, paralysis of the tail muscles may result in a transfer of the active contractile role of the type I myofibers during posture to a passive postural role of *all* myofiber types in bearing the mass of the tail. Thus, paradoxically, both due to and in spite of the dramatic reduction in neuromuscular activity after spinal isolation, it is possible that the unexpected type IID(X) to type IIA myofiber transformation observed in the tail muscles of spinal isolated animals in our study is the result of passive stretch experienced by these muscles. This is supported by the observation that in the rat hindlimb gastrocnemius, which like segmental tail muscles is a mixed type muscle dominated by fast myosin heavy chain isoforms, passive stretch robustly upregulates the MyHC IIa gene and downregulates the MyHC IIb gene (Loughna et al. 1990).

3.4.6 Summary

Early after sacral spinal cord transection, there is little tail muscle activity, a condition that is associated with considerable myofiber atrophy and a transformation toward a faster myofiber distribution in young chronic spinal rats. After long-term spinal isolation (spinal cord transection combined with bilateral deafferentation), there is a permanent near-elimination of muscle activity, which is associated with further myofiber atrophy

and a transformation toward a faster myofiber distribution in spinal isolated rats. However, many months after spasticity develops in older chronic spinal rats, tail muscles recover from these deleterious changes with a partial re-establishment of normal myofiber types and morphology.

3.5 REFERENCES FOR CHAPTER 3

Ansved T and Larsson L. Effects of ageing on enzyme-histochemical, morphometrical and contractile properties of the soleus muscle in the rat. *J Neurol Sci* 93: 105-124, 1989.

Bamford JA, Lopaschuk GD, MacLean IM, Reinhart ML, Dixon WT, and Putman CT. Effects of chronic AICAR administration on the metabolic and contractile phenotypes of rat slow- and fast-twitch skeletal muscles. *Can J Physiol Pharmacol* 81: 1072-1082, 2003.

Bennett DJ, Gorassini M, Fouad K, Sanelli L, Han Y, and Cheng J. Spasticity in rats with sacral spinal cord injury. *J Neurotrauma* 16: 69-84, 1999.

Bennett DJ, Li Y, Harvey PJ, and Gorassini M. Evidence for plateau potentials in tail motoneurons of awake chronic spinal rats with spasticity. *J Neurophysiol* 86: 1972-1982, 2001.

Bennett DJ, Sanelli L, Cooke CL, Harvey PJ, and Gorassini MA. Spastic long-lasting reflexes in the awake rat after sacral spinal cord injury. *J Neurophysiol* 91: 2247-2258, 2004.

Brink EE and Pfaff DW. Vertebral muscles of the back and tail of the albino rat (Rattus norvegicus albinus). *Brain Behav Evol* 17: 1-47, 1980.

Cope TC, Bodine SC, Fournier M, and Edgerton VR. Soleus motor units in chronic spinal transected cats: physiological and morphological alterations. *J Neurophysiol* 55: 1202-1220, 1986.

Crameri RM, Cooper P, Sinclair PJ, Bryant G, and Weston A. Effect of load during electrical stimulation training in spinal cord injury. *Muscle Nerve* 29: 104-111, 2004.

Delp MD and Duan C. Composition and size of type I, IIA, IID/X, and IIB fibers and citrate synthase activity of rat muscle. *J Appl Physiol* 80: 261-270, 1996.

Dupont-Versteegden EE, Houle JD, Gurley CM, and Peterson CA. Early changes in muscle fiber size and gene expression in response to spinal cord transection and exercise. *Am J Physiol Cell Physiol* 275: C1124-1133, 1998.

Eldridge L. Lumbosacral spinal isolation in cat: surgical preparation and health maintenance. *Exp Neurol* 83: 318-327, 1984.

Fry AC, Allemeier CA, and Staron RS. Correlation between percentage fiber type area and myosin heavy chain content in human skeletal muscle. *Eur J Appl Physiol Occup Physiol* 68: 246-251, 1994.

Fujimori B, Shimamura M, Kato M, Yamauchi T, Aoki M, and Tanji J. Studies on the mechanisms of spasticity and rigidity following spinal lesions and ischaemia. *Proc Aust Assoc Neurol* 5: 35-39, 1968.

Hansen G, Martinuk KJ, Bell GJ, MacLean IM, Martin TP, and Putman CT. Effects of spaceflight on myosin heavy-chain content, fibre morphology and succinate dehydrogenase activity in rat diaphragm. *Pflügers Arch* 448: 239-247, 2004.

Harris RLW, Bobet J, Sanelli L, and Bennett DJ. Tail muscles become slow but fatigable in chronic sacral spinal rats with spasticity. *J Neurophysiol* 95: 1124-1133, 2006.

Harris RLW, Sanelli L, Putman CT, and Bennett DJ. Spasticity reverses atrophy and transformation of skeletal muscle fibers after spinal cord injury. *XXXV International Congress of the Physiological Sciences*, San Diego, CA, 2005.

Hartkopp A, Andersen JL, Harridge SD, Crone C, Gruschy-Knudsen T, Kjaer M, Masao M, Ratkevicius A, Quistorff B, Zhou S, and Biering-Sorensen F. High expression of MHC I in the tibialis anterior muscle of a paraplegic patient. *Muscle Nerve* 22: 1731-1737, 1999.

Hartkopp A, Harridge SD, Mizuno M, Ratkevicius A, Quistorff B, Kjaer M, and Biering-Sorensen F. Effect of training on contractile and metabolic properties of wrist extensors in spinal cord-injured individuals. *Muscle Nerve* 27: 72-80, 2003.

Heckman CJ. Alterations in synaptic input to motoneurons during partial spinal cord injury. *Med Sci Sports Exerc* 26: 1480-1490, 1994.

Hidler JM, Harvey RL, and Rymer WZ. Frequency response characteristics of ankle plantar flexors in humans following spinal cord injury: relation to degree of spasticity. *Ann Biomed Eng* 30: 969-981, 2002.

Kern H, Boncompagni S, Rossini K, Mayr W, Fano G, Zanin ME, Podhorska-Okolow M, Protasi F, and Carraro U. Long-term denervation in humans causes degeneration of both contractile and excitation-contraction coupling apparatus, which is reversible by functional electrical stimulation (FES): a role for myofiber regeneration? *J Neuropathol Exp Neurol* 63: 919-931, 2004.

Kuhn RA and Macht MB. Some manifestations of reflex activity in spinal man with particular reference to the occurrence of extensor spasm. *Bull Johns Hopkins Hosp* 84: 43-75, 1948.

Lance JW and Burke D. Mechanisms of spasticity. *Arch Phys Med Rehabil* 55: 332-337, 1974.

Lieber RL, Friden JO, Hargens AR, and Feringa ER. Long-term effects of spinal cord transection on fast and slow rat skeletal muscle. II. Morphometric properties. *Exp Neurol* 91: 435-448, 1986a.

Lieber RL, Johansson CB, Vahlsing HL, Hargens AR, and Feringa ER. Long-term effects of spinal cord transection on fast and slow rat skeletal muscle. I. Contractile properties. *Exp Neurol* 91: 423-434, 1986b.

Lotta S, Scelsi R, Alfonsi E, Saitta A, Nicolotti D, Epifani P, and Carraro U. Morphometric and neurophysiological analysis of skeletal muscle in paraplegic patients with traumatic cord lesion. *Paraplegia* 29: 247-252, 1991.

Loughna PT, Izumo S, Goldspink G, and Nadal-Ginard B. Disuse and passive stretch cause rapid alterations in expression of developmental and adult contractile protein genes in skeletal muscle. *Development* 109: 217-223, 1990.

McGuigan MR, Kraemer WJ, Deschenes MR, Gordon SE, Kitaura T, Scheett TP, Sharman MJ, and Staron RS. Statistical analysis of fiber area in human skeletal muscle. *Can J Appl Physiol* 27: 415-422, 2002.

Murphy RJ, Hartkopp A, Gardiner PF, Kjaer M, and Beliveau L. Salbutamol effect in spinal cord injured individuals undergoing functional electrical stimulation training. *Arch Phys Med Rehabil* 80: 1264-1267, 1999.

Oakley BR, Kirsch DR, and Morris NR. A simplified ultrasensitive silver stain for detecting proteins in polyacrylamide gels. *Anal Biochem* 105: 361-363, 1980.

Ohira Y, Yoshinaga T, Nomura T, Kawano F, Ishihara A, Nonaka I, Roy RR, and Edgerton VR. Gravitational unloading effects on muscle fiber size, phenotype and myonuclear number. *Adv Space Res* 30: 777-781, 2002.

Pierotti DJ, Roy RR, Bodine-Fowler SC, Hodgson JA, and Edgerton VR. Mechanical and morphological properties of chronically inactive cat tibialis anterior motor units. *J Physiol* 444: 175-192, 1991.

Putman CT, Conjard A, Peuker H, and Pette D. Alpha-cardiac-like myosin heavy chain MHCI alpha is not upregulated in transforming rat muscle. *J Muscle Res Cell Motil* 20: 155-162, 1999.

Putman CT, Dusterhoft S, and Pette D. Satellite cell proliferation in low frequency-stimulated fast muscle of hypothyroid rat. *Am J Physiol Cell Physiol* 279: C682-690, 2000.

Putman CT, Kiricsi M, Pearcey J, MacLean IM, Bamford JA, Murdoch GK, Dixon WT, and Pette D. AMPK activation increases uncoupling protein-3 expression and mitochondrial enzyme activities in rat muscle without fibre type transitions. *J Physiol* 551: 169-178, 2003.

Putman CT, Sultan KR, Wassmer T, Bamford JA, Skorjanc D, and Pette D. Fiber-type transitions and satellite cell activation in low-frequency-stimulated muscles of young and aging rats. *J Gerontol A Biol Sci Med Sci* 56: B510-519, 2001.

Ritz LA, Friedman RM, Rhoton EL, Sparkes ML, and Vierck CJ, Jr. Lesions of cat sacrocaudal spinal cord: a minimally disruptive model of injury. *J Neurotrauma* 9: 219-230, 1992.

Rosenblatt JD and Parry DJ. Gamma irradiation prevents compensatory hypertrophy of overloaded mouse extensor digitorum longus muscle. *J Appl Physiol* 73: 2538-2543, 1992.

Roy RR, Kim JA, Grossman EJ, Bekmezian A, Talmadge RJ, Zhong H, and Edgerton VR. Persistence of myosin heavy chain-based fiber types in innervated but silenced rat fast muscle. *Muscle Nerve* 23: 735-747, 2000.

Roy RR, Pierotti DJ, Flores V, Rudolph W, and Edgerton VR. Fibre size and type adaptations to spinal isolation and cyclical passive stretch in cat hindlimb. *J Anat* 180 (Pt 3): 491-499, 1992.

Roy RR, Talmadge RJ, Hodgson JA, Oishi Y, Baldwin KM, and Edgerton VR. Differential response of fast hindlimb extensor and flexor muscles to exercise in adult spinalized cats. *Muscle Nerve* 22: 230-241, 1999.

Roy RR, Talmadge RJ, Hodgson JA, Zhong H, Baldwin KM, and Edgerton VR. Training effects on soleus of cats spinal cord transected (T12-13) as adults. *Muscle Nerve* 21: 63-71, 1998.

Roy RR, Zhong H, Hodgson JA, Grossman EJ, Siengthai B, Talmadge RJ, and Edgerton VR. Influences of electromechanical events in defining skeletal muscle properties. *Muscle Nerve* 26: 238-251, 2002a.

Roy RR, Zhong H, Monti RJ, Vallance KA, and Edgerton VR. Mechanical properties of the electrically silent adult rat soleus muscle. *Muscle Nerve* 26: 404-412, 2002b.

Shields RK and Dudley-Javoroski S. Musculoskeletal Plasticity after Acute Spinal Cord Injury: Effects of Long-Term Neuromuscular Electrical Stimulation Training. *J Neurophysiol*, 2006.

Steg G. Efferent muscle innervation and rigidity. *Acta Physiol Scand* 61 supplementum 225: 1-53, 1964.

Talmadge RJ, Roy RR, and Edgerton VR. Persistence of hybrid fibers in rat soleus after spinal cord transection. *Anat Rec* 255: 188-201, 1999.

Taylor JS, Friedman RF, Munson JB, and Vierck CJ, Jr. Stretch hyperreflexia of triceps surae muscles in the conscious cat after dorsolateral spinal lesions. *J Neurosci* 17: 5004-5015, 1997.

Thomas CK. Contractile properties of human thenar muscles paralyzed by spinal cord injury. *Muscle Nerve* 20: 788-799, 1997.

Thomas CK and Ross BH. Distinct patterns of motor unit behavior during muscle spasms in spinal cord injured subjects. *J Neurophysiol* 77: 2847-2850, 1997.

Tower SS. Function and structure in the chronically isolated lumbo-sacral spinal cord of the dog. *J Comp Neurol* 67: 109-131, 1937.

Zijdewind I and Thomas CK. Motor unit firing during and after voluntary contractions of human thenar muscles weakened by spinal cord injury. *J Neurophysiol* 89: 2065-2071, 2003.

CHAPTER 4: Contractile and metabolic phenotypes are independently regulated in cat medial gastrocnemius muscles and motor units following long-term hemisection and unilateral deafferentation

4.1 INTRODUCTION

It is of considerable importance to understand the impact of paralysis on mammalian skeletal muscles and their motor units. A variety of factors may contribute to muscle paralysis in clinical settings and in experimental conditions, so that it is important to attempt to distinguish between those motor unit and muscle properties that are activity-dependent (i.e., determined by neuromuscular electrical impulses) and those that are activity-independent (e.g., determined by factors such as muscle length and muscle loading). To this end, the elimination of muscle activity has been achieved experimentally by a tetrodotoxin (TTX) blockade of nerve impulses, but this model cannot be maintained for periods of more than 4-6 weeks (Martinov and Nja 2005; St-Pierre et al. 1987; St-Pierre et al. 1988). Moreover, TTX nerve blockade interrupts the motoneuron-muscle connection and thus the impact of TTX-induced paralysis on intact motor units cannot be assessed with this method. A long-term neuromuscular disuse paradigm, in which the motor units remain physically intact, may be accomplished with a spinal isolation preparation (Tower et al. 1941a; Tower et al. 1941b; Tower 1937). Spinal isolation involves transecting the spinal cord at two spinal levels and cutting the dorsal roots that exit the spinal cord between the transections. Thereby the skeletal muscles are completely bilaterally deafferented at those spinal levels. The motor units with motoneuron cell bodies located between the transections remain intact but they are isolated from descending, afferent, and infraspinal inputs, permitting the investigation of the near-elimination of muscle activity (Harris et al. 2007; Pierotti et al. 1991) for as long as 3 years (Eldridge et al. 1981). Thus theoretically, the spinal isolation animal model can be employed to perform a long-term assessment of the activity-independent plasticity of intact muscles and their motor units and, in this light, the consequences of central nervous system injuries and related experimental models can be better interpreted.

When lumbar spinal cord hemisection (HS) is accompanied by unilateral deafferentation (DA) ipsilateral to the spinal cord lesion, severe behavioral impairment results: the leg is passively extended and unable to participate in locomotion, and most reflexes in the paralyzed limb are depressed, although crossed extensor reflexes (mediated by contralateral afferents on the uninjured side) quickly recover (Goldberger and Murray 1974). This supports the notion that hemisection combined with deafferentation (HSDA) can produce a unilateral near-elimination of muscle activity, similar to the bilateral inactivity observed due to spinal isolation. Thus Kernell and colleagues used HSDA to eliminate muscle activity in one hindlimb in order to assess the effects of chronic electrical stimulation on whole muscle properties in adult cats (Donselaar et al. 1987; Kernell et al. 1987a; Kernell et al. 1987b). Remarkably, Kernell and colleagues observed few differences in the morphology or the contractile properties of the unstimulated whole cat peroneus longus muscle after chronic HSDA lasting 4-8 weeks, despite the loss of critical ipsilateral descending and afferent inputs to the hemi-isolated motoneurons and despite the evident impact of this intervention on muscle function in the behaving animal

(Goldberger and Murray 1974). That is, following long-term HSDA in the adult cat, paralyzed whole muscles did not exhibit significant changes in histochemical myofiber type composition, myofiber size, or twitch contractile properties (Donselaar et al. 1987; Kernell et al. 1987b), although whole muscle endurance decreased (Kernell et al. 1987a). These surprising findings indicate that although neuromuscular activity following long-term HSDA must be substantially reduced in the paralyzed muscles compared to in normal muscles, some residual muscle activity is sufficient to sustain some whole muscle contractile properties and muscle fiber properties. Such activity in muscles paralyzed by HSDA would likely be due to activity of the "hemi-isolated" motoneurons and, in turn, contralateral descending and afferent inputs to the hemisected and unilaterally deafferented spinal cord would likely drive this motoneuronal activity.

In order to better understand this interesting experimental model of unilateral hindlimb paralysis, we examined the properties of single motor units of the medial gastrocnemius (MG) muscle paralyzed by HSDA in adult cats, and compared them to motor units of the normal MG. Additionally, at the whole muscle level, we assessed contractile properties, myosin ATPase (mATPase) enzyme histochemistry and myosin heavy chain (MyHC) immunohistochemistry, and metabolic enzyme activities. The goal of these investigations was to answer the following questions. (1) At the whole muscle level, is the response of the MG muscle to HSDA over periods of up to 52 weeks similar to that observed by Kernell and colleagues for the peroneus longus muscle over shorter periods of 4-8 weeks? (2) In the MG of adult cats, how does HSDA affect the distribution and properties of *single motor units*? (3) Following HSDA, what is the relationship between the observed motor unit properties and the observed whole muscle properties? (4) Why do hindlimb muscles paralyzed by HSDA become substantially more fatigable even though their twitch or tetanic contractile properties do not change significantly? Parts of this work have previously been reported in abstract form (Harris et al. 2005).

4.2 MATERIALS AND METHODS

4.2.1 Animals and experimental models

Eleven adult cats (body weight 3.0-3.5 kg, five females and six males) were used in this study with the approval of the University of Alberta Health Sciences Animal Policy and Welfare Committee. All procedures involving the use of these animals were conducted in accordance with the regulations of the Canadian Council for Animal Care. The cats were numbered (Table 4-1) for an unrelated group of experiments as a subset of HSDA cats that were hemisected (HS) and deafferented (DA) ipsilateral to the hemisection. The cats were sacrificed at a variety of times following HSDA, and it was originally intended that the data obtained from each cat would be used to construct a point in the time course of the changes that take place in motor unit and muscle properties in response to HSDA. It was observed, as discussed in the results below, that changes in motor unit and muscle contractile properties were stable at approximately 8-10 weeks after HSDA, and thus the results focus principally on mean values determined from all animals in the data set, although time course data are also reported. As also described below, one animal

Table 4-1

Wet masses, in grams, of the medial gastrocnemius (MG) and other selected hindlimb muscles from paralyzed (PARA) hindlimbs and from normal (NOR) contralateral control hindlimbs of adult cats. Cats were paralyzed due to long-term (see "Time after injury") hemisection and complete unilateral deafferentation, except where deafferentation involved the sparing of some dorsal afferent rootlets (*), or where hemisection alone was not accompanied by deafferentation (†). "‡" indicates two cats in which paralysis began 2 or 6 months after stimulator implants (see MATERIALS AND METHODS). Also shown are the percent differences (%Δ) between normal and paralyzed experimental values. LG, lateral gastrocnemius. SOL, soleus. PLA, plantaris. TA, tibialis anterior. EDL, extensor digitorum longus.

Cat #	Time after injury (wks)	MG			LG			SOL			PLA			TA			EDL		
		NOR	PARA	%Δ	NOR	PARA	%Δ	NOR	PARA	%Δ	NOR	PARA	%Δ	NOR	PARA	%Δ	NOR	PARA	%Δ
5	6	8.7	9.3	6.9	8.9	9.1	1.7	1.8	1.8	4.5	6.0	4.9	-18.8	5.9	4.3	-27.4	3.2	3.3	1.9
14	9	6.8	6.2	-8.8	—	—	—	—	—	—	—	—	—	—	—	—	—	—	—
11‡	15	8.0	7.3	-8.8	10.3	7.8	-24.3	2.3	1.5	-34.8	5.3	3.3	-37.7	4.7	4.0	-14.9	—	—	—
22	19	8.4	9.0	7.2	9.1	9.9	8.2	1.8	1.3	-27.2	5.7	5.2	-9.1	6.6	5.9	-10.8	—	—	—
24*	32	9.3	8.0	-14.6	10.6	8.8	-16.9	3.1	2.7	-11.7	5.6	5.0	-11.2	5.4	5.6	4.5	2.9	2.9	2.5
8*‡	36	7.0	7.5	7.9	9.0	7.1	-21.8	3.0	2.7	-10.5	3.7	3.6	-3.0	4.7	4.7	0.4	2.4	2.8	17.1
12	40	9.9	9.3	-6.1	10.5	7.4	-29.0	5.5	5.2	-3.9	3.4	1.8	-48.4	5.3	5.2	-1.5	2.6	2.6	3.5
13*	42	10.8	11.6	7.4	10.2	9.3	-8.5	3.6	3.0	-15.5	6.3	5.1	-19.2	5.9	5.6	-5.2	2.8	3.3	17.0
21	46	11.4	10.4	-9.1	12.7	10.8	-15.3	3.3	2.2	-33.7	7.0	5.7	-18.9	5.2	5.9	13.2	2.8	3.5	23.7
25†	50	11.5	12.4	8.2	11.8	11.3	-4.3	3.9	3.5	-11.2	8.0	7.1	-11.0	7.8	7.5	-3.9	3.5	3.6	3.2
28*	52	12.8	12.0	-6.3	14.4	14.2	-1.4	4.3	3.7	-14.0	—	—	—	7.8	9.0	15.4	4.4	5.4	22.7
mean	32	9.5	9.4	-1.5	10.7	9.6	-11.2	3.3	2.8	-15.8	5.7	4.6	-19.7	5.9	5.8	-3.0	3.1	3.4	11.4
±SD	±16.6	±2.0	±2.1	±8.9	±1.8	±2.1	±12.2	±1.1	±1.2	±12.6	±1.5	±1.6	±14.5	±1.1	±1.5	±12.8	±0.6	±0.9	±9.6

underwent only hemisection (HS), while in 3 animals some dorsal afferent rootlets were spared (HSDA-SP) during deafferentation. As previously described in detail by Goldberger and Murray (1974), some differences were noted in the behaviour of the paralyzed hindlimbs under these conditions, but no differences were observed in the time course or mean values of motor unit or muscle properties in the paralyzed medial gastrocnemius (MG). In some chronic experiments paralyzed animals served as their own internal controls, with normal control data derived either from tests of the paralyzed muscle prior to surgery or from tests of the contralateral unparalyzed MG. For all other experiments, control data were derived from normal animals assessed using the same methods in a separate study (n = 10; Gordon et al., 1997).

4.2.2 Surgery, electrodes, and unilateral hindlimb paralysis

Each cat received subcutaneous injections of antibiotics (ampicillin 10 mg/kg) one hour prior to surgery and repeated twice at 6 hour intervals following surgery in postoperative care. The animal was pre-operatively sedated with acepromazine (0.25 mg, intramuscular) and Robinul (glycopyrrolate, 0.04 mg/kg, subcutaneous). Deep surgical anaesthesia was achieved with intraperitoneal sodium pentobarbital (40 mg/kg); insertion of a pediatric endotracheal tube permitted closed-loop control of anaesthesia. Deeper surgical anaesthesia was maintained, when necessary, by administration of gaseous halothane anaesthesia. Heart rate was monitored throughout using a toe clip. The skin of the mid and lower back and the lower hindlimbs were shaved, cleaned, and disinfected.

Under strict sterile conditions, an incision was made in the right hindlimb, and fine incisions were made on the lower lumbar part of the back above the spinal cord. In 9 cats, the nerve to the MG muscle was freed over 12 mm and a flexible nerve cuff stimulating electrode of 3 stainless steel wires sewn into a silastic membrane (Dow Corning 500-1), and separated by distances of 2 mm, was carefully placed around the nerve. Two dacron threads loosely closed this cuff electrode so that it loosely apposed the nerve without damaging it. In 2 cats, 3 intramuscular stainless steel stimulating electrodes with 1-cm deinsulated tips were inserted at the motor point using 21-guage needles. In each cat, an EMG recording electrode comprised of 3 stainless steel wires with 1-cm deinsulated tips sewn into a sterile silastic pad was sutured onto the fascia of the MG. The Dacron ® insulated wires were placed such that they flexed loosely within the hindlimb to allow free limb motion without pulling of the nerve, muscle, or electrodes.

Wires from all electrodes were led from the hindlimbs under the skin to the right-hand side of the lumbar back where they were sutured to the paravertebral fascia via sterile Prolene ® (Ethicon PM-L) mesh to ensure that they did not break or retreat through the skin into the animal once muscle, connective tissue, and skin layers were sutured. The electrodes exited the skin at the L7 vertebral level. After closing all incisions from the implantation and paralysis (see below) surgeries, two Prolene ® sutures were passed through the paravertebral musculature of the back in order to secure a lightweight hexalite harness above the L7 lumbar process. External wires were soldered onto lightweight machine pin-integrated circuit connectors for regular stimulation, recording, or monitoring of electrode impedance under halothane anaesthesia.

During the electrode implantation surgery or, in two cats, during a subsequent operation carried out 2 months and 6 months later, the muscles below the knee were paralysed in the right hindlimb. An incision over the lower thoracic spinal cord exposed the vertebrae, and a small hemi-laminectomy exposed half the spinal cord at the T13/T12 level. The dura mater was cut and 0.2 mL of 2% Xylocaine was dripped onto the spinal cord. The level of anaesthesia was deepened, and the T12 spinal cord was carefully hemisected with a #12 scalpel taking care not to damage the blood supply (ventral artery) to the spinal cord. High magnification visual observation confirmed that the hemisection was complete. Hemostasis was ensured and the dura mater was closed.

In all animals except one (hemisection only, HS, #25; see Table 4-1), the paralyzed limb was also deafferented by cutting the S2 to L2 dorsal roots (hemisection and deafferentation, HSDA, #5, 11, 12, 14, 21, 22) or partially deafferented by sparing a few dorsal afferent rootlets (hemisection and spared root deafferentation, HSDA-SP, #8, 13, 24, 28). The dorsal roots were sectioned either intradurally using a method similar to Kernell and colleagues (Eerbeek et al. 1984) or extradurally using a method similar to Goldberger and colleagues (Pubols and Goldberger 1980). An incision over the lumbar cord exposed the vertebrae above the L2 to S1 dorsal roots, and a hemi-laminectomy exposed the L2 to S1 afferent sensory nerves where they enter the spinal cord on the right side. The dura mater was cut and 1 mL of 2% Xylocaine was dripped onto the spinal cord above the L2 to S1 dorsal roots on this side. The level of anaesthesia was deepened, and the dorsal root ganglia from L2 to S1 were very gently lifted with #5 forceps to permit cutting of the central processes. Haemostasis was ensured, and the dura mater, muscle, connective tissue, and skin layers were closed.

Following surgery animals were carefully monitored until they could maintain their own body temperature. Buprenorphine (0.01 mg/kg, subcutaneously) was delivered for 3-5 days and antibiotics (oral amoxicillin) were administered twice daily over the first week. Soft fleece bedding was effective in preventing accidental "catching" of the limb in the bars of the cage. Manual bladder voiding was performed for 5-10 days after injury and in all cats bladder function was normal by 10 days. Only the lower hindlimb on one side was paralyzed so mobility at the hip joint allowed effective rotation of that limb. Animals recovered well and were actively mobile using a 3-legged gait (or 4-legged gait for HS and HSDA-SP animals; (Goldberger and Murray 1974). For the duration of the study, animals were closely monitored for bladder dysfunction, infections, skin abrasions, and general health.

4.2.3 Chronic muscle recording

Under halothane anesthesia, the nerve cuff and EMG electrodes in each cat were attached via the external plug to a switch box to allow recording of impedances as well as evoked maximal EMG and ankle extension in response to stimulation of the MG nerve. The impedances of the implanted nerve cuff and EMG pad electrodes in the cat were measured to check for electrical continuity and for constancy, using a Hewlett-Packard impedance meter (Model 4800A). Then the cat was laid on the right side and the right foot was placed in an adjustable boot that was connected to a force-displacement

transducer (Grass Instruments, Model #FT-10C) in order to record isometric ankle extension at optimal muscle length, in response to stimulation via the nerve cuff as explained in detail previously (Davis et al. 1978; Gordon et al. 1997). Torque is defined by the equation $\tau = \mathbf{r}\mathbf{F}sin\theta$ where: τ is torque; **F** is the applied force; **r** is the length of the moment arm extending from the pivot point (i.e., the connection between the boot and the force-displacement transducer) about which the force acts and against which the force is applied, and θ is the angle through which the force is applied. In this preparation the same boot-transducer apparatus was used for all animals so **r** was the same for every animal, and the distance of the strain gauge from the ankle was constant because when muscle length was altered the boot-transducer apparatus moved with the foot. Thus **F** varied directly with τ, isometric torque measurements could be measured in units of force for any one animal, and force measurements were comparable among animals.

In order to evoke maximal twitch and tetanic isometric forces, the optimal length was determined for the maximal twitch contractions by stimulation of the nerve cuff at a low frequency (0.1-1 Hz). A Textronix 5221 oscilloscope and Gould pen recorder was used to monitor the amplitude and time course of the contractions. Subsequently, a PDP-11 computer performed online averaging of 2 to 5 muscle contractions and the associated EMG responses in response to supramaximal stimulation of the MG nerve (2-2.5 V, 10 μs). The following stimuli were applied. (1) Single supramaximal twitches were evoked by 1 ms pulses delivered at 1 Hz. (2) Sag of unfused tetani was assessed by generating 800-ms-long trains with interpulse intervals of 1.25 × time-to-peak twitch (TTP). From these unfused tetani, sag ratios were calculated as the ratio of the maximum force achieved during the final pulse of the tetanus to the absolute maximum force achieved during the entire tetanus. Sag was present if the sag ratio ≥ 1.0, and sag was absent if the sag ratio < 1.0. (3) Fused tetani were evoked by 210-, 310-, or 410-ms-long supramaximal stimulus trains at 100 Hz.

Muscle fatigability was assessed by supramaximal stimulation in 300 ms-long 40 Hz trains, delivered at 1 Hz for 120 s. The endurance index (EI) was then calculated as the ratio of the peak force measured in the 120th train to the peak force measured in the 1st train, where both of these values were measured relative to the baseline force prior to the 1st contraction. EI ≥ 0.75 indicated fatigue resistance, $0.25 <$ EI < 0.75 indicated intermediate fatigability, and EI ≤ 0.25 indicated fatigability.

4.2.4 Final acute motor unit and muscle recording

Our technique of ventral root splitting is described in detail elsewhere (Rafuse and Gordon 1996b, c; Rafuse et al. 1992). In this preparation ventral root splitting was used to obtain large motor unit samples (15-58 motor units per animal) that represented the motor unit population for each cat studied. In brief, the spinal cord and appropriate leg musculature were surgically exposed under deep sodium pentobarbital anaesthesia (40 mg/kg). Initially, isometric whole muscle contractions were recorded from paralyzed and contralateral unoperated MG muscles using the same stimuli described above for chronic recordings, but the muscles were not subjected to the fatigue test because this would compromise the later measurement of motor unit contractile properties. Final EI values

for whole MG muscles were derived from the final chronic recording session for each cat. Then, L7 and S1 ventral roots on the right-hand side were cut centrally for teasing, in order to stimulate single motor axons to the paralyzed MG motor units. Filaments were split until antidromic stimulation of a single filament evoked a single, reproducible, all-or-none extracellular action potential recorded on the isolated MG nerve; the same stimulation parameter yielded both a single, reproducible EMG potential and discrete, reproducible twitch response from the muscle. The filament was subsequently stimulated at 2 × threshold to record twitch and tetanic contractions. Over a 12 to 15-hour period, 16-58 motor units were sampled, during which time whole muscle tetanic force did not change by more than ± 5%.

Motor unit twitch, sag, tetanus, and endurance were recorded as already described for the whole muscle.

Finally, a single motor unit was isolated for physiological characterization and glycogen depletion by repetitive stimulation. As described previously (Rafuse and Gordon 1996b), 5 fused tetani were evoked by delivering 5 successive 100 Hz stimuli (210, 310, or 410 ms in length as determined earlier in the experiment), delivered at progressively shorter intervals from 1 s (1 Hz) to ~0.14 s (7 Hz) until the evoked force declined to less than 10%. Thereafter the motor unit was stimulated tetanically at a regularity of 0.1 Hz until the maximal tetanic force reached a plateau (i.e., peak tension no longer increased). Then, this repetitive fatiguing regime followed by recovery was repeated at least 5 times until the motor unit tetanic force failed to recover. The muscles were then immediately and rapidly removed, and processed as described below.

4.2.5 Enzyme histochemistry, and immunohistochemistry for myosin heavy chain isoforms

Upon extraction, MG muscles were cut evenly into 5 sections along the longitudinal axis, secured on cork circles with Tissue Tek Embedding Medium (Sakura Finetek U.S.A. Inc., Torrance CA) and frozen in liquid nitrogen-cooled melting isopentane. The tissue blocks were stored at -70°C. Twelve μm muscle cross-sections were cut from the middle block in a cryostat at -20°C, following 30 min of equilibration at this temperature. These sections were stained, as described below, using enzyme histochemistry to determine their metabolic profile and using immunohistochemistry for myosin heavy chain (MyHC) isoforms to determine their contractile profile.

There are three MyHC isoforms found in normal adult cat skeletal myofibers. In order to determine the MyHC-based myofiber type composition of the paralyzed and normal MG, sections were immunohistochemically stained with the following monoclonal (primary) antibodies, as described in detail elsewhere (Putman et al. 2000; Putman et al. 2003): (1) clone BA-D5, IgG, which stains type I myofibers (specific for MyHCI); (2) clone SC-71, IgG, which stains type IIA myofibers (specific for MyHCIIa); (3) clone BF-35, IgG, which stains type I and type IIA myofibers, but not type IID(X) myofibers (specific for both MyHC I and MyHC IIa). Preliminary staining with clone F88-12F8.1, IgG (specific

for cardiac-like MyHCIα), and clone BF-45, IgG (specific for embryonic $MyHC_{emb}$), yielded no staining in paralyzed or normal MG, and thus were not used further.

Following primary antibody application, sections were treated with horse anti-mouse IgG (rat absorbed, affinity purified; Vector Laboratories, Burlingame, CA), a biotinylated secondary antibody directed against the IgG primaries. Each immunohistochemical stain included negative control slides to which these biotinylated secondary antibodies were applied without prior treatment with primary antibodies. Color development of sections (Putman et al. 1999) was achieved by incubation in a biotin-avidin horseradish peroxidase complex followed by a buffered mixture of diaminobenzidine (DAB) and hydrogen peroxide (Vector Laboratories, Burlingame, CA). Type-I and type-IIA myofibers were identified by positive staining reactions with their corresponding primary antibodies, while type-IID(X) myofibers were identified by the absence of staining reactions with any of the primary antibodies used. Hybrid type I/IIA myofibers were observed in proportions of the total myofiber number that were not significantly different from zero (0.74 ± 0.77%, on average). Additionally, our series of antibodies cannot identify hybrid myofibers expressing MyHCIId(x). Therefore, hybrid myofibers were not included in our analysis. Representative immunohistochemical staining of myofibers is shown in Figure 4-1.

In order to determine the *metabolic* myofiber type composition of the paralyzed and normal MG muscles, cross-sections were stained for the following enzyme complexes: (1) mATPase after preincubation at pH = 4.55 as modified by Green and colleagues (Green et al. 1982) and after preincubation at pH = 10.5 as described by Guth and Samaha (Guth and Samaha 1970); (2) a glycolytic activity marker, menadione-linked α-glycerophosphate dehydrogenase (α-GPD, E.C.1.1.1.8), as described by Dubowitz and Brooke (Dubowitz and Brooke 1973); and (3) an oxidative activity marker, NADH tetrazolium reductase (NADH-TR, E.C.1.6.4.3) as described by Dubowitz and Brooke (Dubowitz and Brooke 1973). Myofiber types were identified according to the method used routinely in our laboratory (Gordon et al. 1997) and by Edgerton and colleagues (Peter et al. 1972). Myofibers were classified as slow oxidative (SO) on the basis of dark mATPase staining after preincubation at pH = 4.55 (acid stability) and light mATPase staining after preincubation at pH = 10.5 (alkali labiality), as well as dark NADH-TR staining (high oxidative activity) and light α-GPD staining (low glycolytic activity). Myofibers were classified as fast according to dark mATPase staining after preincubation at pH = 10.5 (alkali stability). Fast oxidative-glycolytic (FOG) myofibers were distinguished from fast glycolytic (FG myofibers) on the basis of *high* oxidative and *high* glycolytic activities in FOG myofibers compared to *low* oxidative and *high* glycolytic activities in FG myofibers. Moreover, after preincubation at pH = 4.55, FOG myofibers are lightly stained (acid labiality) and FG myofibers are darkly stained (acid stability). Representative enzyme histochemical staining of myofibers is shown in Figure 4-2.

Stained MG muscle cross-sections were photomicrographed at 160× in grayscale. Myofibers were assessed in photomicrographs for reactions with antibodies against myosin heavy chain isoforms, for enzyme staining, and for cross-sectional area using custom-designed image analysis software (Putman et al. 2000). For each muscle, an

Figure 4-1

Representative serial photomicrographs show similar regions of the paralyzed medial gastrocnemius (MG) of an adult cat with long-term hemisection and deafferentation (right-hand column) and of the control MG of a normal adult cat (left-hand column), in which myofibers have been labeled according to their *contractile* profile using immunohistochemical staining with antibodies against isoforms of the myosin heavy chain (MyHC) contractile proteins. Myofibers labeled "I" were identified as type I myofibers by dark grey staining with the clone BA-D5 antibody, which reacts positively with MyHCI (A, B). Myofibers labeled "IIA" were identified as type IIA myofibers by grey staining with the clone SC-71 antibody, which reacts positively with MyHCIIa (C, D). Myofibers labeled "IID(X)" were identified as type IID(X) myofibers by no staining with either of these antibodies, as well as by no staining with the clone BF-35 antibody that does not react with MyHCIId(x) and does react positively with both MyHCI and MyHCIIa (E, F).

Figure 4-1

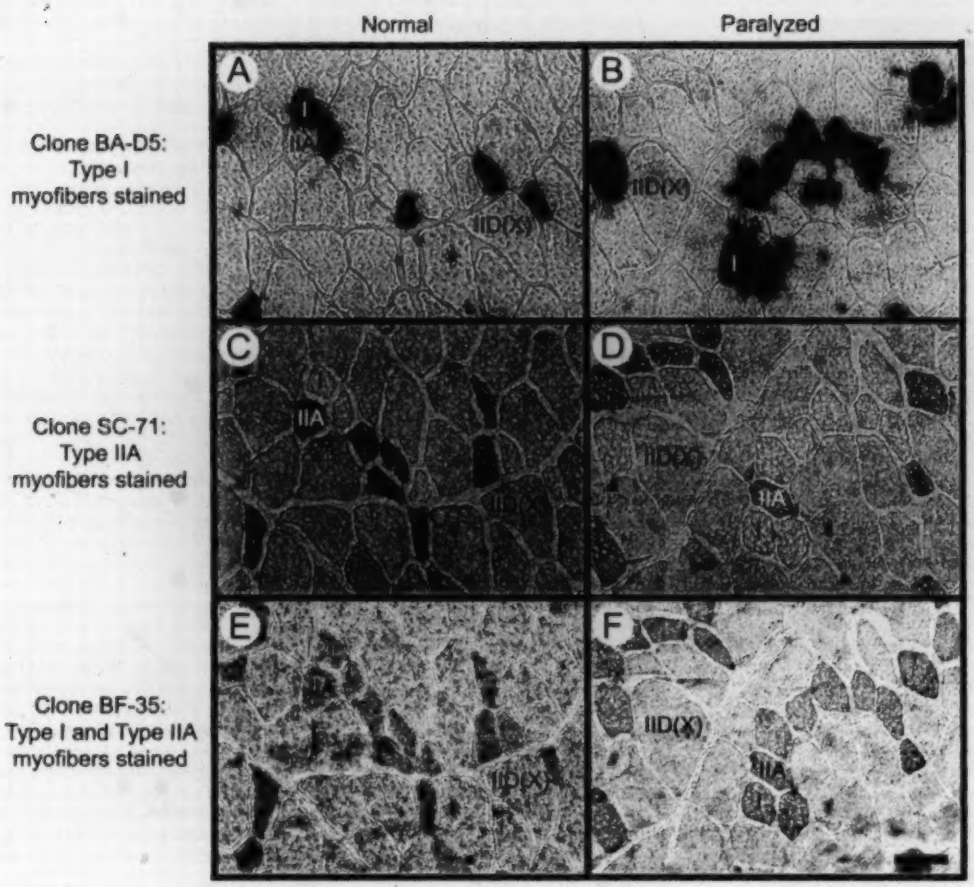
Normal
Paralyzed
A
I
IIA
IID(X)
B
IID(X)
I
C
IIA
IID(X)
D
IID(X)
IIA
E
I
IIA
IID(X)
F
IID(X)
IIA
Clone BA-D5:
Type I
myofibers stained
Clone SC-71:
Type IIA
myofibers stained
Clone BF-35:
Type I and Type IIA
myofibers stained

average of 636 ± 190 myofibers was assessed, ensuring adequate numbers of myofibers for statistical analyses of myofiber proportions and sizes (McGuigan et al. 2002). Moving from the deepest to the most superficial regions of the cat MG there is a progressive increase in type FG myofibers and a progressive decrease in type SO myofibers (Rafuse and Gordon 1996a), so myofibers were selected from five regions spanning the muscle cross-section (i.e., deep, mid-deep, middle, mid-superficial, and superficial), and these regions were similar for all muscles. For each muscle, the number of myofibers exhibiting a particular metabolic or contractile staining profile was reported as a proportion of the total number of myofibers counted. The cross-sectional area of individual myofibers was calculated by the analysis software (Putman et al. 2000) using a conversion factor determined from a 160× photomicrograph of a 1-μm graticule (Leitz Wetzlar, Germany).

4.2.6 Electrophoretic determination of relative MyHC isoform contents

The MyHC compositions of paralyzed and normal MG muscles were also determined electrophoretically by separating bands of MyHCI, MyHCIIa, and MyHCIId/x protein isoforms, as previously described (Putman et al. 2003). Briefly, MyHC protein was isolated from frozen muscle tissue homogenates and separated on an acrylamide gel by SDS-PAGE for 24 hours at 275 V. Protein bands were visualized by developing the gels using a linear silver staining method (Oakley et al. 1980). Individual isoform amounts were determined by integrated densitometry (ChemiGenius, GeneSnap™, and GeneTools™, Syngene, Frederick MD), and these amounts were expressed as relative proportions of the total myosin heavy chain protein present in each sample.

4.2.7 Biochemical measurements of oxidative and glycolytic enzyme activities

Whole muscle homogenates were also prepared for activity determinations of the oxidative marker enzyme citrate synthase (CS, E.C.4.1.3.7) and the glycolytic marker enzyme glyceraldehyde phosphate dehydrogenase (GAPDH, E.C.1.2.1.12). CS activity was measured in a 10 volume muscle homogenate as described by Suarez and colleagues (Suarez et al. 1986). The complete extraction of soluble and structure-bound GAPDH was ensured by extraction in a high-salt 0.1 M sodium potassium phosphate buffer with 5 mM EDTA (pH = 7.2), as described by Reichmann and colleagues (Reichmann et al. 1983), with the addition of 0.1% Triton X-100 to assist in the destabilization of cellular and organellar membranes. Following extraction, CS and GAPDH activities were immediately measured at 30°C according to, respectively, Srere (Srere 1969) and Bass and colleagues (Bass et al. 1969). Soluble protein was subsequently determined using the Bradford assay (BioRad, Hercules CA).

4.2.8 Statistical analyses

Where relevant, regression lines were obtained by least-squares criteria, and the Pearson correlation coefficients were calculated. Correlation of X and Y variables was accepted if the regression slopes were significantly different from zero at $P < 0.05$. A one-way

Figure 4-2

Representative serial photomicrographs show similar regions of the paralyzed medial gastrocnemius (MG) of an adult cat with long-term hemisection and deafferentation (right-hand column) and of the control MG of a normal adult cat (left-hand column), in which myofibers have been labeled according to their *metabolic* profile using histochemical staining for three enzyme complexes. *1)* Myosin ATPase (mATPase) following preincubation at pH = 4.55 (G, H) or at pH = 10.5 (C, D). *2)* The oxidative marker NADH tetrazolium reductase (NADH-TR, E.C.1.6.4.3; E, F). *3)* The glycolytic marker α-glycerophosphate dehydrogenase (α-GPD, E.C. 1.1.1.8; G, H). Myofibers labeled "SO" were identified as slow oxidative myofibers by acid stable mATPase staining (dark staining after preincubation at pH = 4.55), alkali labile mATPase staining (light staining after preincubation at pH = 10.5), high oxidative activity (dark NADH-TR staining), and low glycolytic activity (light α-GPD staining). Myofibers were identified as fast (labeled FOG and FG) by alkali stable (dark) mATPase staining, and FOG (fast oxidative-glycolytic) myofibers were further differentiated from FG (fast glycolytic) myofibers because FG myofibers are more alkali stable (more darkly stained) than FOG myofibers, and FOG myofibers are acid labile (lightly stained). Further, FOG myofibers have high oxidative *and* glycolytic activities, but FG myofibers have low oxidative activity and high glycolytic activity.

Figure 4-2

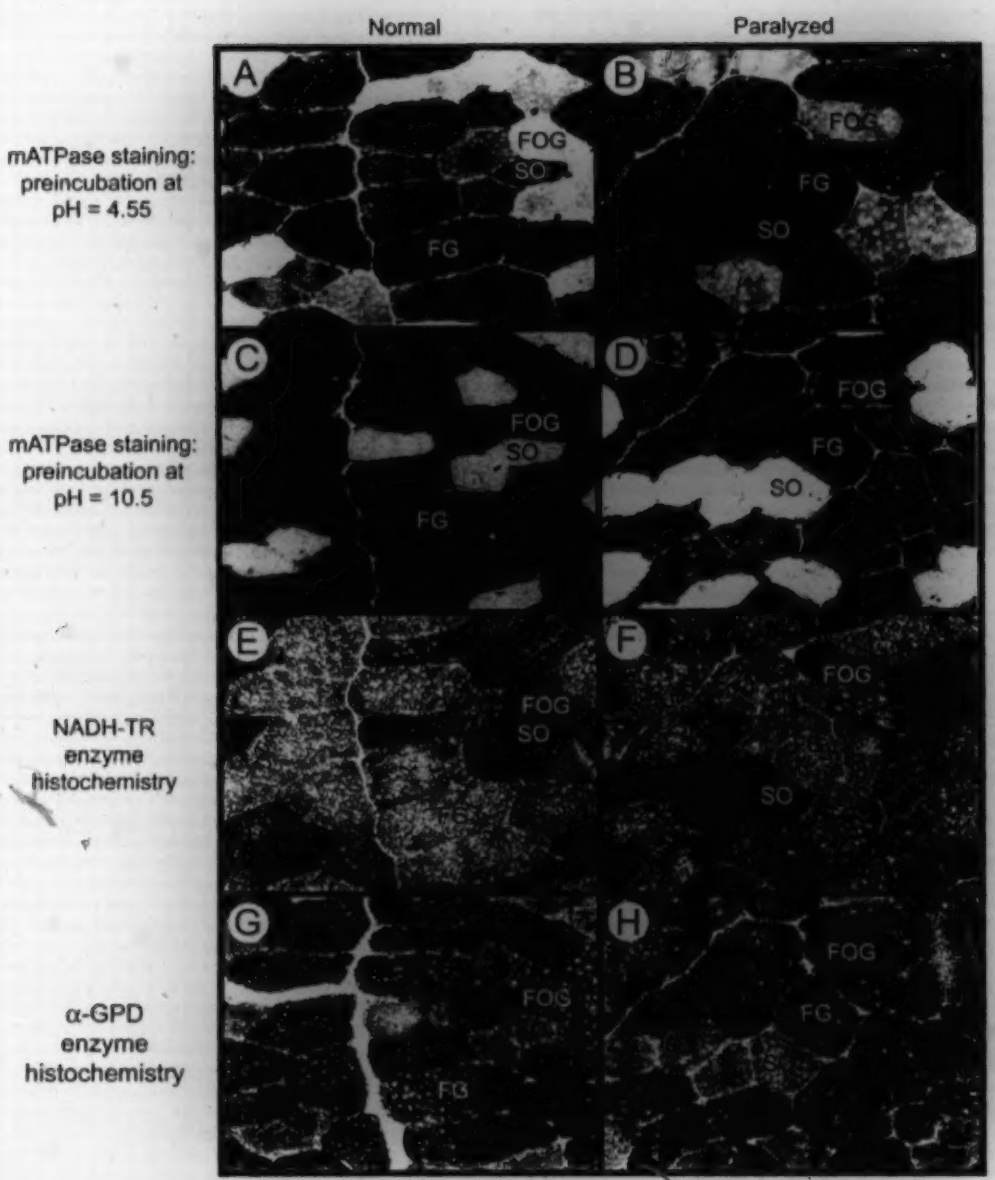
Normal
Paralyzed
A
B
C
D
E
F
G
H
FOG
SO
FG
mATPase staining:
preincubation at
pH = 4.55
mATPase staining:
preincubation at
pH = 10.5
NADH-TR
enzyme
histochemistry
α-GPD
enzyme
histochemistry

analysis of variance (ANOVA) was used to determine statistical significance between mean values at $P < 0.05$. Significant differences were accepted at $P < 0.05$.

4.3 RESULTS

4.3.1 Behavior of the paralyzed hindlimb

Our general observations of the behavior of the paralyzed limb were essentially consistent with those of Goldberger and Murray (1974), although it was not our intent to document such behavior in detail. In hindlimbs paralyzed by hemisection only (HS, n = 1) and by hemisection with spared root unilateral deafferentation (HSDA-SP, n = 4) flaccid paralysis ended within a few days and by approximately one week post-injury, the limb began to be involved in weight bearing under resting (standing) conditions. Over the subsequent three weeks, participation of the paralyzed limb in locomotion increased and gradually improved, until at one month after surgery it appeared almost normal to the casual observer. However, the limb often migrated medially during swing, and brushed against the unparalyzed contralateral limb as if being guided by tactile feedback. Moreover, the paralyzed limb usually walked on the dorsal surface of the paw. Additionally, in the HSDA-SP paralyzed hindlimb but *not* in the HS paralyzed limb, spastic paralysis gradually developed over a period of 15 weeks so that, under resting conditions, spastic co-contractions were observed when the limb was perturbed (e.g., when the animal rested on it or when it was jolted by another limb). These observations suggest that MG muscles paralyzed by HS and HSDA-SP experienced some neuromuscular activity both in the resting state as well as during locomotion despite behavioral impairment, and this activity is likely to have been mediated by ipsilateral afferents as well as by contralateral pathways (Helgren and Goldberger 1993).

Following an initial period of flaccid paralysis (~1 week) the hindlimb paralyzed by hemisection with complete unilateral deafferentation (HSDA, n = 6) developed substantial rigidity and failed to participate in voluntary movements, instead remaining passively extended anteriorly at rest, or being dragged in passive extension posteriorly during locomotion. The paralyzed limb rarely exhibited flexor contractions, demonstrating some extensor hypertonus most of the time. Interestingly, when the paw of the unparalyzed limb in HSDA animals was manipulated, the toes of the paralyzed paw twitched, consistent with previous observations that hindlimbs paralyzed by HSDA (and by HS) exhibit normal crossed extensor reflexes (Goldberger and Murray 1974). MG muscles paralyzed by HSDA clearly experienced some neuromuscular activity due to ongoing motoneuron activity (extensor hypertonus) and due to contralateral pathways (perhaps descending but most likely afferent inputs). However, this residual activity was qualitatively very different from and appeared to be considerably less than the activity observed following HS and HSDA-SP, as previously described by Goldberger and Murray (Goldberger and Murray 1974; Murray and Goldberger 1974).

4.3.2 Muscle force, contractile speed and endurance

We used implanted nerve cuff electrodes to evoke maximal contractile responses in the medial gastrocnemius muscle (MG), and the resulting ankle extensor forces were measured under isometric conditions at optimal muscle length (see MATERIALS AND METHODS). Figure 4-3 shows representative recordings of twitch and tetanic contractions of the whole MG, 0 and 78 days after paralysis by hemisection and deafferentation (HSDA; animal # 21). In the 78-d paralyzed muscle compared to in the normal muscle, no substantial changes were observed in the amplitude and speed of the twitch contraction (Figure 4-3A) or in the maximum tetanic force (Figure 4-3C). However, the paralyzed muscle did appear to sag more during an unfused tetanus (Figure 4-3B). Surprisingly, in the paralyzed MG muscle compared to the normal MG muscle, there was an increase in whole muscle endurance during the first minute of the fatigue test (Figure 4-3D). Thereafter, the force produced during the 2-min fatigue test declined rapidly in the paralyzed MG compared to in the normal MG, and by the end of the test the paralyzed MG generated considerably lower forces than did the normal MG (Figure 4-3D).

We compared the time course of the effects of hindlimb paralysis (Figure 4-4) as induced by hemisection alone (HS; animal # 25), hemisection with unilateral spared root deafferentation (HSDA-SP; animal # 24), and hemisection with complete unilateral deafferentation (HSDA; animal # 12). Surprisingly, with time after paralysis no substantial differences were observed in time-to-peak twitch (Figure 4-4A-C) or in sag (Figure 4-4D-F). However, following paralysis peak tetanic force dropped transiently, and then fully recovered to pre-paralysis levels within approximately 1 week (Figure 4-4D-F). The reduction in tetanic force production immediately after paralysis could not be accounted for by damage to the ventral roots during the extradural dorsal rhizotomy because this drop in tetanic force was also observed when the spinal cord was only hemisected and the dorsal roots remained intact (Figure 4-4A, D, G, J). The reduction in tetanic force production also could not be accounted for by nerve pressure block by the nerve cuff stimulating electrode because it was observed in animals in which the

electrode implantation and the paralysis surgeries were carried out in separate operations (see MATERIALS AND METHODS). Paralysis also resulted in a progressive loss of MG muscle fatigue resistance, as indicated by a relatively rapid decline in the endurance index (EI; Figure 4-4J-L). It is important to note that, according to time-to-peak twitch, sag, peak tetanic force, and EI, no obvious differences were evident among the HS, HSDA-SP, and HSDA preparations in their response to paralysis (Figure 4-4) despite the fact that the limbs differed in their usage (see above) and reflex characteristics (Goldberger and Murray 1974; Murray and Goldberger 1974).

Given the remarkable similarity in the time course of changes in time-to-peak twitch, sag, peak tetanic force, and EI under the 3 paralysis conditions (HS, HSDA-SP, and HSDA), we combined all the longitudinal MG contractile property data that was collected from animals assessed using chronic methods (n = 9; Figure 4-5). The data for time-to-peak twitch (Figure 4-5A) and for sag (Figure 4-5B) reveal that these parameters did not change significantly with time after paralysis, since the slopes of the fitted regression

Figure 4-3

Typical isometric recordings of twitch and tetanic contractions of the adult cat medial gastrocnemius (MG) muscle in response to suprathreshold stimulation of the MG nerve. These are chronic recordings (see MATERIALS AND METHODS) made under fluorothane anesthesia at 0 (normal) and 78 days (paralyzed) of hemisection combined with unilateral deafferentation (HSDA). Stimulation at 1 Hz was used to evoke twitch contractions (A). Repetitive stimulation with an interpulse interval of 1.25 × the time-to-peak twitch (i.e., contraction time) was applied to evoke unfused tetanic contractions in order to observe the presence or absence of sag (B). 100 Hz stimulation was used to evoke maximum fused tetanic contractions (C). 40Hz unfused tetanic contractions were repeated every second for 2 minutes to determine the endurance index and hence the fatigability of the muscle (D). The most substantial change in muscle contractile properties with long-term paralysis was a substantial decline in resistance to fatigue (D).

Figure 4-3

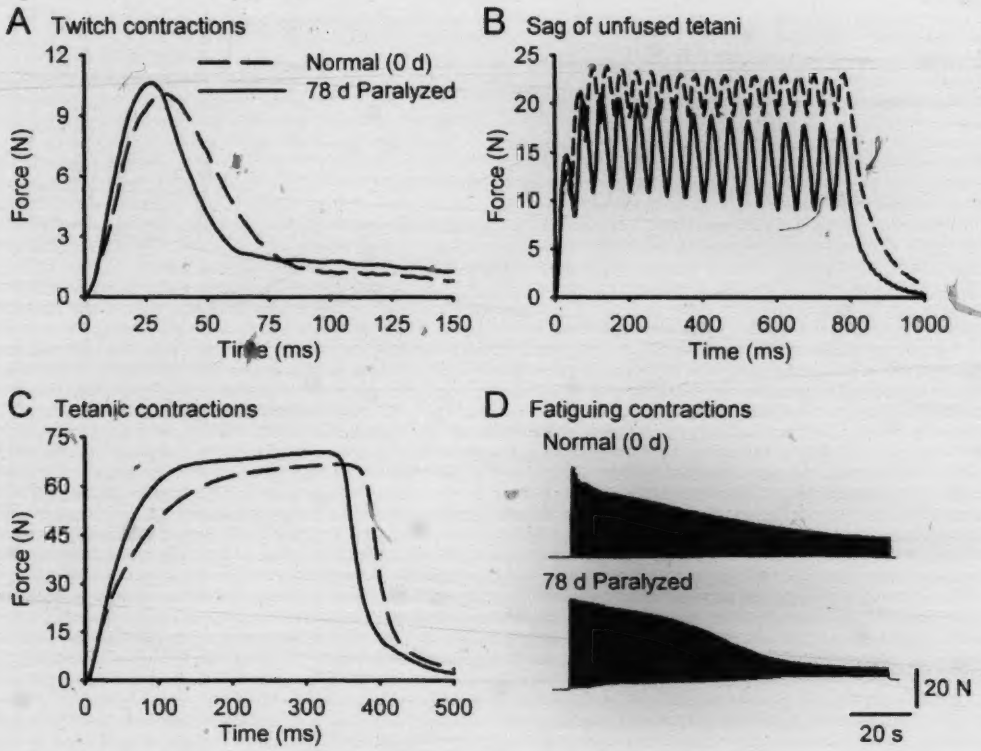
A
Twitch contractions
Normal (0 d)
78 d Paralyzed
Force (N)
Time (ms)
B
Sag of unfused tetani
Force (N)
Time (ms)
C
Tetanic contractions
Force (N)
Time (ms)
D
Fatiguing contractions
Normal (0 d)
78 d Paralyzed
20 N
20 s

Figure 4-4

The time-to-peak twitch force (TTP; A-C), muscle sag during unfused tetani (D-F), the maximal isometric tetanic force (G-I), and the endurance index (J-L) of the whole medial gastrocnemius (MG) muscle are plotted as a function of time after hemisection (HS, animal # 25; A, D, G, J), after hemisection and deafferentation with spared rootlets (HSDA-SP, animal # 24; B, E, H, K) and after hemisection and complete unilateral deafferentation (HSDA, animal # 12; C, F, I, L). The plots show data from a representative animal from each paralysis subgroup. The sag ratio was calculated from an unfused tetanus where the interpulse interval was 1.25 × TTP; the calculation used was the ratio of the maximum force achieved during the final pulse of the tetanus to the absolute maximum force achieved during the entire tetanus. The endurance index is measured from repetitive tetanic contractions at 40 Hz during the Burke fatigue test, and is calculated as the ratio of the maximum tetanic force recorded during the 120^{th} train to the maximum tetanic force recorded during the 1^{st} train of this test. Control values recorded at day 0 are indicated with closed circles in order to differentiate them from the longitudinal data points that are indicated with open circles. Note that in each group, following an initial drop in tetanic forces, the maximal tetanic force in long-term paralyzed muscles does not decline below values recorded immediately after surgery (day 1) and recovers to normal levels (day 0) after approximately one week (also see MATERIALS AND METHODS). There appear to be no longitudinal changes in TTP or sag. Again, in each group the most dramatic change in the paralyzed MG muscles was the decline in the endurance index. No obvious differences among the HS, HSDA-SP, and HSDA subgroups are evident in any of these parameters.

Figure 4-4

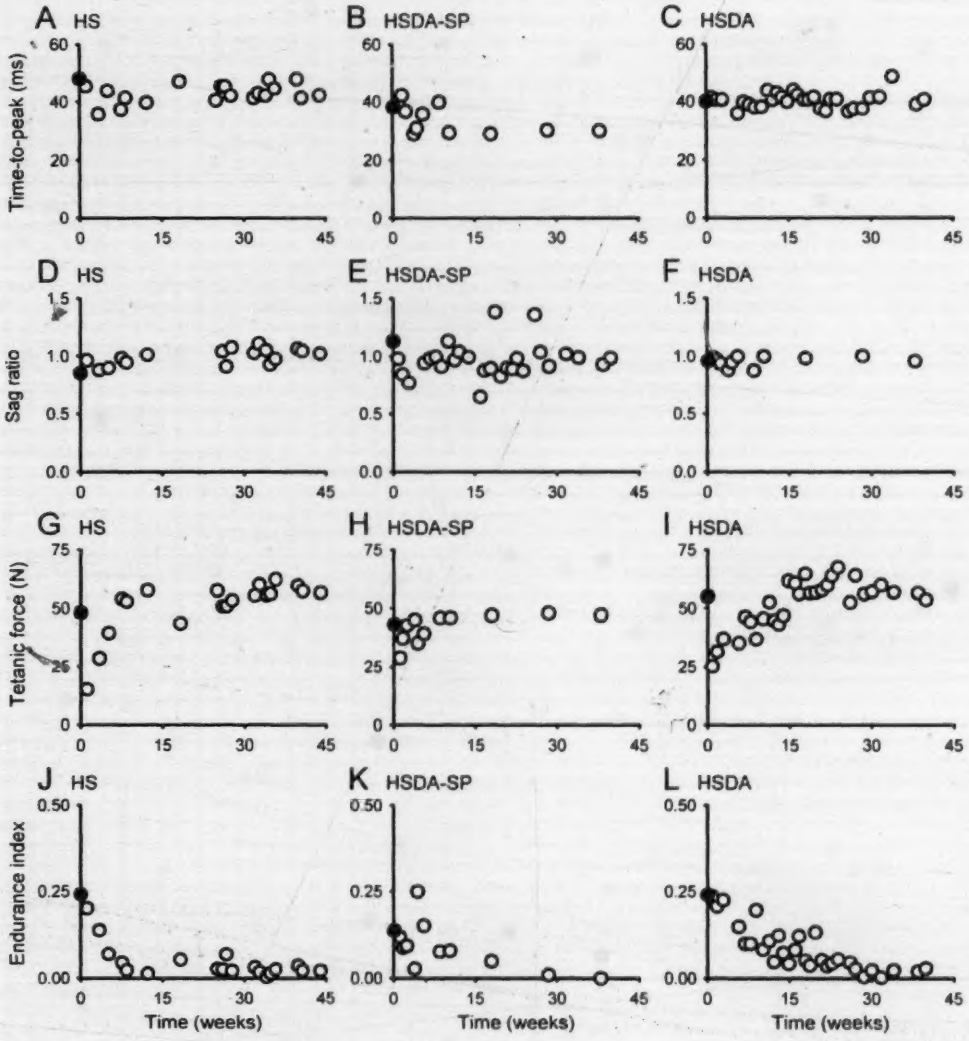
A HS
B HSDA-SP
C HSDA
D HS
E HSDA-SP
F HSDA
G HS
H HSDA-SP
I HSDA
J HS
K HSDA-SP
L HSDA
Time-to-peak (ms)
Sag ratio
Tetanic force (N)
Endurance index
Time (weeks)
Time (weeks)
Time (weeks)

Figure 4-5

Changes in time-to-peak twitch (A), sag ratio (B), peak tetanic force (C), and endurance index (D) of the whole medial gastrocnemius (MG) muscle are shown as a function of time (weeks) after long-term hemisection and unilateral deafferentation (HSDA). These plots show all the data points collected from all paralyzed cats used to perform chronic recordings (n = 9). The tetanic force has been normalized to the initial force recorded at day 0 in order to combine the data from all cats. The slopes of the plots for time-to-peak twitch (A) and sag (B) were not significantly different from 0 at the $P < 0.05$ level. After an immediate and transient decline, peak tetanic force recovered exponentially to normal values with a time constant of 11 days (C). Fatigue resistance dropped dramatically and progressively with an exponential time constant of 8.6 weeks (D).

Figure 4-5

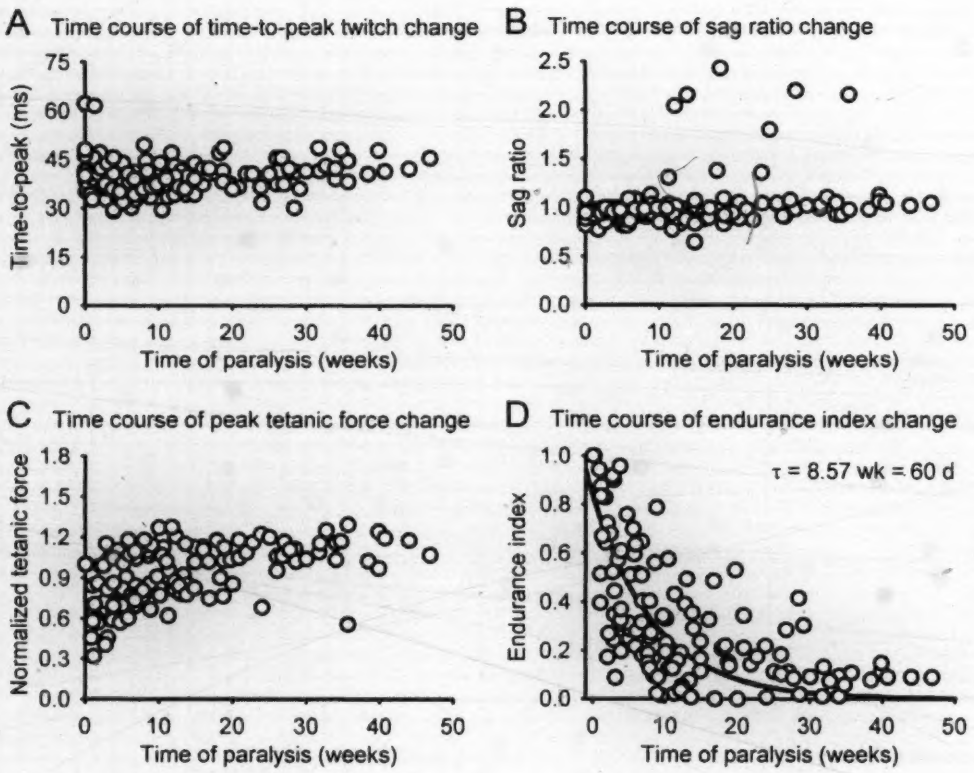
A
Time course of time-to-peak twitch change
Time-to-peak (ms)
75
60
45
30
15
0
0
10
20
30
40
50
Time of paralysis (weeks)
B
Time course of sag ratio change
Sag ratio
2.5
2.0
1.5
1.0
0.5
0.0
0
10
20
30
40
50
Time of paralysis (weeks)
C
Time course of peak tetanic force change
Normalized tetanic force
1.8
1.5
1.2
0.9
0.6
0.3
0.0
0
10
20
30
40
50
Time of paralysis (weeks)
D
Time course of endurance index change
τ = 8.57 wk = 60 d
Endurance index
1.0
0.8
0.6
0.4
0.2
0.0
0
10
20
30
40
50
Time of paralysis (weeks)

lines are not significantly different from zero (and are therefore not drawn in Figure 4-5). However, as already noted, the peak tetanic force initially dropped following paralysis but then recovered to pre-surgery levels after about one week, and did not change subsequently (Figure 4-5C). As described above, this rapid decline and recovery of tetanic force immediately after HSDA is not associated with pressure block of the MG nerve due to the nerve cuff, nor with damage to the intradural portion of the ventral roots to the MG. However, these acute changes in isometric force may be due to acute depletion and then rapid recovery of muscle glycogen, associated with recovery from surgery, as similarly observed immediately following the onset of chronic stimulation (Green et al. 1992). Again, the endurance index of the paralyzed MG fell on a rapid exponential time course, with a time constant of 8.6 weeks (Figure 4-5D).

Our observations of the medial gastrocnemius (MG) paralyzed by hemisection and deafferentation HSDA demonstrated that, compared to in the normal MG, there were no significant longitudinal changes (up to 52 weeks) at the whole muscle level in time-to-peak twitch, in sag, or in peak tetanic force, but whole muscle fatigue resistance dropped dramatically and did not recover. These surprising observations are consistent with the identical findings of Kernell and colleagues, made for the peroneus longus paralyzed by HSDA over periods of 4 to 8 weeks (Kernell et al. 1987a; Kernell et al. 1987b). The unexpected finding that the contractile force and speed properties of an apparently paralyzed hindlimb remained essentially intact over time while the endurance declined indicated that, under some paralytic conditions, the metabolic profile of a muscle may be regulated by mechanisms separate from those that determine the contractile profile of a muscle. Thus we wanted to examine what changes take place at the level of the single motor unit in the MG paralyzed by HSDA.

4.3.3 Motor unit contractile properties

The properties of 235 motor units sampled from the paralyzed MG of adult cats with long-term HSDA (n = 7) were compared to the properties of 273 motor units sampled from the control MG of normal age-matched adult cats (n = 10). First, the properties of all the motor units from each animal studied were averaged with respect to time-to-peak twitch, sag, peak tetanic force, and endurance index. Then we determined group means and standard deviations from these intra-animal motor unit averages. These motor unit data were compared to whole muscle group means (Figure 4-4) that were calculated for the same parameters in the MG of paralyzed adult cats (n = 11) and in the MG of normal adult cats (n = 5). The results were identical both for whole MG and for MG motor units with respect to contractile force and speed. The normal mean times-to-peak twitch were 45 ± 7 ms for whole muscles and 48 ± 11 ms for motor units (Figure 4-6A, open bars), and these were not significantly different in the paralyzed muscles and their constituent motor units (Figure 4-6A, closed bars). The normal mean sag ratios were 1.3 ± 0.4 for whole muscles and 1.7 ± 0.8 for motor units (Figure 4-6B, open bars), and these were not significantly different after HSDA (Figure 4-6B, closed bars). The normal mean peak tetanic forces were 66 ± 11 N for whole muscles and 310 ± 89 mN for motor units (Figure 4-6C, open bars), and these were not significantly different after HSDA (Figure

Figure 4-6

Time-to-peak twitch (A), sag (B), peak tetanic force (C), and endurance index (D) are shown as measured acutely (see MATERIALS AND METHODS) both for whole muscles and for motor units from the paralyzed medial gastrocnemius (MG) of adult cats with hemisection and unilateral deafferentation (closed bars), and from the control MG of normal adult cats (open bars). 235 motor units were sampled from 7 paralyzed cats, and 273 motor units were sampled from 10 control cats. Whole muscle bars show the mean ± standard deviation of the measurements from all cats in the normal (n = 5) and paralyzed (n = 11) groups. Motor unit bars show the mean ± standard deviation of the average motor unit values from each cat in the normal or paralyzed group. Both for whole muscles and for motor units, time-to-peak (A), sag (B), and peak tetanic force (C) in paralyzed cats were not significantly different from in control cats, but the endurance index (D) in paralyzed cats was significantly lower than in normal cats. Not that mean whole muscle EI was calculated from the final chronic recordings because fatiguing hte whole muscle during the acute experiments would have compromised single motor unit contractile properties. * denotes statistical significance accepted at the $P < 0.05$ level as determined using a one-way ANOVA.

Figure 4-6

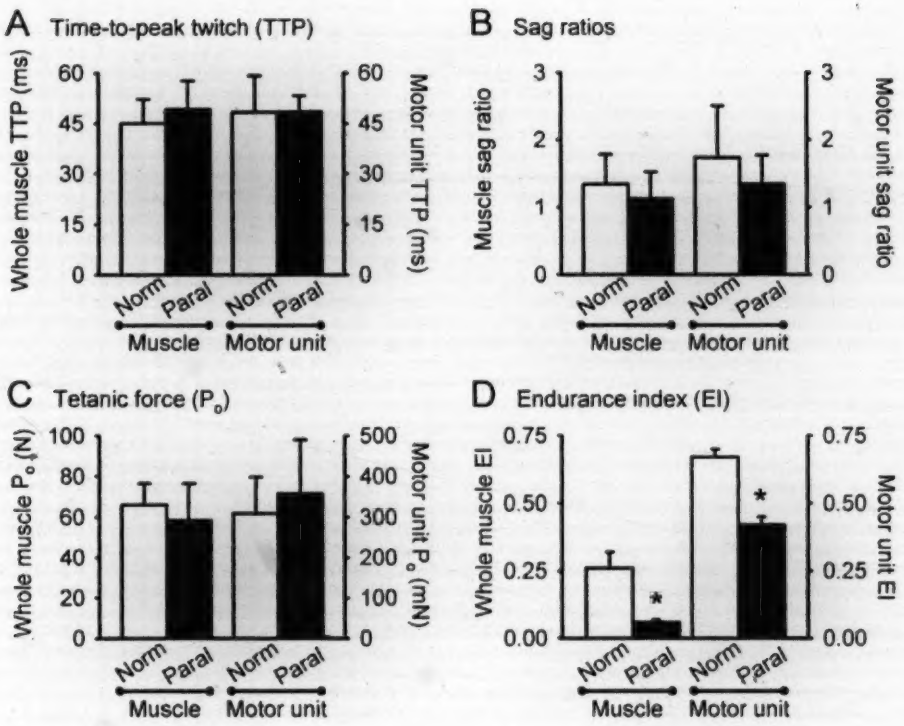
A
Time-to-peak twitch (TTP)
Whole muscle TTP (ms)
Motor unit TTP (ms)
60
45
30
15
0
Norm
Paral
Muscle
Motor unit
B
Sag ratios
Muscle sag ratio
Motor unit sag ratio
3
2
1
0
C
Tetanic force (P$_o$)
Whole muscle P$_o$ (N)
Motor unit P$_o$ (mN)
100
80
60
40
20
500
400
300
200
D
Endurance index (EI)
Whole muscle EI
Motor unit EI
0.75
0.50
0.25
0.00
*

4-6C, closed bars). Consistent with these findings, we also observed normal mean twitch half-fall times (not shown) of 30 ± 7 ms for whole MG muscles and of 43 ± 23 ms for motor units, and these were not significantly different in paralyzed muscles (32 ± 8 ms) or in paralyzed motor units (47 ± 21 ms).

The mean endurance index (Figure 4-4D) was significantly reduced in the paralyzed MG muscle compared to in the normal MG muscle. Specifically, the mean normal endurance indices were 0.26 ± 0.06 for the whole MG muscles and 0.67 ± 0.03 for the MG motor units (Figure 4-6D, open bars), and the mean paralyzed endurance indices were significantly decreased both for the whole MG muscle (0.06 ± 0.01) and for the MG motor units (0.42 ± 0.03; Figure 4-6D, closed bars). As an aside, it is important to note that the endurance indices are measured from normalized force values, and for the motor units these values include normalized forces from slow (S) and fast fatigue resistant (FR) motor units, which during fatigue tests are relatively much higher than those produced by fast fatigue intermediate (FI) and fast fatigable (FF) motor units. Thus, motor unit endurance indices appear much higher than those measured in whole muscles where the contribution of the S and FR motor units to whole muscle force is masked by the much greater contribution, overall, of the FI and FF motor units to whole muscle force.

Distribution frequency histograms for time-to-peak twitch, sag, peak tetanic force, and endurance index were constructed from the pooled data for all motor units sampled in the paralyzed (closed bars) and normal (open bars) groups (Figure 4-7). The distributions of times-to-peak twitch were almost identical for paralyzed and normal motor units, being unimodal with peaks about 40-50 ms in both conditions (Figure 4-7A). The distributions of sag ratios for paralyzed and normal motor units were very similar, being unimodal with a peak at 1.0 in both conditions (Figure 4-7B). However, in the paralyzed motor units compared to in the normal motor units there were small decreases in the number of observed sag ratios of 1.5 and 2.0 and a small increase in the number of observed sag ratios of 1.0, and thus the mean sag ratio of paralyzed motor units tended to decrease slightly, on average (see arrow, Figure 4-7B). The distributions of peak tetanic forces

were also almost identical for paralyzed and normal motor units, resembling either a left-skewed distribution with a principal, obvious peak at approximately 500-600 mN, or a bimodal distribution with a second, less obvious peak at approximately 50-100 mN (Figure 4-7C). Again, the distribution of endurance indices were qualitatively similar between paralyzed and normal MG motor units, but there were clear quantitative differences between these bimodal distributions (Figure 4-7D). Specifically, in paralyzed motor units, although the two peaks remained at EI = 1.0 and at EI = 0.1 as in the normal motor units, the peak at EI = 1.0 was substantially smaller, and that at EI = 0.1 was substantially larger, resulting in a significantly smaller mean EI in the paralyzed motor units compared to in the normal motor units (see arrow in Figure 4-7D; also see Figure 4-6D).

Figure 4-7

Motor unit data are plotted as frequency histograms for time-to-peak twitch (A), sag (B), peak tetanic force (C), and endurance index (D), from the paralyzed medial gastrocnemius (MG) of adult cats with long-term hemisection and unilateral deafferentation (closed bars) and from the control MG of normal adult cats (open bars). These data are the pooled data for 235 motor units sampled from 7 paralyzed cats and 273 motor units sampled from 10 normal cats. The group means (also shown in Figure 4-4) are indicated by the arrows above and below each histogram. * denotes statistical significance accepted at the $P < 0.05$ level as determined using a one-way ANOVA.

Figure 4-7

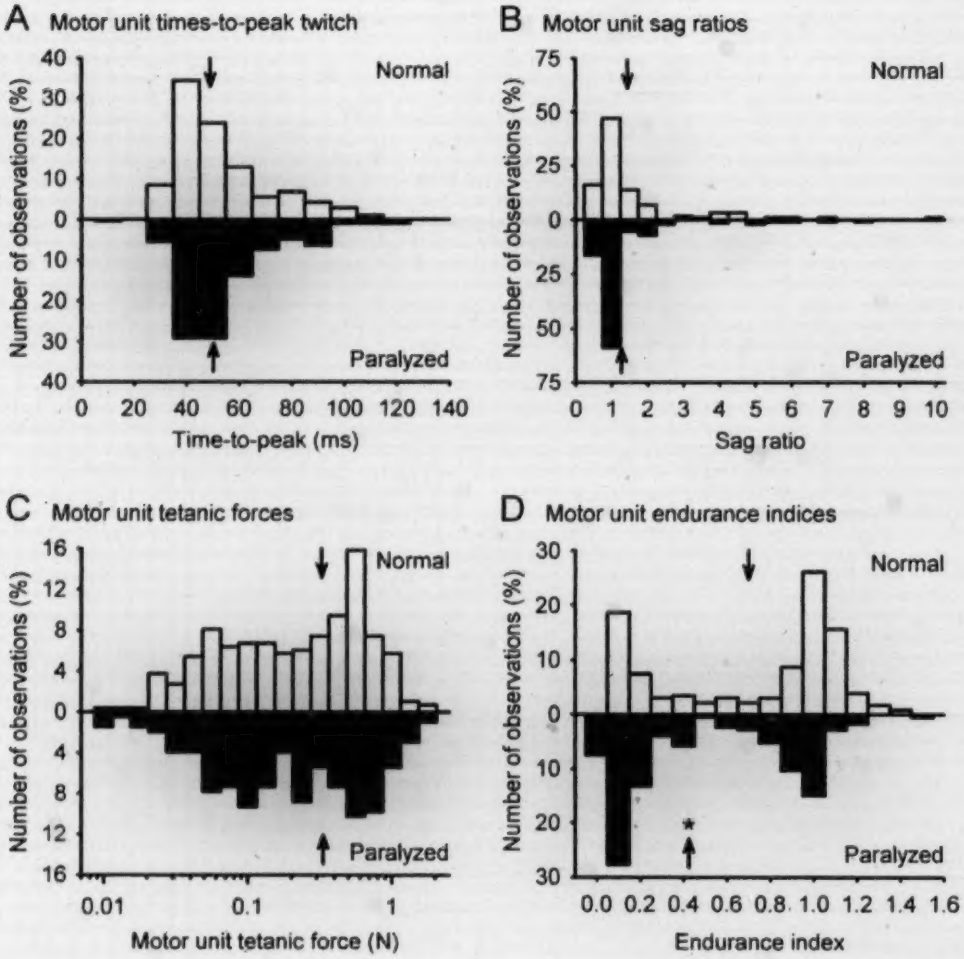
A
Motor unit times-to-peak twitch
Normal
Paralyzed
Number of observations (%)
Time-to-peak (ms)
B
Motor unit sag ratios
Normal
Paralyzed
Number of observations (%)
Sag ratio
C
Motor unit tetanic forces
Normal
Paralyzed
Number of observations (%)
Motor unit tetanic force (N)
D
Motor unit endurance indices
Normal
Paralyzed
Number of observations (%)
Endurance index

4.3.4 Relationships among motor unit contractile properties

As observed for whole MG muscles, no substantial changes were observed in the times-to-peak twitch, sag ratios, or peak tetanic tensions of MG motor units paralyzed by long-term HSDA, compared to normal motor units (Figure 4-6A-C, Figure 4-7A-C). However, a small but statistically non-significant tendency for motor unit sag ratios to decrease with paralysis (Figure 4-6C, Figure 4-7C) suggested the possibility of a transformation from slow (S) to fast (F) motor units since F type motor units exhibit sag (i.e., lower sag ratios) and S type motor units do not (Burke et al. 1973). Moreover, there was a large and significant decline of fatigue resistance in paralyzed motor units compared to in normal motor units (Figure 4-6D, Figure 4-7D), and this was a clear indication that a transformation had occurred in the motor unit population.

In order to investigate these putative motor unit type transformations further, we subdivided the paralyzed (n = 235 MG motor units from 7 cats) and normal (n = 273 MG motor units from 10 cats) pooled motor unit populations into S and F motor units on the basis of the presence or absence of sag. That is, sag of each motor unit was assessed during an unfused tetanus that was induced by a stimulation train with an interpulse interval of 1.25 × time-to-peak (Burke et al. 1973). Then the sag ratio was calculated as the ratio of the peak force recorded during the last pulse of the tetanus to the absolute peak force recorded during the entire tetanus. If a motor unit had a sag ratio ≥ 1.0 this indicated the absence of sag and the motor unit was classified as S and if a motor unit had a sag ratio < 1.0 this indicated the presence of sag and the motor unit was classified as F. Finally, we plotted endurance index (EI) against time-to-peak twitch (TTP; Figure 4-8A, B), against sag (Figure 4-8C, D), and against peak tetanic force (P_o; Figure 4-8E, F) for both S (closed circles) and F (open circles) motor units.

Slow motor units appeared to have somewhat prolonged times-to-peak twitch in the paralyzed MG (60 ms < TTP < 120 for most S motor units; Figure 4-8B) compared to in the normal MG (40 ms < TTP < 80 for most S motor units; Figure 4-8A), even though such a finding was not obvious from the mean TTP (Figure 4-6A) or from the TTP distribution frequency (Figure 4-7A). Fast motor units with relatively short times-to-peak appeared relatively evenly dispersed across the range of endurance indices in normal cats (Figure 4-8A), but fell predominantly in the EI ≤ 0.25 range in paralyzed cats (Figure 4-8B), suggesting that among the fastest contracting F motor units paralysis due to HSDA causes a reduction in fatigue resistance. One major change among the paralyzed F motor units compared to the normal F motor units was especially obvious when looking at F motor unit fatigue indices with respect to their distribution across the range of peak tetanic forces (Figure 4-8E, F). Specifically, among normal F motor units there appeared to be a roughly inverse correlation between endurance index and peak tetanic force (Figure 4-8E), because high endurance indices (EI > 0.75) were generally associated with low tetanic forces (~0-400 mN), while intermediate (0.25 < EI < 0.75) and low endurance indices (EI < 0.25) were generally associated with high tetanic forces (~200-1000 mN), consistent with the well-documented properties of normal mammalian motor units (Burke et al. 1973). However, among paralyzed F motor units this relationship appeared much less robust (Figure 4-8F), because higher endurance indices (0.50 < EI < 1.00) were now

Figure 4-8

For each motor unit sampled, the endurance index (EI) is plotted as a function of time-to-peak twitch (A, B), of sag (C, D), or of peak tetanic force (E, F), for the paralyzed medial gastrocnemius (MG) of adult cats after long-term hemisection and unilateral deafferentation (B, D, F) and for the control MG of normal adult cats (A, C, E). These data are the pooled data for 235 motor units sampled from 7 paralyzed cats and 273 motor units sampled from 10 control cats. Motor units were classified as slow or fast according to the absence or presence of sag, which was assessed using unfused tetani evoked by stimulus trains with interpulse intervals of 1.25 × TTP. The sag ratio was calculated as the ratio of the maximum force achieved during the final pulse of the unfused tetanus to the absolute maximum force achieved during the entire tetanus. Closed circles represent slow motor units, which were identified by the absence of sag (sag ratio $\geq$ 1.0), and open circles represent fast motor units, which were identified by the presence of sag (sag ratio < 1.0).

Figure 4-8

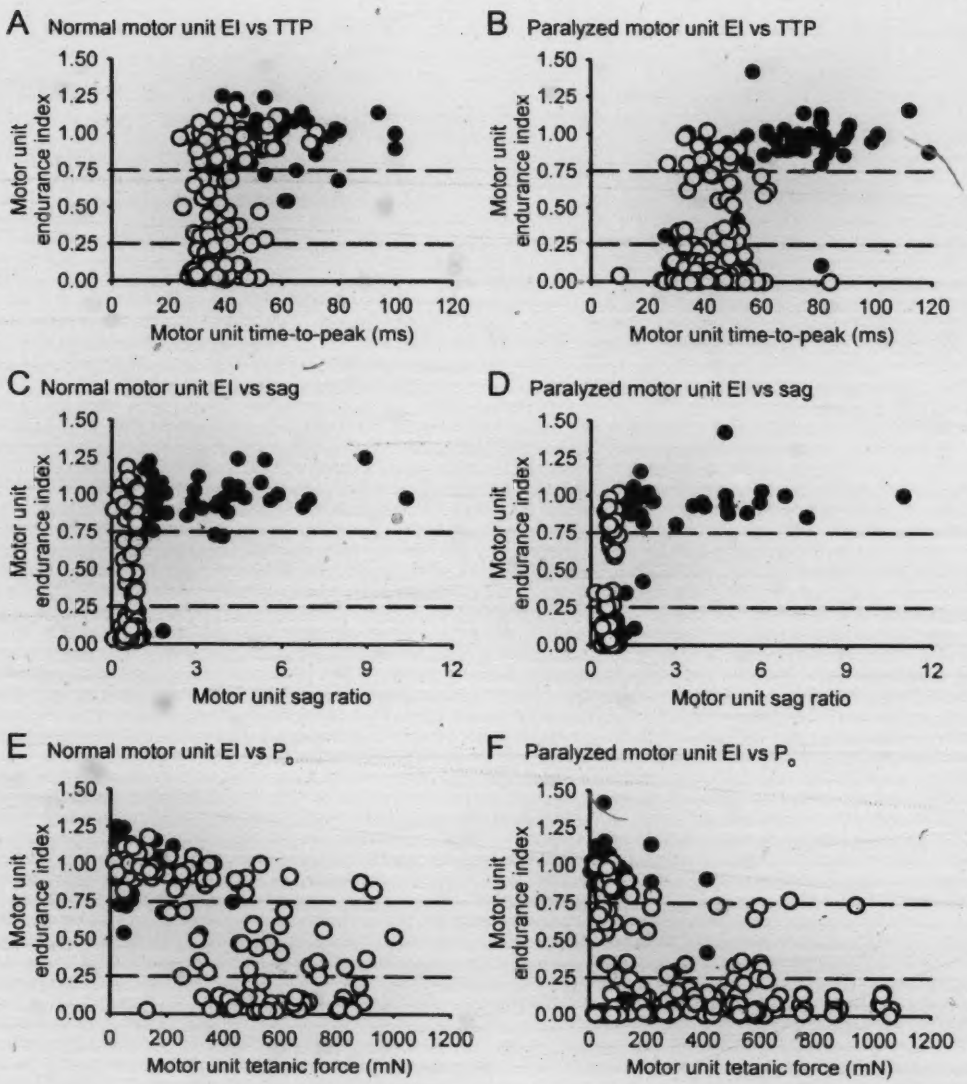
A Normal motor unit EI vs TTP
B Paralyzed motor unit EI vs TTP
C Normal motor unit EI vs sag
D Paralyzed motor unit EI vs sag
E Normal motor unit EI vs P_o
F Paralyzed motor unit EI vs P_o
Motor unit endurance index
1.50
1.25
1.00
0.75
0.50
0.25
0.00
0 20 40 60 80 100 120
Motor unit time-to-peak (ms)
0 3 6 9 12
Motor unit sag ratio
0 200 400 600 800 1000 1200
Motor unit tetanic force (mN)

generally associated with very low tetanic forces (~0-200 mN), and lower endurance indices ($0 < EI < 0.50$) were now generally associated with the full range of tetanic forces (~0-1000 mN). Overall, there were many fewer F motor units with high endurance indices ($EI > 0.75$) among paralyzed motor units (Figure 4-8F) than among normal motor units (Figure 4-8F).

4.3.5 Distributions of motor unit types and motor unit forces

From our observations it was clear that there was a major shift in the fatigability profile of motor units paralyzed by HSDA (n = 235 motor units from 7 adult cats) compared to normal motor units (n = 273 motor units from 10 adult cats). Specifically, compared to normal F motor units paralyzed F motor units had transformed from a population with a relatively broad distribution of endurance indices from 0 to 1.00, to a population exhibiting a very large number of endurance indices < 0.25 and many fewer endurance indices > 0.50 (Figure 4-8E, F). Thus we sub-categorized the F motor units according to fatigability as described by Burke and colleagues (Burke et al. 1973). Motor units demonstrating sag and with $EI \geq 0.75$ were reclassified as fast fatigue resistant (FR). Motor units demonstrating sag and with $0.25 < EI < 0.75$ were reclassified as fast fatigue intermediate (FI). Motor units demonstrating sag and with $EI \leq 0.25$ were reclassified as fast fatigable (FF). Theoretically, slow (S) motor units should always demonstrate $EI \geq 0.75$ (Burke et al. 1973) but in practice, because the properties of individual motor units fall along a continuum, a few S motor units in both paralyzed and normal MG muscles demonstrated relatively low resistance to fatigue (in Figure 4-8 see closed circles that fall below EI = 0.50). However, these anomalous motor units were very rare compared to the overall number of S motor units, and thus the S motor units were not reclassified.

In paralyzed cats (Figure 4-9B) compared to in normal cats (Figure 4-9A), there were large transformations in the proportions of motor unit types. Specifically, the normal motor unit distribution was 36 ± 14% S, 22 ± 9% FR, 9 ± 6% FI, and 33 ± 6% FF (Figure 4-9C, open bars) in good agreement with previous studies (Gordon et al. 2004). Among motor units paralyzed due to HSDA (Figure 4-9C, closed bars), compared to the motor units in the normal MG muscle, there were no significant differences in the proportions of S (27 ± 16%) or FI motor units (14 ± 10%), but there was a large and significant decrease in the proportion of FR motor units (12 ± 14%) and a large and significant increase in the proportion of FF motor units (47 ± 13%). Despite these changes in motor unit proportions, the peak force produced by motor units of any type in paralyzed cats was unchanged, compared to the motor unit forces in normal cats (Figure 4-9D). Specifically, among normal MG motor units mean peak tetanic tensions were 98 ± 41 mN for S motor units, 218 ± 97 mN for FR motor units, 533 ± 255 mN for FI motor units, and 497 ± 150 mN for FF motor units (Figure 4-9D, open bars), and these were not significantly different among paralyzed motor units (Figure 4-9D, closed bars).

Under conditions where neuromuscular activity or muscle loading is altered, due to paralysis or exercise for example, it is difficult to interpret changes in motor unit numbers and motor unit force production independently since their impact on whole muscle behavior is interdependent. Thus we developed a measure that estimates the overall

Figure 4-9

Slow (S), fast fatigue resistant (FR), fast fatigue intermediate (FI), and fast fatigable (FF) motor units are differentiated according to cumulative force histograms (A, B), proportions of individual motor unit types (C), mean peak tetanic forces (D), and mean force density (E). These data are the means ± SD of the averaged motor unit data for each of 7 paralyzed cats (total n = 235 motor units; closed symbols/bars) and for each of 10 control cats (total n = 273 motor units; open symbols/bars). Cumulative force distributions (A, B) were prepared by arranging motor unit groups in the order S, FR, FI, and FF, and then by ordering the motor units within each group from the smallest to the largest peak tetanic force; then the motor units, in this order, were plotted against the cumulative number of motor units expressed as a percentage of the total number of motor units. Mean proportions of motor unit types (B) and mean peak tetanic forces (C) are shown. Mean force density (D) is the sum of peak tetanic forces produced by motor units of each type, expressed as a percentage of the sum total force produced by all motor units of all types combined.

Figure 4-9

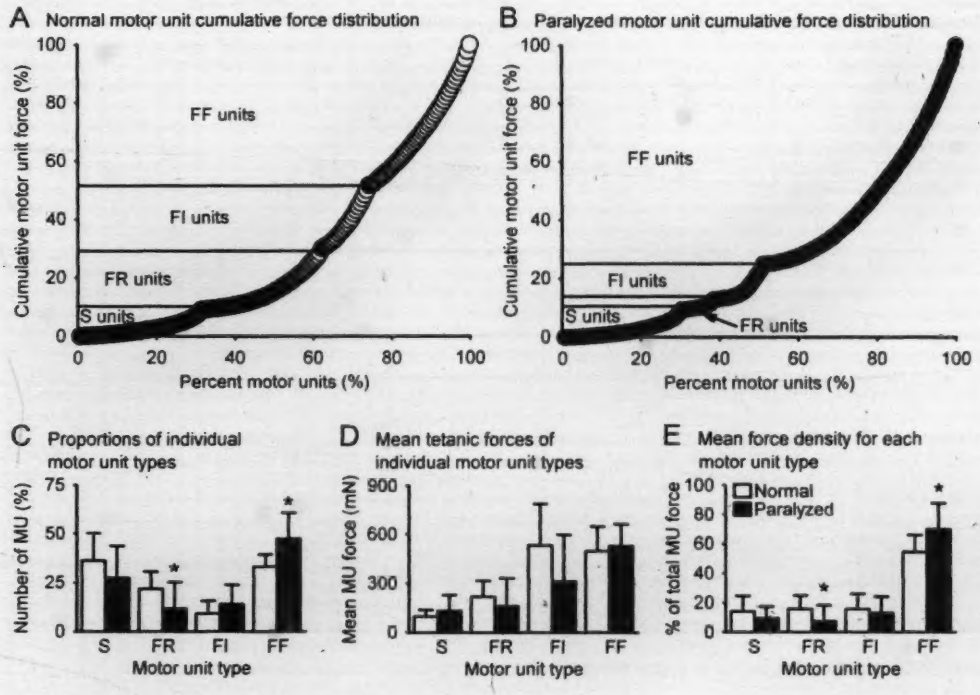
A Normal motor unit cumulative force distribution
Cumulative motor unit force (%)
FF units
FI units
FR units
S units
Percent motor units (%)
B Paralyzed motor unit cumulative force distribution
Cumulative motor unit force (%)
FF units
FI units
S units
FR units
Percent motor units (%)
C Proportions of individual motor unit types
Number of MU (%)
S
FR
FI
FF
Motor unit type
D Mean tetanic forces of individual motor unit types
Mean MU force (mN)
S
FR
FI
FF
Motor unit type
E Mean force density for each motor unit type
Normal
Paralyzed
% of total MU force
S
FR
FI
FF
Motor unit type

combined effect on whole muscle behavior of experimentally induced changes in motor unit proportions and peak tetanic forces, which we called motor unit force density (Figure 4-9E). To calculate the percentage force density of each motor unit type in paralyzed and normal MG muscles, the sum of the peak tetanic forces produced by all the motor units of a given type within the paralyzed or normal group was expressed as a percentage of the sum total tetanic force produced by all the motor units of all types within that group. Thus the percent motor unit force density is an estimate of the contribution of the number of motor units of each type *and* the peak force produced by the motor units of that type, on average, to the force produced by the entire motor unit pool (i.e., whole muscle) during maximum recruitment of all the motor units. There was a significant transformation in the motor unit force densities after HSDA, from FR to FF. Specifically, among paralyzed motor units (Figure 4-9E, closed bars) compared to among normal motor units (Figure 4-9E, open bars) there were no changes in the force densities of S (9 ± 8% paralyzed vs 14 ± 10% normal) or FI (13 ± 11% paralyzed vs 16 ± 10% normal) motor units. However, there was a significant decrease in the FR motor unit force density (8 ± 11% paralyzed vs 16 ± 9% normal) and a significant increase in the FF motor unit force density (70 ± 18% paralyzed vs 54 ± 12% normal). This force density transformation toward a more fatigable motor unit distribution due to paralysis is consistent with the large decreases observed, on average, in the endurance indices of both whole MG muscles and single MG motor units.

The dramatic impact of these relative changes in the distributions of the fast motor unit types in paralyzed compared to normal MG muscle is best illustrated by the cumulative distribution plots in Figures 9A and 9B. While the proportion of S motor units and the cumulative force developed by the small S motor units is not changed after paralysis, the reduced mean force density of the FR units and the increase in the mean force density of the FF motor units means that the majority of the cumulative motor unit force (~75%, Figure 4-9B) is generated by FF motor units in the paralyzed MG muscles. In comparison, only approximately one half (~50%, Figure 4-9A) of the cumulative motor unit force is generated by FF motor units in the normal muscles. In other words, in the normal muscles more than 60% of the motor unit population is recruited to develop 30% of the cumulative muscle force *without* fatigue (Figure 4-9A), while in the paralyzed muscles approximately 40% of the motor unit population is recruited to develop less than 15% of the cumulative muscle force *without* fatigue (Figure 4-9B). Consequently, the development of large cumulative forces during motor unit recruitment in the paralyzed muscles will result in rapid onset of fatigue.

4.3.6 Relationships among muscle unit and motor axon properties

We wanted to determine if the motor unit transformations due to paralysis had any effect on the normal size relationships observed between basic properties of the muscle units (the non-neural components of the motor units) and those of the innervating motor axons. Thus in paralyzed MG motor units (Figure 4-10A, C, E, G) compared to in normal MG motor units (Figure 4-10B, D, F, H) we compared the relationships between motor axon conduction velocity (CV; Figure 4-10A, B) or peak-to-peak amplitude of the motor axon extracellular action potential (neural P-P; Figure10, D), and motor unit peak tetanic force

Figure 4-10

Motor axon conduction velocity (CV; A, B), peak-to-peak amplitude of extracellular motor axon action potential (neural P-P; C, D), and motor unit time-to-peak twitch (TTP; E, F) are plotted against motor unit tetanic force. CV is also plotted against TTP (G, H). The relationships shown are for all the motor units sampled from the paralyzed medial gastrocnemius (MG) of a representative adult cat with long-term hemisection and unilateral deafferentation (# 13, right-hand column), and from the control MG of a representative normal adult cat. In every plot the line reflects a correlation, between the dependent and independent variables, that was found to be significant at the $P < 0.05$ level.

Figure 4-10

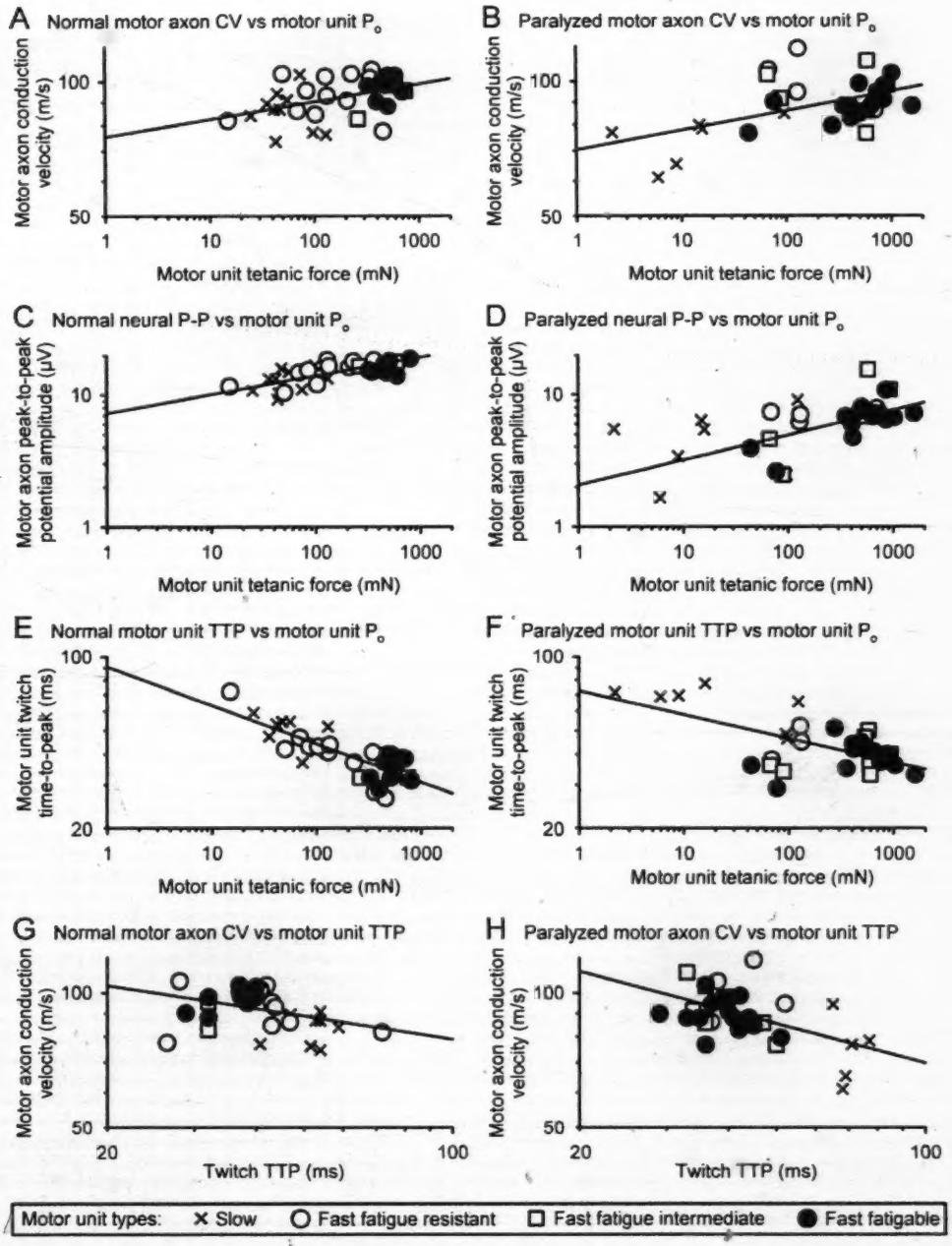
A Normal motor axon CV vs motor unit P_o
B Paralyzed motor axon CV vs motor unit P_o
C Normal neural P-P vs motor unit P_o
D Paralyzed neural P-P vs motor unit P_o
E Normal motor unit TTP vs motor unit P_o
F Paralyzed motor unit TTP vs motor unit P_o
G Normal motor axon CV vs motor unit TTP
H Paralyzed motor axon CV vs motor unit TTP
Motor axon conduction velocity (m/s)
Motor axon peak-to-peak potential amplitude (μV)
Motor unit twitch time-to-peak (ms)
Motor unit tetanic force (mN)
Twitch TTP (ms)
Motor unit types: × Slow ○ Fast fatigue resistant □ Fast fatigue intermediate ● Fast fatigable

(P_o; Figure 4-10A-D) or motor unit time-to-peak twitch (TTP; Figure 4-10G, H). Motor unit TTP is also plotted against motor unit P_o (Figure 4-10E, F). These comparisons are displayed on logarithmic scales in Figure 4-10, and the regression lines that are shown in all plots show that the slope of the relationship between the variables is significantly different from zero at the $P < 0.05$ level.

In normal motor units, the size principle dictates that higher (faster) CV values and larger neural P-P values indicate larger motor axons, while larger P_o values and lower (faster) TTP values indicate the larger muscle units that should be innervated by these larger motor axons (Gordon et al. 2004). In normal adult cat motor units, as expected based upon these normal motor axon-muscle unit size relationships (Gordon et al. 2004), we observed that both neural P-P (Figure 4-10A) and CV (Figure 4-10C) varied directly with P_o, that TTP (Figure 4-10E) varied inversely with P_o, and that CV varied inversely with TTP (Figure 4-10G). Predictably, these relationships also tended to be hierarchical with respect to motor unit types, because the smallest S motor units tended to be clustered toward one end of the regression plot and the largest FF motor units at the other end, while the FR and FI motor units fell between these clusters (Figure 4-10A, C, E, G). Importantly, following long-term paralysis due to HSDA, these size relationships were not altered. That is, among paralyzed motor units as among normal motor units, both neural P-P (Figure 4-10B) and CV (Figure 4-10D) varied directly with P_o, TTP (Figure 4-10F) varied inversely with P_o, and CV varied inversely with TTP (Figure 4-10H). Nevertheless, it was obvious in these size relationships (Figure 4-10), as it was in the motor unit proportions and force densities (Figure 4-9), that the motor unit population in paralyzed MG compared to in normal MG had transformed toward a distribution that included more fatigable motor units (see closed circles in Figure 4-9). This provides an example of dramatic changes in motor unit fatigue resistance that lead to altered motor unit classification *without* affecting the normal size relationships between contractile indicators of muscle unit size (i.e., tetanic force and time-to-peak twitch) and electrophysiological indicators of motor axon size (i.e., axon conduction velocity and extracellular axon potential amplitude).

Although the normal motor axon-muscle unit size relationships were not altered by paralysis due to long-term HSDA, we noted that in the paralyzed MG compared to in the normal MG the properties of slow motor units tended to be more distinct from those of fast motor units, and that the individual motor units were somewhat more disorganized about the lines of regression (Figure 4-8). Both of these outcomes resemble the effects of nerve section followed by nerve suture and reinnervation (Gordon and Stein 1982; Gordon et al. 2004). Although these two experimental approaches cannot be compared directly, it is interesting that the qualitative effects of long-term HSDA on muscle unit-motor axon size relationships resemble those of nerve section followed by recovery.

4.3.7 Changes in myofiber types and myofiber sizes

We observed that in whole MG muscles and single MG motor units that were paralyzed due to long-term HSDA, compared to in normal whole MG muscles and single MG motor units, there were no changes in time-to-peak twitch, sag, or peak tetanic force, but

there was a large and significant decrease in the fatigue resistance both of whole MG and of MG motor units (Figure 4-6). This increase in fatigability was accompanied by a transformation in the motor unit distribution from fatigue resistant motor units to fatigable motor units (Figure 4-9). These results indicated that the HSDA intervention resulted in a dis-coordinate regulation of the metabolic and contractile profiles of the paralyzed whole MG and its motor units. We wanted to investigate the possible sources of this dis-coordinate regulation, so we assessed myofibers in the paralyzed MG (n = 6 cats) and in the normal MG (n = 6 cats) for myofiber type proportions and myofiber sizes using two approaches. In order to determine the contractile profile of the myofibers, we stained muscle cross-sections using routine immunohistochemistry for myosin heavy chain (MyHC) isoforms using primary antibodies specific for type I and type IIA myofibers. We identified type IID(X) myofibers as those remaining unstained (Figure 1; also see MATERIALS AND METHODS). In order to determine the metabolic profile of the paralyzed and normal myofibers, we stained muscle cross-sections using routine enzyme histochemistry for mATPase activity following preincubation at pH = 4.55 (Figure 4-9G, H) and at pH = 10.5 as well as for a marker of oxidative metabolic activity, NADH-TR (E.C.1.6.4.3), and for a marker of glycolytic metabolic activity, α-GPD (E.C.1.1.1.8). These enzyme histochemical stains were used to classify the myofibers as slow oxidative (SO), fast oxidative-glycolytic (FOG), and fast glycolytic (FG; Figure 4-2; also see MATERIALS AND METHODS for a complete description of our histochemical approach to myofiber classification.) We also used these contractile (MyHC) and metabolic (mATPase, NADH-TR, and α-GPD) histochemical stains to analyze myofiber sizes in units of cross-sectional area (CSA, μm^2).

The most important outcome of our immunohistochemical and metabolic histochemical analyses was that paralyzed MG myofibers, compared to normal MG myofibers, exhibited the same independence of the contractile and metabolic profiles that was observed at the levels of motor units and whole muscle. In normal MG muscles (Figure 4-11A, open bars) there were MyHC-classified myofiber proportions of 21 ± 1% type I, 27 ± 6% type IIA, and 52 ± 7% type IID(X). Additionally, in normal MG muscles the metabolically-classified myofiber proportions (Figure 4-11D, open bars) of 26 ± 6% SO, 36 ± 3% FOG, and 38 ± 4% FG were not clearly equivalent to the MyHC-classified myofiber proportions. In paralyzed MG muscles, compared to in normals MG muscles, according to immunohistochemistry for contractile MyHC isoforms (Figure 4-11A) there were no changes in type I, type IIA, or type IID(X) myofiber proportions, but according to metabolic histochemistry for mATPase, NADH-TR, and α-GPD, there was a transformation from FOG to FG myofibers (Figure 4-11D). Specifically, in the paralyzed MG muscles (Figure 4-10D, closed bars), although there were no changes in the proportion of SO myofibers (23 ± 4%), the FOG myofiber proportion decreased significantly (18 ± 8%) and the FG myofiber proportion increased significantly (59 ± 4%). Thus, consistent with the idea that HSDA dis-coordinately (i.e., independently) alters the contractile and metabolic profiles of paralyzed MG muscles and motor units, there were no changes in the MyHC-identified myofiber types that are known to be involved directly in the contractile phenotype defined by time-to-peak twitch, sag, and tetanic force (Gallo et al. 2004), but there were changes toward a more fatigable myofiber

Figure 4-11

The numbers and sizes of myofibers in the medial gastrocnemius (MG) are shown from adult cats paralyzed by long-term hemisection and unilateral deafferentation (n = 6; closed bars) or from normal adult cats (n = 6; open bars). Myofibers in serial muscle sections were classified according to their contractile profile using immunohistochemistry against isoforms of the myosin heavy chain MyHC contractile proteins (A-C) or according to their metabolic profile using enzyme histochemistry for mATPase, NADH-TR, and α-GPD (D-F; see MATERIALS AND METHODS). The numbers of myofibers classified as type I, type IIA, and type IID(X) using immunohistochemistry (A) or as slow oxidative (SO), fast oxidative-glycolytic (FOG), and fast glycolytic (FG) using metabolic histochemistry (D) are expressed as a mean percentage of the total number of myofibers. The mean size of myofibers of each type (B, E) or the mean size of all myofibers combined (C, F) is expressed in units of cross-sectional area (μm^2). Values are expressed as means ± standard deviations. * denotes statistical significance accepted at the $P < 0.05$ level as determined using a one-way ANOVA.

Figure 4-11

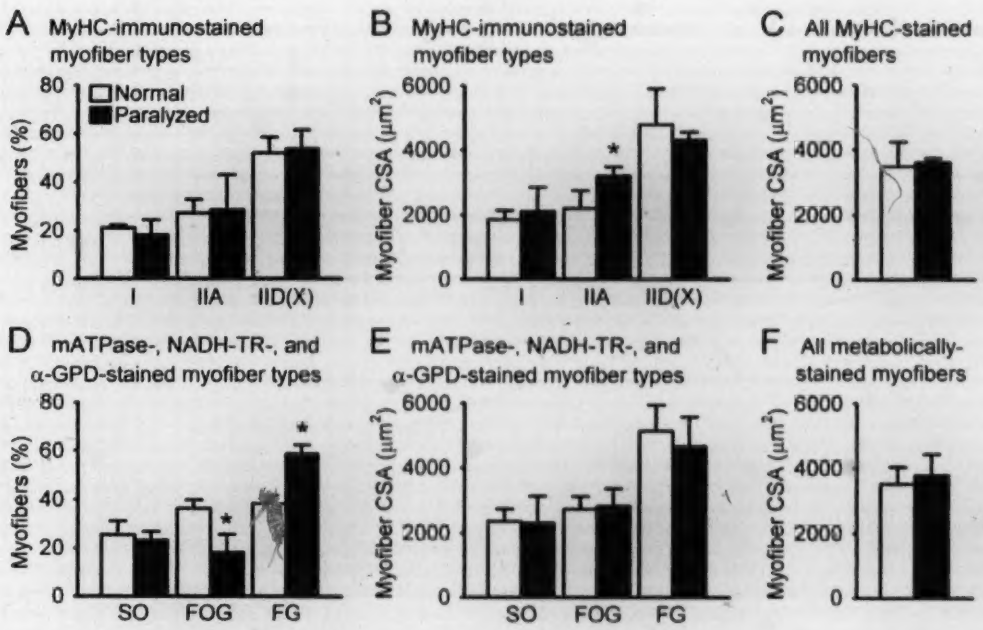
A MyHC-immunostained myofiber types
Normal
Paralyzed
Myofibers (%)
80
60
40
20
0
I
IIA
IID(X)
B MyHC-immunostained myofiber types
Myofiber CSA (μm²)
6000
4000
2000
0
*
I
IIA
IID(X)
C All MyHC-stained myofibers
Myofiber CSA (μm²)
6000
4000
2000
0
D mATPase-, NADH-TR-, and α-GPD-stained myofiber types
Myofibers (%)
80
60
40
20
0
*
*
SO
FOG
FG
E mATPase-, NADH-TR-, and α-GPD-stained myofiber types
Myofiber CSA (μm²)
6000
4000
2000
0
SO
FOG
FG
F All metabolically-stained myofibers
Myofiber CSA (μm²)
6000
4000
2000
0

composition according to the mATPase-identified myofiber types that are known to be correlated with fatigue resistance during repetitive, high-intensity contractile activity (Clarkson et al. 1980; Colliander et al. 1988; Kugelberg 1973).

Another interesting outcome of our histochemical analyses was that the mean myofiber cross-sectional area of all paralyzed myofibers did not change compared to that of all normal myofibers. Specifically, the mean CSA of all myofibers in normal MG muscles was 3481 ± 759 μm^2 according to measurements of myofibers classified using immunohistochemical criteria (Figure 4-11C, open bar) and was 3518 ± 517 μm^2 according to measurements of myofibers classified uisng metabolic histochemistry (Figure 4-11F, open bar). These values were not different in paralyzed MG muscles (Figure 4-11C, F, closed bars). Similarly, the mean CSAs of individual myofiber types changed very little after paralysis. Specifically, mean myofiber CSAs in normal MG muscles were 1858 ± 272 μm^2 for type I, 2189 ± 551 μm^2 for type IIA, and 4779 ± 1120 μm^2 for type IID(X) according to measurements of myofibers classified using immunohistochemical criteria (Figure 4-11B, open bars), and mean normal myofiber CSAs were 2347 ± 391 μm^2 for type SO, 2725 ± 401 μm^2 for type FOG, and 5134 ± 807 μm^2 for type FG according to measurements of myofibers classified using metabolic histochemistry (Figure 4-11E, open bars). In paralyzed MG muscles, the mean CSAs of type I and type IID(X) myofibers were not significantly different from those in normal myofibers (Figure 4-10B, closed bars), nor were the mean CSAs of SO, FOG, and FG myofibers (Figure 4-11E, closed bars). However, the mean CSA of type IIA myofibers increased significantly (3191 ± 290 μm^2; Figure 4-10B, closed bars). Likely this increase was the result of the transformation toward a more fatigable muscle profile including increased reliance on high energy phosphates as a fuel source, requiring the upregulation of enzymes such as creatine kinase, a structural protein (Turner et al. 1973), and hence to increased myofiber size. Type IIA myofibers are most likely to be found within the muscle units involved in the transformation from FR to FF after HSDA, which means that among myofibers classified according to contractile criteria (i.e., MyHC isoforms) the type IIA myofibers are most likely to exhibit this increase in myofiber size. The fact that this myofiber size increase is not observed among any of the myofiber groups classified according to metabolic criteria (i.e., staining for mATPase, NADH-TR, and α-GPD) suggests that this change is masked by the FOG to FG myofiber type transformation that was also observed.

In order to further elucidate the observed myofiber type proportions and myofiber CSAs in normal MG muscles and in MG muscles paralyzed due to long-term HSDA, each myofiber type was organized into frequency distribution plots according to cross-sectional area (CSA) bins of 0-500 μm^2, 501-1000 μm^2, and so on, up to 11501-12000 μm^2 (Figure 4-12). Type I (Figure 4-12A, B) and SO (Figure 4-12C, D) myofibers are represented by closed bars. Type IIA (Figure 4-12A, B) and FOG (Figure 4-12C, D) myofibers are represented by hatched bars. Type IID(X) (Figure 4-12A, B) and FG (Figure 4-12C, D) myofibers are represented by open bars. Myofiber CSA frequency distribution histograms were prepared for both paralyzed (Figure 4-12B, D) and normal (Figure 4-12A, C) MG muscles. In paralyzed MyHC-identified myofibers (Figure 4-12B)

Figure 4-12

For each immunohistochemically classified (A, B) or metabolically classified (C, D) myofiber type in the medial gastrocnemius (MG) muscle from adult cats paralyzed by long-term hemisection and unilateral deafferentation (n = 6; B, D) or from normal adult cats (n = 6; A, C), the number of myofibers within each of a series of size ranges is plotted as a percentage of the total number of myofibers of all types. In A and B, type I myofibers are represented by closed bars, type IIA myofibers are represented by hatched bars, and type IID(X) myofibers are reperesented by open bars. In C and D, slow oxidative (SO) myofibers are represented by closed bars, fast oxidative-glycolytic (FOG) myofibers are represented by hatched bars, and fast glycolytic myofibers are represented by open bars (C, D). In each plot, the total number of myofibers of each type is shown numerically as a percentage of the total number of myofibers of all types, and the mean myofiber size of each myofiber type is represented at the top of the plot with a triangle of a colour matching the bars for that myofiber type. The data in each plot comprise the pooled data for all myofibers from every animal analyzed in the paralyzed or normal groups.

Figure 4-12

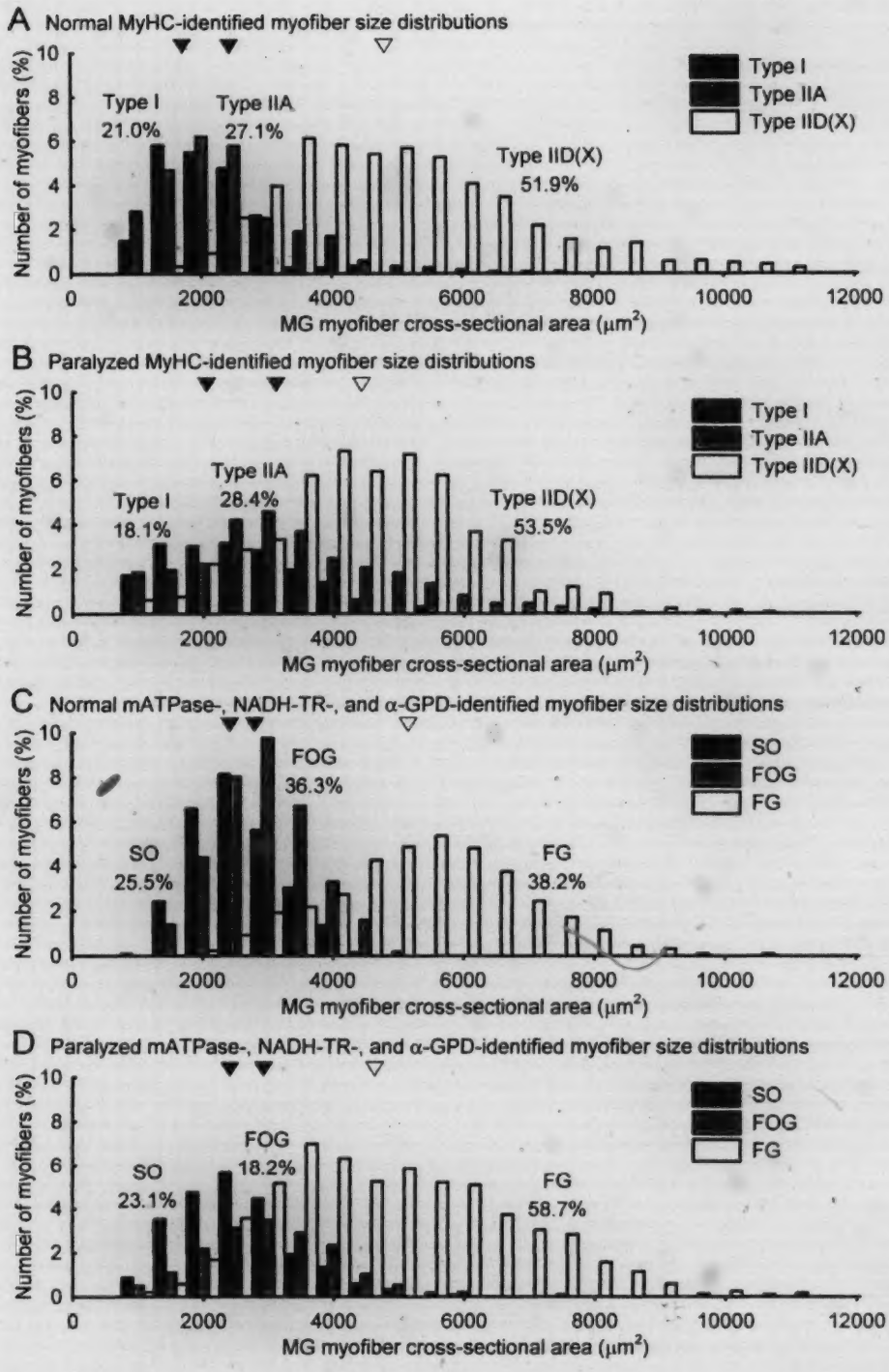
A Normal MyHC-identified myofiber size distributions
Number of myofibers (%)
Type I
21.0%
Type IIA
27.1%
Type IID(X)
51.9%
Type I
Type IIA
Type IID(X)
MG myofiber cross-sectional area (μm²)
B Paralyzed MyHC-identified myofiber size distributions
Number of myofibers (%)
Type I
18.1%
Type IIA
28.4%
Type IID(X)
53.5%
Type I
Type IIA
Type IID(X)
MG myofiber cross-sectional area (μm²)
C Normal mATPase-, NADH-TR-, and α-GPD-identified myofiber size distributions
Number of myofibers (%)
SO
25.5%
FOG
36.3%
FG
38.2%
SO
FOG
FG
MG myofiber cross-sectional area (μm²)
D Paralyzed mATPase-, NADH-TR-, and α-GPD-identified myofiber size distributions
Number of myofibers (%)
SO
23.1%
FOG
18.2%
FG
58.7%
SO
FOG
FG
MG myofiber cross-sectional area (μm²)

compared to in normal MyHC-identified myofibers (Figure 4-12A) the range of myofiber CSAs for each immunohistochemically classified myofiber type appears to broaden, without any obvious changes in myofiber type proportions. Similarly, in paralyzed metabolically-identified myofibers (Figure 4-12D) compared to in normal metabolically-identified myofibers (Figure 4-12C) the range of myofiber CSAs for each enzyme histochemically classified myofiber type also appears to broaden. However, among mATPase defined myofiber types this broadening appears to be accompanied by myofiber type transformations, especially from FOG toward FG (Figure 4-12D). This FOG to FG myofiber type transformation with paralysis is highlighted not only by, respectively, the decreased and increased FOG and FG myofiber proportions, but also by a relatively stable frequency distribution of FG myofibers with CSA > ~5000 μm^2, combined with a large increase in the proportion of FG myofibers with CSA < ~5000 μm^2, as well as a large decrease in the proportion of FOG myofibers that almost all exhibit CSA < ~5000 μm^2 (Figure 4-12D). In other words, in paralyzed MG (Figure 4-12D) compared to in normal MG (Figure 4-12C), the small (and non-significant) decrease in the mean CSA of FG myofibers (see white triangles in Figure 4-12C, D) was likely not due to atrophy of FG myofibers *per se*, but rather to a broadening of the FG myofiber size distribution due to the transformation of smaller FOG myofibers into an FG phenotype. Moreover, the FOG myofiber distribution in the paralyzed muscles clearly loses these myofibers. Consequently, the total CSA distribution for all myofibers does not change due to HSDA. Rather, in paralyzed MG muscles compared to normal MG muscles, some myofibers are included in a different metabolically-defined population as a result of changes both in the pH sensitivity of their mATPase and in their oxidative and glycolytic activities. Thus there was a classical transformation in the metabolic myofiber type distribution toward faster, more fatigable myofibers as revealed by a decrease in the proportion of FOG myofibers, and an increase in the proportion of FG myofibers (Figure 4-12C, D), consistent with the corresponding changes in the distribution FR and FF motor units, respectively (Figure 4-9), and in muscle endurance (Figure 4-5D).

The changes in the CSAs of the myofibers belonging to a single glycogen depleted motor unit in a paralyzed MG muscle (Figure 4-13B) were compared to the myofibers of a single glycogen depleted motor unit in a normal MG muscle (Figure 4-13A). The changes were consistent with the findings for the whole MG (Figure 4-12). Specifically, as similarly observed for the range of sizes of each myofiber type in paralyzed muscles, compared to normal muscles, the range of myofiber CSAs of glycogen depleted single motor units in the paralyzed muscles (Figure 4-13B) was substantially broadened compared to glycogen depleted single motor units in the normal muscles (Figure 4-13A). In fact, while the range of myofiber CSAs in the normal motor unit is only ~50% of the range of myofiber CSAs in the whole muscle (Figure 4-13A), the range of myofiber CSAs in the paralyzed motor unit spans almost the entire range of myofiber sizes in the whole muscle (Figure 4-13B). In both paralyzed and normal muscles, the mean myofiber CSA of the glycogen depleted motor unit myofibers (indicated by arrows above and below each histogram) was significantly different (not shown) from that of all the myofibers in the muscle.

Figure 4-13

Representative distribution frequency histograms from the paralyzed medial gastrocnemius (MG) of an adult cat with hemisection and unilateral deafferentation (B) and from the control MG of a normal adult cat (A) demonstrate the range of sizes of myofibers comprising a single motor unit in each muscle (closed bars) compared to the range of sizes of all myofibers in that muscle (open bars). Myofibers were identified in glycogen depleted motor units using periodic acid-Schiff staining (Pearse 1960). The arrows in each plot indicate the mean cross-sectional area, in μm^2, of the myofibers in the histogram.

Figure 4-13

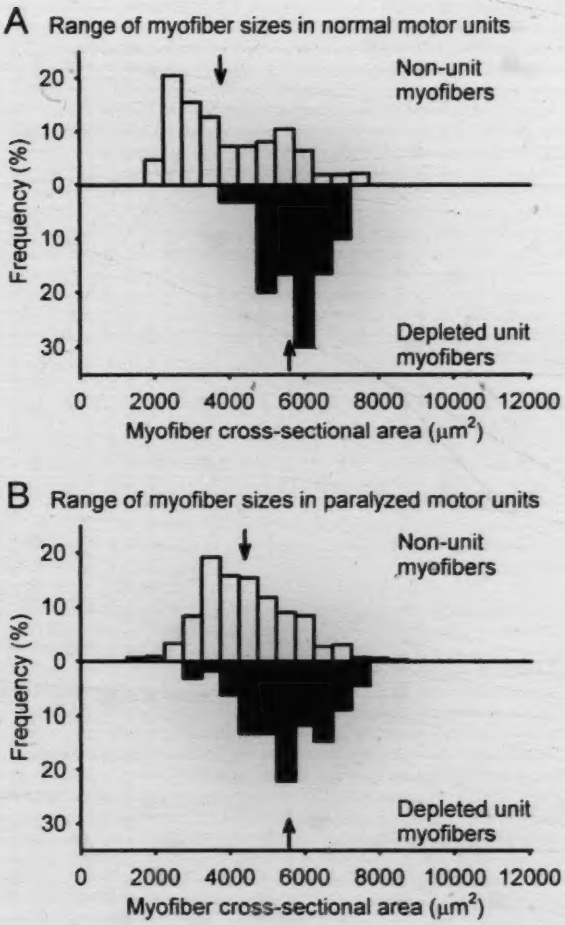
A Range of myofiber sizes in normal motor units
Non-unit myofibers
Depleted unit myofibers
Frequency (%)
20
10
0
10
20
30
0
2000
4000
6000
8000
10000
12000
Myofiber cross-sectional area (μm²)
B Range of myofiber sizes in paralyzed motor units
Non-unit myofibers
Depleted unit myofibers
Frequency (%)
20
10
0
10
20
30
0
2000
4000
6000
8000
10000
12000
Myofiber cross-sectional area (μm²)

4.3.8 Changes in contractile protein isoform contents and in metabolic enzyme activities

The maintained contractile force and speed at the whole MG muscle and MG motor unit levels after HSDA, compared to normal, are consistent with there being no changes in the proportions of myofibers classified according to their expression of contractile proteins (myosin heavy chain, or MyHC, isoforms). In contrast, the reduced muscle fatigue resistance was accompanied by a transformation toward a more fatigable profile both in the motor unit distribution and in the proportions of myofibers classified according to metabolic criteria (staining for mATPase, NADH-TR, and α-GPD). In other words, HSDA results in independent regulation of contractile and metabolic muscle phenotypes for prolonged periods (e.g., one year). Consequently, we wanted to quantify directly any possible changes in contractile proteins and metabolic enzymes in paralyzed MG muscles compared to in normal MG muscles that were likely to underlie these observed contractile and metabolic properties of whole muscles, motor units, and myofibers under the paralyzed and normal conditions. We quantified the relative contents of MyHC isoforms by using electrophoresis (SDS-PAGE) to separate these proteins (Figure 4-14A) in whole muscle extracts from paralyzed MG muscles (n = 5) and from normal MG muscles (n = 4), we also quantified the biochemical activities of oxidative and glycolytic marker enzymes (Figure 4-15) in whole muscle extracts from paralyzed MG (n = 8) and from normal MG muscles (n = 5).

In normal MG muscles gel electrophoresis (Figure 4-14A) demonstrated relative whole muscle MyHC isoform contents of 21 ± 5% MyHCI, 16 ± 3% MyHCIIa, and 63 ± 5% MyHCIId(x) (Figure 4-14B, open bars), and these were not different in paralyzed MG muscles (Figure 4-14B, closed bars). In order to compare these results from the electrophoretic separation of MyHC isoforms to the results of immunohstochemical identification of myofibers expressing MyHC isoforms we calculated the MyHC area density, which is defined as the measured cross-sectional area of a muscle that is positively identified as expressing a particular MyHC isoform, expressed as a percentage of the total cross-sectional area of all myofibers in that muscle (Fry et al. 1994; Hansen et al. 2004). We also calculated the area density defined according to metabolic criteria (staining for mATPase, NADH-TR, and α-GPD) in order to more accurately compare these measures of MyHC contractile proteins to the results of enzyme histochemical identification of myofibers with different metabolic properties. Mathematically, area density is the product of the mean proportion of a given myofiber type and the mean size of that myofiber type, normalized to the mean size of all myofibers, and thus area density calculated from immunohistochemistry is better correlated with the proportion of gel-separated MyHC isoforms than either myofiber proportion or myofiber size alone (Harris et al. 2007). In normal MG muscles, consistent with the whole muscle relative contents of MyHC isoforms (Figure 4-14B), the MyHC area densities were 12 ± 5% MyHCI, 17 ± 4% MyHCIIa, and 71 ± 8% MyHCIId(x) (Figure 4-14C, open bars), and these were not different in paralyzed MG muscles (Figure 4-14C, closed bars). As expected based upon the distributions of metabolically-classified myofiber types (Figure 4-11D), there was a significant transformation in metabolically-defined area density compared to in normal MG muscles. Specifically, in normal MG muscles the metabolic area densities were 16 ±

Figure 4-14

Representative lanes from SDS-PAGE gel electrophoresis (A) show the separation of myosin heavy chain (MyHC) isoforms I, IIa, and IId(x) in muscle extracts from the paralyzed medial gastrocnemius (MG) of adult cats with long-term hemisection and unilateral deafferentation (n = 5; right-hand lane) and from the control MG of normal adult cats (n = 4; left-hand lane). Mean relative contents of each MyHC isoform in paralyzed (closed bars) or normal (open bars) MG are shown as measured from MyHC bands separated by gel electrophoresis (B). The area density of myofiber types is shown as computed either from immunohistochemistry (type I, type IIA, and type IID[X] myofibers; C) or from metabolic histochemistry (slow oxidative [SO], fast oxidative-glycolytic [FOG], and fast glycolytic [FG] myofibers; D). The area density is the measured cross-sectional area of a muscle that is positively identified as a given myofiber type, calculated as a percentage of the total cross-sectional area of all myofibers measured (also see MATERIALS AND METHODS). Values are means ± standard deviations. * denotes statistical significance accepted at the $P < 0.05$ level as determined using a one-way ANOVA.

Figure 4-14

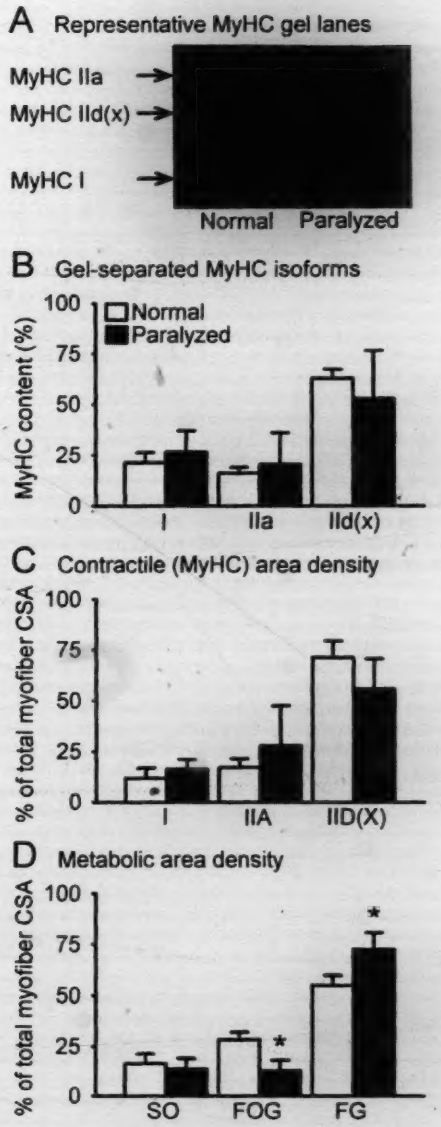
A Representative MyHC gel lanes
MyHC IIa
MyHC IId(x)
MyHC I
Normal
Paralyzed
B Gel-separated MyHC isoforms
MyHC content (%)
Normal
Paralyzed
100
75
50
25
0
I
IIa
IId(x)
C Contractile (MyHC) area density
% of total myofiber CSA
100
75
50
25
0
I
IIA
IID(X)
D Metabolic area density
% of total myofiber CSA
100
75
50
25
0
SO
FOG
FG

Figure 4-15

A: biochemical activities in units of activity per milligram of soluble protein are shown for the oxidative marker enzyme citrate synthase (CS, E.C.4.1.3.7) and for the glycolytic marker enzyme glyceraldehyde phosphate dehydrogenase (GAPDH, E.C.1.2.1.12), as determined photometrically in extracts from the paralyzed medial gastrocnemius (MG) muscle of adult cats with hemisection and unilateral deafferentation (n = 8; closed bars) and from the control MG of normal adult cats (n = 5; open bars). B: the mean oxidative (CS) and glycolytic (GAPDH) enzyme activities (shown in A) are compared as ratios for the normal and paralyzed groups. Values are means ± standard deviations. * denotes statistical significance accepted at the $P < 0.05$ level, as determined using a one-way ANOVA in A or using a one-tailed t-test in B.

Figure 4-15

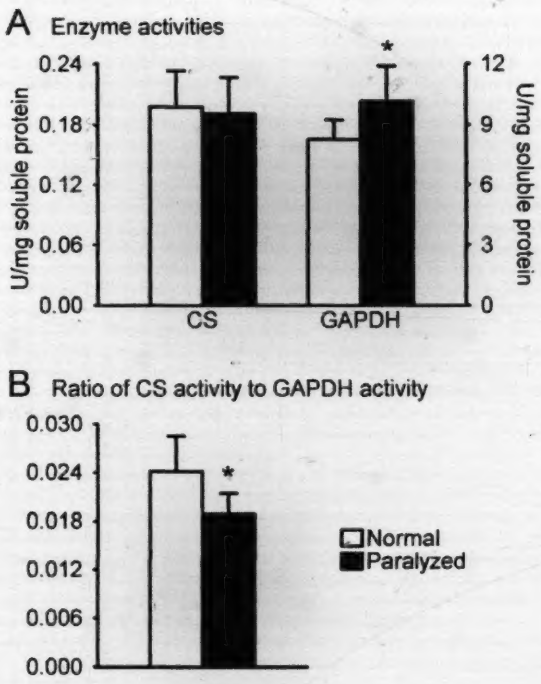
A Enzyme activities
U/mg soluble protein
0.24
0.18
0.12
0.06
0.00
12
9
6
3
0
U/mg soluble protein
*
CS
GAPDH
B Ratio of CS activity to GAPDH activity
0.030
0.024
0.018
0.012
0.006
0.000
*
Normal
Paralyzed

5% SO, 28 ± 4% FOG, and 55 ± 5% FG (Figure 4-14D, open bars), and in paralyzed MG muscles (Figure 4-14D, closed bars), although the SO area density did not change (14 ± 5%), the FOG area density decreased significantly (13 ± 5%) and the FG area density increased significantly (73 ± 8%).

In normal MG muscles the mean whole muscle biochemical activity of citrate synthase (CS), a marker of oxidative metabolism, was 0.20 ± 0.05 U/mg soluble protein (Figure 4-15), and the CS activity in paralyzed MG muscles was not significantly different from normal (0.18 ± 0.05 U/mg soluble protein; Figure 4-15A). However, in normal MG muscles the mean whole muscle biochemical activity of glyceraldehyde phosphate dehydrogenase (GAPDH), a marker of glycolytic metabolism, was 13.1 ± 5.7 U/mg soluble protein (Figure 4-15), and the GAPDH activity in paralyzed MG muscles was significantly greater (17.9 ± 4.4 U/mg soluble protein; Figure 4-15A). The increased ratio of glycolytic to oxidative enzyme activities in paralyzed MG compared to in normal MG (Figure 4-15B) is consistent with the significant decline in muscle and motor unit fatigue resistance and with the significant transformation toward more fatigable myofiber types observed as a result of paralysis.

4.3.9 Muscle masses

In adult cats paralyzed by hemisection and unilateral deafferentation, the mean wet mass of the normal contralateral control medial gastrocnemius (MG) muscle was 9.5 ± 2.0 g (Table 4-1). In comparison, the mean wet mass of the paralyzed MG concurred with myofiber size analyses, demonstrating no significant difference from the normal MG (Table1). There were also no significant differences between mean muscle masses of paralyzed and normal lateral gastrocnemius (LG), soleus (SOL), plantaris (PLA), tibialis anterior (TA), or extensor digitorum longus (EDL; Table 4-1). However, it should be noted that with the exception of MG and TA, for which the mean percent change in muscle mass was less than 5% in both cases, all these muscles exhibited mean percent changes in muscle mass of > 10%, indicating a tendency for muscle atrophy. Moverover, within the triceps surae, the -15.8 ± 12.6% decrease in SOL muscle mass and the -11.2 ± 12.2% decrease in LG muscle were significantly different neither from 0 nor from each other, but they were both significantly different from the -1.5 ± 8.9% decrease in MG muscle mass (Table 4-1, significant differences not indicated).

4.4 DISCUSSION

4.4.1 Muscle weakness after paralysis: force versus fatigue

The results of this study show that compared to the normally active medial gastrocnemius (MG) muscles and motor units in normal adult cats, MG muscles paralyzed by hemisection and deafferentation (HSDA) exhibit normal whole muscle and motor unit contractile speed and force, normal myosin heavy chain (MyHC) contractile protein distributions, and normal MyHC-classified myofiber proportions, as well as resistance to atrophy at both the whole muscle and myofiber levels. However, MG muscles paralyzed

by HSDA become dramatically more fatigable with reduced muscle and motor unit endurance and with transformations in the frequency distributions both of motor unit types and of metabolically-classified myofiber types. These transformations lead to a larger number of fast fatigable (FF) motor units and a larger number of fast glycolytic (FG) myofibers at the expense of fast fatigue resistant (FR) motor units and fast oxidative glycolytic myofibers (FOG). The ratio of whole muscle oxidative to glycolytic enzyme activities is also reduced. Such changes demonstrate that HSDA causes a dramatic shift in the metabolic profile of the paralyzed MG muscle such that most of the cumulative motor unit force is developed by the FF motor units, although there is no change overall in the mean tetanic forces of either the whole muscle or of the motor units. In other words after long-term HSDA, compared to normal, the muscle maintains its ability to generate large isometric forces but it becomes extremely susceptible to fatigue. Consequently the force densities of MG motor units observed after HSDA mean that the development of large cumulative forces during motor unit recruitment in the paralyzed muscles will result in a rapid onset of fatigue.

These changes in fatigability after long-term HSDA are comparable to those observed following long-term muscle paralysis due to spinal cord injury in humans (Castro et al. 1999). Hence our data highlight an important outcome of paralysis: the functional weakness of muscles after both spinal cord injury and HSDA is not necessarily a consequence of the muscles' inability to produce force, but rather of their inability to *sustain* force. This is particularly evident in studies of the effects of electrical stimulation training of muscles that have been paralyzed by chronic (2 years or more) spinal cord injury. These investigations always document poor fatigue resistance at the outset of the study and a recovery of endurance with many weeks of training (Hartkopp et al. 2003). However, as similarly observed following HSDA muscles paralyzed by spinal cord injury do not always exhibit an impaired ability to generate isometric forces compared to unparalyzed control muscles (Stein et al. 1992), *or* an increased ability to generate force as training progresses even while contractile speed slows and endurance improves (Harridge et al. 2002; Stein et al. 1992).

From a clinical perspective, it is interesting to reiterate (see INTRODUCTION) that cats with unilateral hindlimb paralysis due to chronic HSDA have been used previously to investigate the effects of long-term electrical stimulation (Donselaar et al. 1987; Gordon et al. 1997; Kernell et al. 1987a; Kernell et al. 1987b). We observed that paralyzed and stimulated MG muscles experience dramatic increases in endurance and exhibit substantial slowing in the form of prolonged twitch contractions and increased type SO and FOG myofiber proportions at the expense of type FG myofiber proportions, but they also exhibit reduced absolute isometric forces (Gordon et al. 1997). In other words, muscle strength as defined according to absolute isometric force generation is not altered following paralysis due to HSDA but it is in fact reduced following long-term stimulation of muscles paralyzed by HSDA. In contrast, muscle strength as defined according to the ability to sustain force with repeated contractions (endurance) is impaired following HSDA and is improved with long-term stimulation after HSDA. Moreover, when paralyzed muscles under partial voluntary control (e.g., partial spinal cord injury) generate lower absolute isometric forces (unlike muscles paralyzed by HSDA) they must

work at a higher percentage of their maximum force to perform any given functional task and thus they will fatigue more rapidly, especially if they also exhibit compromised endurance (Thomas and Zijdewind 2006). Thus therapies aimed at promoting muscle recovery after chronic paralysis must achieve a balance between improving or maintaining muscle strength *and* improving or maintaining muscle fatigue resistance, without compromising either of these functional attributes. This has in fact been investigated thoroughly in studies of electrical stimulation induced exercise designed both for resistance training (Hartkopp et al. 2003) and for endurance training (Stein et al. 1992) of muscles paralyzed by spinal cord injury.

4.4.2 HSDA is an unique model of altered use

We did not directly quantify the level of activity present in adult cat MG muscles paralyzed by HSDA in this study. However, we can partially clarify the impact of this intervention on muscle activity by comparison with other models of altered use. Based upon the results of chronic stimulation experiments it is known that over extended periods of time (weeks to months) large average daily amounts of muscle activity are correlated with the acquisition (or maintenance) of high levels of muscle and motor unit fatigue resistance (Eerbeek et al. 1984; Gordon et al. 1997; Kernell et al. 1987a). By extension, it appears that HSDA results in a large decrease in the daily neuromuscular activity of the paralyzed MG muscles, compared to normal, because their fatigue resistance is profoundly reduced (see preceding section). This is consistent with data demonstrating significant reductions in the fatigue resistance of soleus and MG muscles and motor units in rats and cats following spinal cord transection and spinal isolation (Mayer et al. 1984; Roy et al. 1998; Roy et al. 2002b; Talmadge et al. 2002), which are known to result in dramatic reductions in neuromuscular activity (Alaimo et al. 1984; Harris et al. 2007; Pierotti et al. 1991; Roy et al. 2007). Importantly, the similarity of the cat MG muscle in the response of its fatigability profile to reduced activity resulting both from HSDA and spinal cord transection is highlighted by the fact that in both cases the motor units transform from type FR to type FF without a significant loss of type S motor units (Munson et al. 1986).

Although it seems very likely that MG muscles paralyzed by HSDA undergo large reductions in activity our results in fact demonstrate that unilateral hindlimb paralysis due to HSDA is not a good model of skeletal muscle disuse, i.e., of inactivity. In particular, observations of the behaviour of hindlimbs paralyzed by HSDA, HSDA-SP, and HS demonstrate that the affected muscles participate in voluntary and/or reflex movements unlike muscles paralyzed by spinal isolation, in which activity is known to be almost completely (≥ 92%) eliminated (Harris et al. 2007; Pierotti et al. 1991; Roy et al. 2007). Moreover, in models where it is well established that a reduction in muscle activity is the result of complete spinal cord transection (Alaimo et al. 1984), *augmented* FR motor unit tetanic force and *reduced* FF motor unit tetanic force have been attributed to, respectively, increased type FOG myofiber CSA and decreased type FG myofiber CSA (Mayer et al. 1984; Munson et al. 1986). Yet in the current study not only is FR motor unit tetanic force slightly (but not significantly) *reduced* and FF motor unit tetanic force slightly (but not significantly) *augmented*, there also are no changes in the mean myofiber

CSA of either type FOG or type FG myofibers. Finally, following HSDA, compared to normal, there are in fact no significant changes in the average motor unit or muscle contractile speed or peak tetanic tension, or in the average whole musle mass. In contrast, the results of experiments investigating the effects of reduced or eliminated activity due to spinal cord transection or spinal isolation, respectively, demonstrate increased contractile speed and decreased tetanic tension of both whole muscles and motor units, as well as muscle mass atrophy (Mayer et al. 1984; Munson et al. 1986; Roy et al. 1999; Roy et al. 2002a; Zhong et al. 2002).

It is also interesting to speculate that even if the reduced fatigue resistance at the MG motor unit and muscle levels observed after HSDA suggests a reduction in muscle activity that may be quantitatively similar to that observed after spinal cord transection, the neuromuscular activity decrease must be *qualitatively* different in these models (i.e., the residual activity occurs in different patterns). Therefore, the associated changes in the myofiber distributions are not the same. Specifically, in the MG muscle following HSDA, transformations in the distributions of myofibers classified according to metabolic criteria (staining for mATPase, NADH-TR, and α-GPD) occur only within the fast types, but *not* the slow types, and transformations do not occur at all in the distribution of myofibers classified according to contractile criteria (immunostaining for myosin heavy chain contractile protein isoforms). However, in the MG and soleus muscles following spinal cord transection and spinal isolation, transformations in the distributions of metabolically-classified *and* contractile protein-based myofibers include reduced proportions of, respectively, type SO and type I myofibers combined with increased proportions of type FOG/FG and type II myofibers (Graham et al. 1992; Jiang et al. 1990a, b; Roy et al. 2002a; Zhong et al. 2002). Similarly, HSDA, spinal cord transection, and spinal isolation all result in a decrease in the ratio of oxidative to glycolytic enzyme activities in the MG muscle, but following HSDA this is due only to increased glycolytic enzyme activity whereas following spinal cord transection and spinal isolation this is due both to decreased oxidative enzyme activity *and* to increased glycolytic enzyme activity (Jiang et al. 1990a; Jiang et al. 1991).

In summary, with respect to reductions in muscle and motor unit fatigability, the effects of HSDA are similar to those of spinal cord transection and spinal isolation, in which muscle activity is known to be significantly reduced. Thus it is likely that muscle activity is also substantially reduced following HSDA. However, we did not measure muscle activity and the extent of the putative activity reduction is unclear because HSDA does not lead to changes in contractile properties or muscle mass and the transformations it induces in motor units, myofiber types, and metabolic enzymes are different from those observed following spinal cord transection and spinal isolation. Further, MG muscles paralyzed by HSDA, HSDA-SP, and HS clearly experience some activity because they participate in reflex and/or voluntary movements.

4.4.3 The contractile and metabolic phenotypes of cat skeletal muscle are regulated independently following HSDA

The metabolic and contractile phenotypes of paralyzed skeletal muscles are independently regulated after long-term paralysis of cat skeletal muscle due to HSDA. There is no change in the distribution of myofibers classified according to their expression of myosin heavy chain protein isoforms, and likewise there are no changes in contractile force or speed of the paralyzed muscles and their motor units. However, there is a large transformation in the distribution of myofibers classified according to metabolic criteria toward more fatigable myofiber types and, accordingly, the paralyzed muscles and their motor units become more fatigable. These observations are consistent with our previous models of altered muscle activity in which conceptually similar dissociations between metabolism and contractile phenotype occured. In rats with chronic sacral spinal cord transection the paralyzed tail muscles exhibit normal amounts of neuromuscular activity, on average, because they become very spastic over many months (Harris et al. 2007). As in the current study these paralyzed but active (spastic) muscles exhibit normal proportions of myosin heavy chain protein isoforms despite their reduced muscle endurance (Harris et al. 2006; Harris et al. 2007). Similarly, in rats that experience a 28-day upregulation of the activity of AMP-activated protein kinase, which mediates skeletal muscle adaptations to increased contractile activity, there is a preservation of myofiber type proportions and contractile protein distributions, coordinate with increases in the ratio of oxidative to glycolytic metabolic enzyme activities (Putman et al. 2003). Hence with altered activity in these three models there is a dis-coordinate or independent regulation of contractile and metabolic properties.

These findings challenge the common view that the metabolic and contractile properties of skeletal muscle are regulated in a coordinate fashion. This view has been reflected in the assumption that immunohistochemistry for MyHC isoforms and enzyme histochemistry for mATPase and metabolic markers provide similar myofiber classifications, especially when the particular techniques used permit the differentiation of only two myofiber types (e.g., type I versus type II, or slow versus fast) and even when there has been a clear alteration in neuromuscular activity (Jiang et al. 1991). It might also be assumed that the comparison between these two methods should be more direct in cats than in smaller mammals, because mATPase can most easily be used to clearly identify three distinct myofiber types and, similarly, adult cat muscles normally express 3 MyHC isoforms (Roy et al. 1999), whereas adult rodent muscles normally express 4 isoforms (Peuker et al. 1999). However, we show in this study that normal adult cat MG muscles exhibit significantly fewer type I and type IIA myofibers than SO and FOG myofibers, respectively, and they exhibit significantly more type IID(X) myofibers than FG myofibers. Thus it is not safe to assume that the results of mATPase enzyme histochemistry and MyHC immunohistochemistry can be directly compared in cat muscle just because each method identifies 3 distinct myofiber types. This conclusion is consistent with data revealing mismatches between immunohistochemical and mATPase myofiber profiles in 40% of myofibers in horse skeletal muscle (Linnane et al. 1999). As emphasized by these authors, such findings demonstrate the need for caution not only in

the interpretation of both staining methods, but also in making comparisons between studies using different methods of myofiber classification.

Indeed, throughout the preceding text we are careful to describe our enzyme histochemical staining in terms of "myofibers classified according to metabolic criteria" because we used enzyme histochemistry for the metabolic markers NADH-TR (oxidative) and α-GPD (glycolytic) in addition to mATPase staining (see MATERIALS AND METHODS). Myosin ATPase enzyme histochemistry is a useful myofiber type classification method if applied rigorously, but it is subjective. Therefore its value is questionable if the exact methodology employed is not considered or described. For example, if optimized and validated for each species examined mATPase staining stands alone (Hämäläinen and Pette 1993). This is time consuming, however, and the accuracy of the method can be compromised easily by minute fluctuations in the pH of the preincubation media. Even when myofiber classification according to mATPase staining is assisted with quantitative measurements of myofiber optical density, the method usually remains subjective because the experimenters must ultimately decide what constitutes the "darkest" or "lightest" myofiber of each type (Castro et al. 1999). Consequently, myofiber classification according to mATPase enzyme histochemistry may be supplemented with oxidative and glycolytic enzyme histochemistry (Peter et al. 1972). Again, this requires a subjective assessment, in which myofibers that stain ambiguously according to mATPase are classified according to metabolic criteria. When cat soleus myofibers are assessed using rigorous quantitation of optical density of mATPase, SDH (oxidative), and α-GPD staining, two distinct groups of myofibers can be discerned, consistent with the motor unit distribution of this muscle (Martin et al. 1988; Zhong et al. 2002). However, it has also been shown that in order for optical density measurements to be a valid means of quantitatively analysing myofiber staining, the method must include careful controls for non-linearities in the relationship between the thickness and the light absorption of the tissue sections, and for possible non-specific staining that can result from mATPase-independent processes (van der Laarse et al. 1984). In large studies such technicalities can be very time consuming, and thus routine staining must be accompanied by acknowledgement of its subjectivity. Finally, although it is well-established that the mATPase staining intensity of a given myofiber is determined by the constituent myosin heavy chains rather than by the myosin light chains (Billeter et al. 1981) there is a multiplicity of myofiber types possible when various combinations of both heavy and light chain isoforms are considered (Staron and Pette 1987). This diversity of myofiber types is further complicated by the numerous proteins involved in contraction including actin, troponins, and tropomyosin, which all exist in multiple isoforms that are differentially expressed across myofiber types and that transform with alterations in activity (Schiaffino and Reggiani 1996). Functionally, these various proteins form a large complex, and thus it is important to consider that, in any given myofiber, subtle changes in the pH sensitivity of mATPase enzyme histochemistry are most likely determined not only by myosin heavy chains but also by numerous other proteins. This will be particularly complicated when altered activity causes changes in expression of different protein isoforms.

In contrast, immunohistochemistry for myosin heavy chain isoforms is a repeatable source of information regarding the contractile phenotype of individual myofibers, so long as the antibodies used have been carefully tested for specificity and cross-reactivity in the species being examined. An appropriate battery of antibodies can be applied to identify myofibers expressing single or multiple myosin heavy chain contractile protein isoforms (Peuker et al. 1999; Putman et al. 1999). Additionally, this semi-quantitative staining method can be validated in each experiment by comparing the area density of each antibody's staining to the quantitative distribution of elecrophoretically separated myosin heavy chain isoforms as we have done here and elsewhere (Hansen et al. 2004; Harris et al. 2007).

In conclusion, careful consideration of the technical aspects of enzyme histochemical staining for mATPase and metabolic enzymes and of immunohistochemistry for myosin heavy chain isoforms emphasizes that these are not equivalent methods of myofiber type classification and thus it is not surprising that there is a mismatch between the myofiber types identified using these methods here and in previous studies (Linnane et al. 1999). However, both methodological approaches are useful in classifying myofibers types according to different criteria: enzyme histochemistry for mATPase and oxidative and glycolytic markers identifies the metabolic profile of myofibers, while immunohistochemistry for myosin heavy chain isoforms identifies the contractile profile of myofibers. In the current study the two methods applied in parallel revealed the metabolic and contractile myofiber distributions that were fundamental to the independent regulation of metabolic and contractile function in paralyzed muscles and motor units following long-term HSDA.

4.4.4 Summary

A combination of hemisection and unilateral deafferentation (HSDA) causes substantial unilateral hindlimb paralysis, resulting in impaired postural and locomotor behaviour of the paralyzed hindlimb and a profound reduction in whole muscle and motor unit endurance. In spite of this paralysis, HSDA does not completely eliminate muscle activity because paralyzed medial gastrocnemius muscles and their motor units still participate in some reflex and voluntary movements, and they exhibit contractile and metabolic profiles that are substantially different from those observed in other models of reduced or eliminated use (Alaimo et al. 1984; Graham et al. 1992; Jiang et al. 1990a; Mayer et al. 1984; Munson et al. 1986; Pierotti et al. 1991; Zhong et al. 2002). Specifically, contractile force, contractile speed, and contractile proteins are all preserved in MG muscles and motor units following HSDA, but there is a loss of fatigue resistance accompanied by transformations toward a more fatigable profile in the distributions of motor units, myofibers, and metabolic enzymes. These findings support the idea that the contractile and metabolic properties of skeletal muscle may be regulated independently when muscle activity is altered due to injury or exercise. At the myofiber level, such independent regulation can be assessed using a combination of methods that classify myofibers according to both metabolic criteria and myosin heavy chain proteins. Physiological classification of motor units according to contractile properties and endurance should reflect any observed changes in myofiber types.

4.5 REFERENCES FOR CHAPTER 4

Alaimo MA, Smith JL, Roy RR, and Edgerton VR. EMG activity of slow and fast ankle extensors following spinal cord transection. *J Appl Physiol* 56: 1608-1613, 1984.

Bass A, Brdiczka D, Eyer P, Hofer S, and Pette D. Metabolic differentiation of distinct muscle types at the level of enzymatic organization. *Eur J Biochem* 10: 198-206, 1969.

Billeter R, Heizmann CW, Howald H, and Jenny E. Analysis of myosin light and heavy chain types in single human skeletal muscle fibers. *Eur J Biochem* 116: 389-395, 1981.

Burke RE, Levine DN, Tsairis P, and Zajac FE, 3rd. Physiological types and histochemical profiles in motor units of the cat gastrocnemius. *J Physiol* 234: 723-748, 1973.

Castro MJ, Apple DF, Jr., Staron RS, Campos GER, and Dudley GA. Influence of complete spinal cord injury on skeletal muscle within 6 mo of injury. *J Appl Physiol* 86: 350-358, 1999.

Clarkson PM, Kroll W, and McBride TC. Plantar flexion fatigue and muscle fiber type in power and endurance athletes. *Med Sci Sports Exerc* 12: 262-267, 1980.

Colliander EB, Dudley GA, and Tesch PA. Skeletal muscle fiber type composition and performance during repeated bouts of maximal, concentric contractions. *Eur J Appl Physiol Occup Physiol* 58: 81-86, 1988.

Davis LA, Gordon T, Hoffer JA, Jhamandas J, and Stein RB. Compound action potentials recorded from mammalian peripheral nerves following ligation or resuturing. *J Physiol* 285: 543-559, 1978.

Donselaar Y, Eerbeek O, Kernell D, and Verhey BA. Fibre sizes and histochemical staining characteristics in normal and chronically stimulated fast muscle of cat. *J Physiol* 382: 237-254, 1987.

Dubowitz V, and Brooke MH. *Muscle biopsy: a modern approach*. Philadelphia: Saunders, 1973, p. 475.

Eerbeek O, Kernell D, and Verhey BA. Effects of fast and slow patterns of tonic long-term stimulation on contractile properties of fast muscle in the cat. *J Physiol* 352: 73-90, 1984.

Eldridge L, Liebhold M, and Steinbach JH. Alterations in cat skeletal neuromuscular junctions following prolonged inactivity. *J Physiol* 313: 529-545, 1981.

Fry AC, Allemeier CA, and Staron RS. Correlation between percentage fiber type area and myosin heavy chain content in human skeletal muscle. *Eur J Appl Physiol Occup Physiol* 68: 246-251, 1994.

Gallo M, Gordon T, Tyreman N, Shu Y, and Putman CT. Reliability of isolated isometric function measures in rat muscles composed of different fibre types. *Exp Physiol* 89: 583-592, 2004.

Goldberger ME, and Murray M. Restitution of function and collateral sprouting in the cat spinal cord: the deafferented animal. *J Comp Neurol* 158: 37-53, 1974.

Gordon T, and Stein RB. Reorganization of motor-unit properties in reinnervated muscles of the cat. *J Neurophysiol* 48: 1175-1190, 1982.

Gordon T, Thomas CK, Munson JB, and Stein RB. The resilience of the size principle in the organization of motor unit properties in normal and reinnervated adult skeletal muscles. *Can J Physiol Pharmacol* 82: 645-661, 2004.

Gordon T, Tyreman N, Rafuse VF, and Munson JB. Fast-to-slow conversion following chronic low-frequency activation of medial gastrocnemius muscle in cats. I. Muscle and motor unit properties. *J Neurophysiol* 77: 2585-2604, 1997.

Graham SC, Roy RR, Navarro C, Jiang B, Pierotti D, Bodine-Fowler S, and Edgerton VR. Enzyme and size profiles in chronically inactive cat soleus muscle fibers. *Muscle Nerve* 15: 27-36, 1992.

Green HJ, Dusterhoft S, Dux L, and Pette D. Metabolite patterns related to exhaustion, recovery and transformation of chronically stimulated rabbit fast-twitch muscle. *Pflugers Arch* 420: 359-366, 1992.

Green HJ, Reichmann H, and Pette D. A comparison of two ATPase based schemes for histochemical muscle fibre typing in various mammals. *Histochemistry* 76: 21-31, 1982.

Guth L, and Samaha FJ. Procedure for the histochemical demonstration of actomyosin ATPase. *Exp Neurol* 28: 365-367, 1970.

Hämäläinen N, and Pette D. The histochemical profiles of fast fiber types IIB, IID, and IIA in skeletal muscles of mouse, rat, and rabbit. *J Histochem Cytochem* 41: 733-743, 1993.

Hansen G, Martinuk KJ, Bell GJ, MacLean IM, Martin TP, and Putman CT. Effects of spaceflight on myosin heavy-chain content, fibre morphology and succinate dehydrogenase activity in rat diaphragm. *Pflügers Arch* 448: 239-247, 2004.

Harridge SD, Andersen JL, Hartkopp A, Zhou S, Biering-Sorensen F, Sandri C, and Kjaer M. Training by low-frequency stimulation of tibialis anterior in spinal cord-injured men. *Muscle Nerve* 25: 685-694, 2002.

Harris RLW, Bobet J, Sanelli L, and Bennett DJ. Tail muscles become slow but fatigable in chronic sacral spinal rats with spasticity. *J Neurophysiol* 95: 1124-1133, 2006.

Harris RLW, Putman CT, Bennett DJ, Tyreman N, and Gordon T. Fatigue-resistance and oxidative metabolism are severely compromised in cat medial gastrocnemius after hemisection and deafferentation. In: *35th Meeting of the Society for Neuroscience*. Washington DC: 2005.

Harris RLW, Putman CT, Rank MM, Sanelli L, and Bennett DJ. Spastic tail muscles recover from myofiber atrophy and myosin heavy chain transformations in chronic spinal rats. *J Neurophysiol* 97: 1040-1051, 2007.

Hartkopp A, Harridge SD, Mizuno M, Ratkevicius A, Quistorff B, Kjaer M, and Biering-Sorensen F. Effect of training on contractile and metabolic properties of wrist extensors in spinal cord-injured individuals. *Muscle Nerve* 27: 72-80, 2003.

Helgren ME, and Goldberger ME. The recovery of postural reflexes and locomotion following low thoracic hemisection in adult cats involves compensation by undamaged primary afferent pathways. *Exp Neurol* 123: 17-34, 1993.

Jiang B, Roy RR, and Edgerton VR. Enzymatic plasticity of medial gastrocnemius fibers in the adult chronic spinal cat. *Am J Physiol* 259: C507-514, 1990a.

Jiang B, Roy RR, and Edgerton VR. Expression of a fast fiber enzyme profile in the cat soleus after spinalization. *Muscle Nerve* 13: 1037-1049, 1990b.

Jiang BA, Roy RR, Navarro C, Nguyen Q, Pierotti D, and Edgerton VR. Enzymatic responses of cat medial gastrocnemius fibers to chronic inactivity. *J Appl Physiol* 70: 231-239, 1991.

Kernell D, Donselaar Y, and Eerbeek O. Effects of physiological amounts of high- and low-rate chronic stimulation on fast-twitch muscle of the cat hindlimb. II. Endurance-related properties. *J Neurophysiol* 58: 614-627, 1987a.

Kernell D, Eerbeek O, Verhey BA, and Donselaar Y. Effects of physiological amounts of high- and low-rate chronic stimulation on fast-twitch muscle of the cat hindlimb. I. Speed- and force-related properties. *J Neurophysiol* 58: 598-613, 1987b.

Kugelberg E. Histochemical composition, contraction speed and fatiguability of rat soleus motor units. *J Neurol Sci* 20: 177-198, 1973.

Linnane L, Serrano AL, and Rivero JL. Distribution of fast myosin heavy chain-based muscle fibres in the gluteus medius of untrained horses: mismatch between antigenic and ATPase determinants. *J Anat* 194: 363-372, 1999.

Martin TP, Bodine-Fowler S, and Edgerton VR. Coordination of electromechanical and metabolic properties of cat soleus motor units. *Am J Physiol* 255: C684-693, 1988.

Martinov VN, and Nja A. A microcapsule technique for long-term conduction block of the sciatic nerve by tetrodotoxin. *Journal of neuroscience methods* 141: 199-205, 2005.

Mayer RF, Burke RE, Toop J, Walmsley B, and Hodgson JA. The effect of spinal cord transection on motor units in cat medial gastrocnemius muscles. *Muscle Nerve* 7: 23-31, 1984.

McGuigan MR, Kraemer WJ, Deschenes MR, Gordon SE, Kitaura T, Scheett TP, Sharman MJ, and Staron RS. Statistical analysis of fiber area in human skeletal muscle. *Can J Appl Physiol* 27: 415-422, 2002.

Munson JB, Foehring RC, Lofton SA, Zengel JE, and Sypert GW. Plasticity of medial gastrocnemius motor units following cordotomy in the cat. *J Neurophysiol* 55: 619-634, 1986.

Murray M, and Goldberger ME. Restitution of function and collateral sprouting in the cat spinal cord: the partially hemisected animal. *J Comp Neurol* 158: 19-36, 1974.

Oakley BR, Kirsch DR, and Morris NR. A simplified ultrasensitive silver stain for detecting proteins in polyacrylamide gels. *Anal Biochem* 105: 361-363, 1980.

Pearse AGE. *Histochemistry: theoretical and applied.* London: Churchill, 1960, p. 998.

Peter JB, Barnard RJ, Edgerton VR, Gillespie CA, and Stempel KE. Metabolic profiles of three fiber types of skeletal muscle in guinea pigs and rabbits. *Biochemistry* 11: 2627-2633, 1972.

Peuker H, Conjard A, Putman CT, and Pette D. Transient expression of myosin heavy chain MHCI alpha in rabbit muscle during fast-to-slow transition. *J Muscle Res Cell Motil* 20: 147-154, 1999.

Pierotti DJ, Roy RR, Bodine-Fowler SC, Hodgson JA, and Edgerton VR. Mechanical and morphological properties of chronically inactive cat tibialis anterior motor units. *J Physiol* 444: 175-192, 1991.

Pubols LM, and Goldberger ME. Recovery of function in dorsal horn following partial deafferentation. *J Neurophysiol* 43: 102-117, 1980.

Putman CT, Conjard A, Peuker H, and Pette D. Alpha-cardiac-like myosin heavy chain MHCI alpha is not upregulated in transforming rat muscle. *J Muscle Res Cell Motil* 20: 155-162, 1999.

Putman CT, Dusterhoft S, and Pette D. Satellite cell proliferation in low frequency-stimulated fast muscle of hypothyroid rat. *Am J Physiol Cell Physiol* 279: C682-690, 2000.

Putman CT, Kiricsi M, Pearcey J, MacLean IM, Bamford JA, Murdoch GK, Dixon WT, and Pette D. AMPK activation increases uncoupling protein-3 expression and mitochondrial enzyme activities in rat muscle without fibre type transitions. *J Physiol* 551: 169-178, 2003.

Rafuse VF, and Gordon T. Self-reinnervated cat medial gastrocnemius muscles. I. comparisons of the capacity for regenerating nerves to form enlarged motor units after extensive peripheral nerve injuries. *J Neurophysiol* 75: 268-281, 1996a.

Rafuse VF, and Gordon T. Self-reinnervated cat medial gastrocnemius muscles. I. comparisons of the capacity for regenerating nerves to form enlarged motor units after extensive peripheral nerve injuries. *J Neurophysiol* 75: 268-281, 1996b.

Rafuse VF, and Gordon T. Self-reinnervated cat medial gastrocnemius muscles. II. analysis of the mechanisms and significance of fiber type grouping in reinnervated muscles. *J Neurophysiol* 75: 282-297, 1996c.

Rafuse VF, Gordon T, and Orozco R. Proportional enlargement of motor units after partial denervation of cat triceps surae muscles. *J Neurophysiol* 68: 1261-1276, 1992.

Reichmann H, Srihari T, and Pette D. Ipsi- and contralateral fibre transformations by cross-reinnervation. A principle of symmetry. *Pflugers Arch* 397: 202-208, 1983.

Roy RR, Talmadge RJ, Hodgson JA, Oishi Y, Baldwin KM, and Edgerton VR. Differential response of fast hindlimb extensor and flexor muscles to exercise in adult spinalized cats. *Muscle Nerve* 22: 230-241, 1999.

Roy RR, Talmadge RJ, Hodgson JA, Zhong H, Baldwin KM, and Edgerton VR. Training effects on soleus of cats spinal cord transected (T12-13) as adults. *Muscle Nerve* 21: 63-71, 1998.

Roy RR, Zhong H, Hodgson JA, Grossman EJ, Siengthai B, Talmadge RJ, and Edgerton VR. Influences of electromechanical events in defining skeletal muscle properties. *Muscle Nerve* 26: 238-251, 2002a.

Roy RR, Zhong H, Khalili N, Kim SJ, Higuchi N, Monti RJ, Grossman E, Hodgson JA, and Edgerton VR. Is spinal cord isolation a good model of muscle disuse? *Muscle Nerve* 35: 312-321, 2007.

Roy RR, Zhong H, Monti RJ, Vallance KA, and Edgerton VR. Mechanical properties of the electrically silent adult rat soleus muscle. *Muscle Nerve* 26: 404-412, 2002b.

Schiaffino S, and Reggiani C. Molecular diversity of myofibrillar proteins: gene regulation and functional significance. *Physiological reviews* 76: 371-423, 1996.

Srere PA. Citrate synthase. In: *Citric Acid Cycle*, edited by Lowenstein JM. New York: Academic Press, 1969, p. 3-11.

St-Pierre DM, Leonard D, and Gardiner PF. Recovery of muscle from tetrodotoxin-induced disuse and the influence of daily exercise. 1. Contractile properties. *Exp Neurol* 98: 472-488, 1987.

St-Pierre DM, Leonard D, Houle R, and Gardiner PF. Recovery of muscle from tetrodotoxin-induced disuse and the influence of daily exercise. 2. Muscle enzymes and fatigue characteristics. *Exp Neurol* 101: 327-346, 1988.

Staron RS, and Pette D. The multiplicity of combinations of myosin light chains and heavy chains in histochemically typed single fibres. Rabbit soleus muscle. *Biochem J* 243: 687-693, 1987.

Stein RB, Gordon T, Jefferson J, Sharfenberger A, Yang JF, de Zepetnek JT, and Belanger M. Optimal stimulation of paralyzed muscle after human spinal cord injury. *J Appl Physiol* 72: 1393-1400, 1992.

Suarez RK, Brown GS, and Hochachka PW. Metabolic sources of energy for hummingbird flight. *Am J Physiol* 251: R537-542, 1986.

Talmadge RJ, Roy RR, Caiozzo VJ, and Edgerton VR. Mechanical properties of rat soleus after long-term spinal cord transection. *J Appl Physiol* 93: 1487-1497, 2002.

Thomas CK, and Zijdewind I. Fatigue of muscles weakened by death of motoneurons. *Muscle Nerve* 33: 21-41, 2006.

Tower S, Bodian D, and Howe H. Isolation of intrinsic and motor mechanism of the monkey's spinal cord. *J Neurophysiol* 4: 388-397, 1941a.

Tower S, Howe H, and Bodian D. Fibrillation in skeletal muscle in relation to denervation and to inactivation without denervation. *J Neurophysiol* 4: 398-401, 1941b.

Tower SS. Function and structure in the chronically isolated lumbo-sacral spinal cord of the dog. *J Comp Neurol* 67: 109-131, 1937.

Turner DC, Wallimann T, and Eppenberger HM. A protein that binds specifically to the M-line of skeletal muscle is identified as the muscle form of creatine kinase. *Proceedings of the National Academy of Sciences of the United States of America* 70: 702-705, 1973.

van der Laarse WJ, Diegenbach PC, and Maslam S. Quantitative histochemistry of three mouse hind-limb muscles: the relationship between calcium-stimulated myofibrillar ATPase and succinate dehydrogenase activities. *The Histochemical journal* 16: 529-541, 1984.

Zhong H, Roy RR, Hodgson JA, Talmadge RJ, Grossman EJ, and Edgerton VR. Activity-independent neural influences on cat soleus motor unit phenotypes. *Muscle Nerve* 26: 252-264, 2002.

CHAPTER 5: INTERPRETATIONS AND APPLICATIONS

5.1 SUMMARY OF RESULTS

It was hypothesized that following the onset of paralysis due to nervous system injuries resulting in the persistence or the recovery of some neuromuscular activity, the contractile phenotypes of whole muscles, motor units, and myofibers would be preserved or would recover over many months, but that the metabolic phenotypes would transform toward a more fatigable profile. This hypothesis was tested in two animal models: (1) chronic sacral spinal cord transection leading to the development of long-term tail muscle spasticity in adult rats, and (2) unilateral hindlimb paralysis due to low thoracic spinal cord hemisection combined with complete unilateral lumbar deafferentation (HSDA) in adult cats. Both models confirm the hypothesis. Specifically, in rat tail muscles the following outcomes are described.

- Daily tail muscle EMG early after sacral spinal cord transection is eliminated almost completely compared to normal tail muscles, and this is associated with a slow-to-fast myofiber type transformation and myofiber atrophy.

- Daily tail muscle EMG after several months of sacrocaudal spinal isolation also is eliminated almost completely compared to normal tail muscles, and this is associated with an even larger slow-to-fast myofiber type transformation and more severe myofiber atrophy than early after transection.

- Daily tail muscle EMG after several months of sacral spinal cord transection and spasticity is not different from normal tail muscles, and this spasticity-associated muscle activity promotes recovery of the normal myofiber type proportions, and complete recovery from myofiber atrophy except in the dominant type IID(X) myofibers.

- Compared to normal, long-term spinal cord transection and spasticity also result in a prolongation both of tail muscle twitch contraction and of twitch and tetanus relaxation, as well as an increase in twitch force. However, the spastic tail muscles become much more fatigable.

In summary, tail muscle activity is decreased acutely after sacral spinal cord transection in adult rats, and this is associated with atrophy and a slow-to-fast myofiber type transformation. However, tail muscle activity recovers with chronic transection and the development of spasticity, and this recovery of activity leads to a recovery of myofiber size, myofiber type proportions, and muscle contractile properties, although muscle fatigue resistance is lost. The recovery observed is due to muscle activity associated with spasticity because when spasticity is eliminated by also cutting the dorsal roots, the recovery of myofiber size and myofiber type proportions is not observed.

Similarly, in cat hindlimb medial gasrocnemius muscles the following outcomes following long-term HSDA are described.

- Paralyzed motor unit contractile speed, sag, and tetanic force are not altered compared to normal, but there is a large reduction in paralyzed motor unit endurance, which is evident as a robust transformation in motor unit types from fast fatigue resistant to fast fatigable.

- Paralyzed whole muscle contraction time, sag, and tetanic force are not altered compared to normal, but there is a large reduction in endurance.

- Compared to normal, paralyzed myofibers are not atrophied and do not exhibit a transformation in myofiber types according to immunohistochemistry for myosin heavy chain isoforms, but they do transform from fast oxidative glycolytic to fast glycolytic myofiber types according to histochemistry for mATPase and for oxidative and glycolytic marker enzymes.

- Paralyzed muscles exhibit a decrease in the ratio of oxidative to glycolytic enzyme activities.

In summary, long-term HSDA causes a transformation in physologically classified motor unit types from fast fatigue resistant to fast fatigable. This is manifested at the level of the paralyzed whole muscle as a loss of muscle endurance, and can be explained by a shift toward a more fatigable metabolic phenotype with respect to both the reduced ratio of oxidative to glycolytic enzyme activities and to the transformation in myofiber types classified according to metabolic criteria. However, HSDA does not alter the proportion of slow motor units, and HSDA does not alter the contractile force or speed, or the sag, of the paralyzed muscles. This sparing of contractile properties is associated with a preservation of the normal myofiber type proportions as determined by immunohistochemistry for myosin heavy chain isoforms. Likely, this preservation of the contractile phenotype in muscles paralyzed by HSDA is associated with hindlimb extensor hypertonus and recovery of reflex function, which are observed in the paralyzed hindlimbs, and which indicates some recovery of muscle activity with long-term injury.

5.2 MUSCLE ACTIVITY AFTER INJURY BENEFITS PARALYZED MUSCLES

The interpretation presented in Chapter 2 is that spastic neuromuscular activity promotes the sparing of some normal-like muscle contractile properties. Such an interpretation seems reasonable when the normal tetanus-to-muscle mass ratio, increased twitch force, prolonged twitch contraction and relaxation, prolonged relaxation from tetanus, decreased post-tetanic potentiation, and increased twitch-to-tetanus ratio of the spastic tail muscles are compared to the dissimilar results of studies in which no spasticity is observed or quantified in hindlimb muscles following spinal cord injury. This interpretation is further supported by the observations in Chapters 3 and 4, taken together, that activity in paralyzed muscles leads to the recovery of myofiber types and sizes and of twitch and tetanic contractile properties. Nevertheless, it must be emphasized that because all paralyzed adult rats in this study developed spasticity it was not possible to compare our findings to tail muscles that had been paralyzed but that had *not* been spastic. Although we did not quantify the amount of activity in the cat MG muscles

paralyzed by HSDA, it is likely that this activity was greatly reduced because the behaviour of these muscles was profoundly impaired, and because they were deafferented and thus the innervating motoneurons received no ipsilateral reflex inputs. This indicates that very little activity is required to preserve the normal tetanic and twitch contractile properties, myofiber size, and myosin heavy chain isoforms in the adult cat MG muscle.

However, it is clear from the results of the experiments described in Chapter 3 that when muscles are paralyzed following spinal cord injury, substantial muscle activity sometimes remains or emerges with time after injury, especially in the form of spasticity. As also shown in Chapter 3, it is useful to quantify the amount of activity associated with spasticity in order to interpret the interaction of spasticity with paralysis, which I have defined as the loss of voluntary control and sensation. Chapter 3 shows that when robust spasticity emerges with long-term injury in adult rats, it generates normal amounts of neuromuscular activity, which benefits paralyzed tail skeletal muscles. Specifically, spastic neuromuscular activity leads to recovery from myofiber atrophy and from transformations in myofiber types and the myosin heavy chain isoforms they express. Unfortunately, as discussed in Chapters 3 and 4, no reliable antibody against type IId(x) myosin heavy chain was available for the immunohistochemical staining. The myofiber distributions presented were validated using the clone BF-35 antibody against all myofibers except type IID(X) and using electrophoretic separation of MyHC isoforms. Further proof that there were not large numbers of hybrid myofibers coexpressing type IId(x) MyHC in any group is the only evidence missing in these studies that would support the conclusion that spasticity leads to the recovery of normal myofiber type proportions.

As shown in Chapter 4, adult cat medial gastrocnemius (MG) muscles paralyzed by hemisection and deafferentation exhibit preservation of muscle properties similar to that in spastic rat tail muscles. Specifically, myofiber size, myofiber type, and myosin heavy chain isoforms are preserved and, importantly, so are the twitch and tetanic contractile properties. The activity level of these MG muscles was not quantified, but their nominal spasm-like and contralateral reflex behaviour suggests that very little activity remained with long-term paralysis. The preserved myofiber properties, as well as the twitch and tetanic contractile properties, are consistent with this assumption. In the case of hemisection and deafferentation the ipsilateral descending and afferent inputs to the MG motoneurons are eliminated. Interestingly, then, the source of any residual, spastic-like activity in these muscles must come from contralateral descending and afferent inputs via interneuronal networks, or from infraspinal inputs (i.e., networks of cells at lower spinal segments). This is interesting because it reveals that critical structural and functional properties of skeletal muscles can be maintained throughout long-term paralysis by inputs from non-ipsilateral sources.

5.3 THE ROLE OF CALCIUM IN CONTRACTION OF PARALYZED MUSCLE

Chapter 2 describes the hypothesis that, secondary to the development of spasticity with long-term spinal cord injury, changes in calcium regulation are responsible for the altered

contractile properties of paralyzed rat tail muscles, independent of changes in myofiber types and the myosin heavy chain contractile protein isoforms they express. This scenario is probable, based upon recent studies that demonstrated virtually identical contractile property changes, compared to normal, of mouse hindlimb muscles in which the myoplasmic calcium buffer, parvalbumin, has been eliminated (Raymackers et al. 2000; Schwaller et al. 1999). These identical changes in spastic rats and parvalbumin-null mice include longer and larger twitches and prolonged relaxation from twitch and from tetanus (as well as no changes in the myofiber type distribution).

The critical role of calcium buffering and reuptake following excitation-contraction coupling in regulating the contractile properties of skeletal muscles was observed many years ago in the clinical setting by Brody (Brody 1969; Brody et al. 1970), who was also the first to demonstrate experimentally that calcium reuptake by the sarcoplasmic reticulum can profoundly impact muscle relaxation, in particular (Brody 1976). In fact, following 4 weeks of complete muscle disuse due to neurally-applied tetrodotoxin (TTX), impaired calcium reuptake by the sarcoplamic reticulum has been implicated as an underlying mechanism for the prolongation and potentiation of muscle twitch as well as of slowed relaxation from twitch and tetanus (St-Pierre and Gardiner 1985), results that are similar to our own. Thus the altered contractile properties of spastic tail muscles are almost certainly due to altered intracellular calcium handling, and this effect must indeed be the result of changes in the sarcoplasmic reticulum or its calcium ATPase, or in the myoplasmic buffer parvalbumin, or both.

It is also relevant to the discussion of calcium handling that the altered twitch contraction time observed in spastic tail muscles is discussed in Chapter 2 as a measure of muscle contractile speed that relates to myosin heavy chain isoforms. In fact, twitch contraction time is not well correlated with the mATPase kinetics that are associated with myosin heavy chain expression (Brody 1976). Not only has it been demonstrated that the muscle maximal shortening velocity, or V_{max}, reflects the best known correlation between muscle function (i.e., speed) and myofiber type distribution (Fitts et al. 1986), the maximal rate of rise of tetanus is a very good estimate of V_{max} (Stevens and Renaud 1985; Turcotte et al. 1991). The liklihood that the altered contractile properties observed with long-term spasticity are due to altered calcium handling remains well-supported by the literature. However, statements referring to the normal myofiber type distribution in spastic muscles should have been made in the context of the maximum rate of rise of tetanus rather than the twitch contraction speed; the former does not change, consistent with no changes in the myofiber type distribution or the in the myosin heavy chain isoform distribution, while the the latter does change, consistent with altered calcium buffering and/or reuptake.

5.4 CALCIUM- AND RATE-DEPENDENCE OF FATIGUE-RESISTANCE

In Chapters 2 through 4 a critical result is the reduction in fatigue resistance that is observed in conjunction with normal proportions of myofiber types classified according to MyHC isoform expression and, in the cat muscles, decreased relative oxidative-to-

glycolytic enzyme activity. The decreased fatigue resistance is observed at the levels both of the whole muscle and of single motor units. This relative reduction in aerobic capacity is consistent with reduced fatigue resistance in motor units and muscles under certain conditions (Nemeth et al. 1981; Parry and Desypris 1985). However, in contrast to the outcomes described in this thesis, 4 weeks of TTX-induced muscle paralysis leads to reduced oxidative capacity *without* large changes in muscle fatigue resistance (St-Pierre et al. 1988). In fact, it has been demonstrated that, without chronic changes in metabolism, factors related to myoplasmic calcium can be more important in determining the response of a muscle to a fatigue test, and such factors are clearly relevant to the changes in fatigue resistance described in this thesis.

It has been demonstrated experimentally that release of calcium ions from the sarcoplasmic reticulum during repetitive muscle contraction can be diminished. This occurs, for example, due to reduced ATP availability leading to impaired function of the SERCA pumps (poor calcium reuptake would lead to reduced calcium available for release). Another putative mechanism is the hydrolysis of creatine phosphate and ATP leading to the build-up of inorganic phospate ions, which bind to sarcoplasmic calcium and prevent its exit to the myoplasm (Westerblad et al. 1998). In order for the former possibility to be effective in contributing to fatigue, the excess myoplasmic calcium would have to diffuse to areas relatively far from the sites of cross-bridge formation, and this degree of myofibrillar compartmentalization is equivocal (Westerblad et al. 1998). The relevance of the latter scenario is meaningful when animals multiple experimental groups are metabolically compromised and thus differ in muscle creatine phosphate and ATP availability. Overall, based upon the fatigue tests described in Chapters 2 and 4, it seems possible that the increased fatigability observed in both models (sacral spinal transection in rats and HSDA in cats) could be due either to metabolic compromise (reduced availability of high energy phosphates) or to reduced calcium release from the SR (consequent to impaired calcium buffering and/or reuptake), or both.

A more likely impact of impaired myoplasmic calcium handling on the results of the fatigue tests used in Chapters 2 and 4 is the impact of prolonged contraction and relaxation on the response of paralyzed muscles to repetetive stimulation at 40 Hz, compared to the response of control muscles to stimulation at this same frequency. As similarly observed in muscles paralyzed by TTX-induced disuse, in which calcium reuptake into the SR is apparently impaired (Gardiner et al. 1992; St-Pierre et al. 1988), the outcome of the fatigue test in spastic rat tail muscles or in cat MG motor units or muscles paralyzed by HSDA will depend to a large extent on the twitch contraction and relaxation properties of the muscle in question. Specifically, because TTX-paralyzed muscles exhibit impaired calcium reuptake and their contraction and relaxation are prolonged, they operate at a higher percentage of their maximum tension when stimulated at lower frequencies, compared to control muscles (Gardiner et al. 1992; St-Pierre et al. 1988). Similarly, spastic rat tail muscles obviously contract and relax more slowly. Although cat MG muscles paralyzed by HSDA are not different from normal in their twitch contraction and relaxation times, the population of slow MG motor units did show a 20-30 ms prolongation of time-to-peak twitch (Figure 4-8 and associated text). As a result these paralyzed muscles operate at a higher percentage of their maximum tension at

40 Hz than do their repsective controls (see Figure 2-6 insets in Chapter 2 and Figure 4-3D in Chapter 4). Thus impaired calcium handling could ultimately cause these paralyzed muscles to fatigue more rapidly than normal muscles at 40 Hz, and thus in these muscles the Burke-like fatigue test may not be the best method for identifying fatigability changes that result from altered oxidative-glycolytic balance in the muscles themselves.

5.5 DISCOORDINATE ALTERATIONS IN METABOLIC AND CONTRACTILE PROFILES

Rat tail muscles that were spastic following low sacral spinal cord transection and cat MG muscles and motor units that were paralyzed by HSDA both demonstrated reduced fatigue resistance, preserved or enhanced twitch and tetanic contractile properties, and preserved or restored myofiber types and myofiber sizes, compared to controls. I have described this phenomenon as a discoordinate, or independent, regulation of metabolism and and contractile properties. The data presented in this thesis (especially Chapter 4) indicate that, under conditions of altered use, fatigue resistance and the associated metabolic properties are relatively plastic but tension-generating mechanisms are relatively stable, while myofiber size is preserved. In contrast, experiments investigating muscles paralyzed by neurally-applied TTX have demonstrated the opposite result: with TTX-induced disuse fatigue resistance and metabolism are relatively much less plastic than contractile properties and the associated myosin heavy chain isoforms, and myofibers undergo considerable atrophy (Cormery et al. 2000; Gardiner et al. 1992; St-Pierre et al. 1988). Regardless of the fact that spastic and HSDA-paralyzed muscles respond differently to their respective changes in activity than do TTX-paralyzed muscles, similar conclusions can be drawn from these models. Specifically, based upon the effects of neurally-applied TTX on muscle properties, it has been suggested that activity is the the principal, but not the only, determinant of myofiber size and metabolic heterogeneity (Michel et al. 1994). This conclusion is consistent, in particular, with the results presented in Chapter 3 where long-term spinal isolation led to considerable myofiber degeneration because muscle activity was almost completely eliminated, but in long-term spinal cord transected rats this myofiber degeneration was not evident because muscle activity was restored to normal levels by spasticity.

Overall, the response of rat tail muscles to long-term spinal cord transection and spasticity and of cat hindlimb MG muscles to long-term HSDA reflect the apparent dose-response relationship of muscles, motor units, and their myofibers to activity. This relationship has been best demonstrated using electrical stimulation paradigms that vary with respect to the site of stimulation delivery (i.e., stimulation of the muscle nerve versus stimulation of the motor point) and, more importantly, the stimulation frequency (Gordon et al. 1997; Sutherland et al. 1998). Depending on these stimulation conditions the muscle sometimes converts completely to a slow/type I myofiber profile with long-term stimulation, and sometimes it converts to a fast fatigue-intermediate/type IIA myofiber profile (Gordon et al. 1997; Sutherland et al. 1998). In these studies the final, steady-state phenotype observed (response) is dependent upon the amount and pattern of activity (dose), and this phenotype sometimes exhibits evidence of metabolic-contractile

discoordination (Gordon et al. 1997; Sutherland et al. 1998), similar to the results described in this thesis.

5.6 FUTURE DIRECTIONS

Although spastic tail muscles clearly are active in the chronic spinal rat, and although the prolonged twitch and tetanic contraction and relaxation properties in these muscles are associated with this activity, the underlying mechanisms for these changes are unknown. With long-term spasticity tail myofiber type proportions recover, with no increase in the proportion of slow type I myofibers, and this is consistent with no changes in the rate of rise of the tetanus in these muscles. Evidently, the altered contractile properties in these muscles are not a result of chronic transformations in contractile proteins, and thus we have proposed that the changes are most consistent with changes in intracellular calcium handling. Specifically, the first step toward revealing the mechanisms for altered contractile properties in spastic tail muscles is to determine whether these muscles downregulate the intracellular calcium binding protein parvalbumin that buffers free intracellular calcium following excitation-contraction coupling, and to determine whether these muscles undergo a type 2 to type 1 transformation in the sarco/endoplasmic reticulum calcium ATPase (SERCA) that pumps free intracellular calcium into the sarcoplasmic reticulum. These changes would both contribute to the altered contractile phenotype observed in tail muscles after long-term spasticity.

In hindlimb cat medial gastrocnemius muscles after chronic HSDA injuries, as in spastic rat tail muscles, the proportions of myofiber types identified according to myosin heavy chain expression also recover or are preserved, and this is associated with preserved motor unit and muscle contractile properties. Likely this preservation of contractile phenotype after HSDA is related to the recovery of some activity in these paralyzed muscles, but this remains to be determined. Consequently, it would be useful to perform 24-hour EMG recordings in normal medial gastrocnemius muscles and in medial gastrocnemius muscles paralyzed by long-term HSDA. This might be done most easily in a rat model of HSDA, which has not previously been attempted. Such a rat model would allow confirmation of the results presented in this thesis for cat muscles, and by using a chronic EMG recording approach similar to that described in this thesis for the rat tail muscles this rat model of HSDA might permit a simpler and more accessible activity measurement than could be accomplished using cats.

After chronic sacral spinal cord injury and spasticity in the rat and after chronic HSDA injury in the cat, the affected muscles and motor units demonstrated profound reductions in fatigue resistance with long-term paralysis. Following HSDA in the cat medial gastrocnemius this was clearly due to changes in the distribution both of the metabolically-classified myofiber types and of the biochemically-determined oxidative and glycolytic enzyme activities. Such changes also are the most likely candidates for the mechanism underlying changes in the fatigue profile of the spastic tail muscles, but tail muscles from chronic spinal rats must be assessed metabolically in order to confirm this. Thus enzyme activities should be quantified in these muscles. Such assays would be easy

to perform in conjunction with quantification of parvalbumin and SERCA isoforms, as suggested above.

The principal drawback of the methodological approach used in the studies reported here was the lack of a reliable immunohistochemical antibody that could identify type IID(X) myofibers and, by extension, a potentially large number of hybrid myofibers in the muscles analyzed. For this reason, it would be extremely useful to identify an effective MyHC IId(x) antibody or, perhaps more relevant to this thesis, identify a protocol that would permit adequate type IID(X) myofiber staining in rat and cat muscle using one of the existing MyHC IId(x) antibodies that currently cross-reacts with MyHC IIa in these tissues.

One final curiosity in this thesis that would be interesting to investigate is the reason for the IID(X) to type IIA myofiber type transformation that was observed in the tail muscles of rats with long-term spinal isolation. Discovering the reason for this transformation would assist in understanding the response of tail muscles to the changes in activity observed in this thesis. One approach to this question is to design a casting procedure that could immobilize the central segments of the tail in shortened, normal, and lengthened positions. This could be done using normal animals, but it would likely be easier using spinal isolated animals because their tails are neither under voluntary control nor subject to spasms as in the transected animals. Obviously, the outcome of such an investigation would be altered by a more effective antibody against MyHC IId(x), as already mentioned.

5.7 CLINICAL RELEVANCE AND APPLICATION

The clinical relevance of these studies should not be overlooked. In the tail muscles of chronic sacral spinal rats, recovery from atrophy and recovery of the normal myofiber type proportions with long-term spasticity, as well as the apparent preservation of some normal-like contractile properties, suggests that muscle activity due to spasticity can have some important benefits for muscle health. This should be investigated further in humans with spinal cord injury, and the results of such investigations should be considered when selecting rehabilitation and treatment approaches for people coping with spasticity due to spinal cord injuries. Additionally, in the medial gastrocnemius muscles of cats with HSDA injuries the contractile properties were preserved, including normal muscle and motor unit tetanic forces, on average, despite paralysis and the loss of fatigue resistance. This suggests that following central nervous system injuries, loss of function may be due to muscle fatigability rather than to loss of muscle force generation per se. More research is required in order to determine if fatigue resistance can be preserved or recovered following paralysis, without compromising muscle force generation. If these issues can be addressed effectively they would clearly have important clinical implications for the management of spinal cord injury, spasticity, and other muscle paralysis conditions.

In fact, based upon the results presented here I would like to propose that for people living with spinal cord injury, if untreated using pharmacological approaches, the potential benefits of spasticity may outweigh its negative consequences and, moreover,

that pharmacological treatment of spasticity may ultimately interfere with effective treatment of spinal cord injury. A comprehensive review of the literature regarding the pathophysiology and management of spasticity provides some helpful insights in this regard (Adams and Hicks 2005; Johnson et al. 1998; Stein et al. 2002; Yu 1998).

- Effective physical therapy and exercise can reduce hypertonus, spasms, and the pain associated with them.
- Effective physical therapy and exercise can improve coordination and strength in spastic limbs with partial voluntary control following spinal cord injury.
- Effective physical therapy and exercise can improve cardiovascular health in individuals that often suffer from life-threatening cardiovascular deterioration secondary to their injury.
- Pharmacological treatments for spasticity present a variety of negative side effects including: addiction; nausea and loss of appetite (leading to poor nutrition and deterioration of general health); dizziness; unwanted suppression of cardiopulmonary function; muscle weakness in limbs with partial or full voluntary control; and nerve and muscle degeneration beyond the direct effects of spinal cord injury (e.g., botulism toxin injections).

Obviously, exercise and physical therapy require substantial inputs of time, effort, motivation, personnel, and money in order to be effective. However, pharmacological therapies are also expensive, and potentially detrimental to the health of individuals living with spinal cord injury. I believe that the combination of exercise-based therapy and, accordingly, properly managed spasticity, has the potential to substantially improve the long-term muscle health and the quality of life of people living with spinal cord injury and thus it should be pursued aggressively as the primary focus of rehabilitation for these individuals.

5.8 REFERENCES FOR CHAPTER 5

Adams MM, and Hicks AL. Spasticity after spinal cord injury. *Spinal Cord* 43: 577-586, 2005.

Brody IA. Muscle contracture induced by exercise. A syndrome attributable to decreased relaxing factor. *The New England journal of medicine* 281: 187-192, 1969.

Brody IA. Regulation of isometric contraction in skeletal muscle. *Exp Neurol* 50: 673-683, 1976.

Brody IA, Gerber CJ, and Sidbury JB, Jr. Relaxing factor in McArdle's disease. Calcium uptake by sarcoplasmic reticulum. *Neurology* 20: 555-558, 1970.

Cormery B, Pons F, Marini JF, and Gardiner PF. Myosin heavy chains in fibers of TTX-paralyzed rat soleus and medial gastrocnemius muscles. *J Appl Physiol* 88: 66-76, 2000.

Fitts RH, Metzger JM, Riley DA, and Unsworth BR. Models of disuse: a comparison of hindlimb suspension and immobilization. *J Appl Physiol* 60: 1946-1953, 1986.

Gardiner PF, Favron M, and Corriveau P. Histochemical and contractile responses of rat medial gastrocnemius to 2 weeks of complete disuse. *Can J Physiol Pharmacol* 70: 1075-1081, 1992.

Gordon T, Tyreman N, Rafuse VF, and Munson JB. Fast-to-slow conversion following chronic low-frequency activation of medial gastrocnemius muscle in cats. I. Muscle and motor unit properties. *J Neurophysiol* 77: 2585-2604, 1997.

Johnson RL, Gerhart KA, McCray J, Menconi JC, and Whiteneck GG. Secondary conditions following spinal cord injury in a population-based sample. *Spinal Cord* 36: 45-50, 1998.

Michel RN, Cowper G, Chi MM, Manchester JK, Falter H, and Lowry OH. Effects of tetrodotoxin-induced neural inactivation on single muscle fiber metabolic enzymes. *Am J Physiol* 267: C55-66, 1994.

Nemeth PM, Pette D, and Vrbova G. Comparison of enzyme activities among single muscle fibres within defined motor units. *J Physiol* 311: 489-495, 1981.

Parry DJ, and Desypris G. Fatiguability and oxidative capacity of forelimb and hind limb muscles of dystrophic mice. *Exp Neurol* 87: 358-368, 1985.

Raymackers JM, Gailly P, Schoor MC, Pette D, Schwaller B, Hunziker W, Celio MR, and Gillis JM. Tetanus relaxation of fast skeletal muscles of the mouse made parvalbumin deficient by gene inactivation. *J Physiol* 527 Pt 2: 355-364, 2000.

Schwaller B, Dick J, Dhoot G, Carroll S, Vrbova G, Nicotera P, Pette D, Wyss A, Bluethmann H, Hunziker W, and Celio MR. Prolonged contraction-relaxation cycle of fast-twitch muscles in parvalbumin knockout mice. *Am J Physiol Cell Physiol* 276: C395-403, 1999.

St-Pierre D, and Gardiner PF. Effect of "disuse" on mammalian fast-twitch muscle: joint fixation compared with neurally applied tetrodotoxin. *Exp Neurol* 90: 635-651, 1985.

St-Pierre DM, Leonard D, Houle R, and Gardiner PF. Recovery of muscle from tetrodotoxin-induced disuse and the influence of daily exercise. 2. Muscle enzymes and fatigue characteristics. *Exp Neurol* 101: 327-346, 1988.

Stein RB, Chong SL, James KB, Kido A, Bell GJ, Tubman LA, and Belanger M. Electrical stimulation for therapy and mobility after spinal cord injury. *Prog Brain Res* 137: 27-34, 2002.

Stevens ED, and Renaud JM. Use of dP/dt and rise time to estimate speed of shortening in muscle. *Am J Physiol* 249: R510-513, 1985.

Sutherland H, Jarvis JC, Kwende MM, Gilroy SJ, and Salmons S. The dose-related response of rabbit fast muscle to long-term low-frequency stimulation. *Muscle Nerve* 21: 1632-1646, 1998.

Turcotte R, Panenic R, and Gardiner PF. TTX-induced muscle disuse alters Ca2+ activation characteristics of myofibril ATPase. *Comparative biochemistry and physiology* 100: 183-186, 1991.

Westerblad H, Allen DG, Bruton JD, Andrade FH, and Lannergren J. Mechanisms underlying the reduction of isometric force in skeletal muscle fatigue. *Acta Physiol Scand* 162: 253-260, 1998.

Yu D. A crash course in spinal cord injury. *Postgrad Med* 104: 109-106, 119, 1998.